Fortschritt-Berichte VDI

Reihe 10

Informatik/
Kommunikation

Junying Niu, M. Sc.,
Shanxi / China

Nr. 851

Suppressing Electromagnetic Interference in Switching-Mode Power Supplies by Chaotic Carrier Frequency Modulation

FernUniversität in Hagen
Schriften zur Informations- und Kommunikationstechnik

Suppressing Electromagnetic Interference in Switching-Mode Power Supplies by Chaotic Carrier Frequency Modulation

DISSERTATION

zur Erlangung des akademischen Grades

DOKTOR-INGENIEURIN

der Fakultät für Mathematik und Informatik

der FernUniversität in Hagen

von

Junying Niu, M.Sc.

Yangquan/China

Hagen, 2016

Fortschritt-Berichte VDI

Reihe 10

Informatik/
Kommunikation

Junying Niu, M. Sc.,
Shanxi / China

Nr. 851

Suppressing Electromagnetic Interference in Switching-Mode Power Supplies by Chaotic Carrier Frequency Modulation

FernUniversität in Hagen
Schriften zur Informations- und Kommunikationstechnik

Niu, Junying
Suppressing Electromagnetic Interference in Switching-Mode Power Supplies by Chaotic Carrier Frequency Modulation
Fortschr.-Ber. VDI Reihe 10 Nr. 851. Düsseldorf: VDI Verlag 2017.
110 Seiten, 89 Bilder, 9 Tabellen.
ISBN 978-3-18-385110-2, ISSN 0178-9627,
€ 43,00/VDI-Mitgliederpreis € 38,70.

Keywords: Chaotic Carrier Frequency Modulation Module – Electromagnetic Interference – Switching Mode Power Supply – Chaotic Frequency Pulse Width Modulation Integrated Circuit – Spread Spectrum

Due to the unpredictable and random-like features of chaotic signals, chaotic carrier frequency modulation (CCFM) technique, by which the spectra of input and output signals can be spread over a wide frequency band without changing the total energy, has been used to suppress electromagnetic interference (EMI) of switching mode power supply (SMPS). So far, the study on CCFM was focused on theoretical analyses, simulations, and experimental verifications, lacking of a practical consideration of applying CCFM in real power supplies, which will be main concern of this dissertation. To provide efficient and economical EMI suppression solutions, a CCFM module is proposed to serve as a plug-in component for power supplies with standard PWM ICs, and for designing a chaotic frequency PWM IC, it is necessary to integrate a chaotic frequency oscillator into the standard PWM IC, which is to be realized both in analogue and digital manners for various practical applications.

Bibliographische Information der Deutschen Bibliothek
Die Deutsche Bibliothek verzeichnet diese Publikation in der Deutschen Nationalbibliographie; detaillierte bibliographische Daten sind im Internet unter http://dnb.ddb.de abrufbar.

Bibliographic information published by the Deutsche Bibliothek
(German National Library)
The Deutsche Bibliothek lists this publication in the Deutsche Nationalbibliographie (German National Bibliography); detailed bibliographic data is available via Internet at http://dnb.ddb.de.

Schriften zur Informations- und Kommunikationstechnik
Herausgeber:
Wolfgang A. Halang, Lehrstuhl für Informationstechnik
Herwig Unger, Lehrstuhl für Kommunikationstechnik
FernUniversität in Hagen

Als Manuskript gedruckt. Printed in Germany.

ISSN 0178-9627

ISBN 978-3-18-385110-2

Preface

It was a day in the winter of 2010, when my colleague, Dr. Ping Li, invited Prof. Halang to visit our lab, where I got to know Prof. Halang. After that meeting, I got a wonderful opportunity to study for Ph.D. in Germany, a country famous for its rigor and diligence, where I joined the team led by Prof. Wolfgang A. Halang and Prof. Zhong Li, and began to work on a practical topic since August 2012: applying chaos to reduce electromagnetic interference (EMI) in commercial electrical products.

Switching mode power supply (SMPS), with the features of high energy conversion efficiency and small size, is increasingly widely used in modern electronic equipments. However, severe EMI is caused by high-frequency switching action of semiconductor devices, which threatens the functions of other electric and electronic devices and health of human beings in the environment, and thus poses a big challenge for scientists and engineers to fight EMI. Traditionally, filtering and shielding techniques have been well deployed in various devices, but they have many drawbacks in cost, size, and efficiency, and new solutions are always desired. Owing to the pseudo-randomness and the continuous spectrum features of chaos, chaotic carrier frequency modulation (CCFM) technique can be well employed to fight EMI on the emission source by spreading the spectra of input and output signals over the entire frequency band. Thus, it has attracted great research interest in the past two decades.

Although there have been a lot of the theoretical and experimental research done on the application of CCFM for EMI reduction, commercial SMPSs with chaotic modulation have not yet been seen on the market. Hence, schemes to implement CCFM in the commercial power supplies are of great practical significance. Then, the mathematical analysis and the experimental research on the schemes have been carried out in the framework of this dissertation.

This dissertation agglomerates painstaking efforts of many persons. Without their help, I would not have been able to complete this dissertation.

First, a great appreciation is due to my supervisor, Prof. Zhong Li, for his instruction with patience. In the meantime, thanks for the concern and consideration of Prof. Li's family members, his wife, Mrs. Juan Mei, and his son, Yifan. With the warm help of Prof. Li and his family both in my work and daily life, I could live and work without worries behind. Additionally, it is worth learning from Prof. Li's humor, the attitude to life and good intention toward others.

Also, I owe my thanks to Prof. Halang for his supervision and kindly help in my work. I was deeply influenced by his scientism and academic consciousness. Thanks also go to Mrs. Halang for her kindness and encouragement.

My special thanks are owned to Dr. Ping Li for recommending me to Prof. Li and Prof. Halang. I would thank Prof. Herwig Unger and Dr. Panchalee Sukjit for their kind help. Thanks also go to my colleagues: Mrs. Yuhong Song, Dr. Guidong Zhang, and Mrs. Jutta During, and my friends around: Mr. Ditter Dannet, Mrs. Ulrike Danner, Mr. Ulrisch Fisher, Mrs. Ulrike Fisher, Mrs. Bing Xiao, Mr. Jiameng Luo and Dr. Yajun Li.

Cordial thanks also go to my parents and parents-in-law for their love and concern from time to time. I would thank my husband, Zongzheng You, for his care for the family and our son, Zhijin, for bringing me a lot of pleasure.

I would thank the support of the project IGF-Vorhaben-Nr.17211 N, "suppressing electromagnetic interference in electronic devices via chaos control", which was funded by the German Federation of Industrial Research Associations. Sincere thanks go to Shunde Polytechnic for supporting my study.

Junying Niu
August 2016

Contents

Abstract

Due to its high efficiency, a switching mode power supply (SMPS) has been increasingly widely applied in electric industry. However, rapid switching action of semiconductor devices, which results in high change rates of voltage and current, leads to severe electromagnetic interference (EMI) problems.

Many engineering techniques have been proposed to suppress EMI of SMPS by taking measurements on interference sources, victims or EMI coupling paths, respectively. The conventional techniques for EMI reduction are shielding and filtering, which are methods to cut off the coupling path and enhance the interference immunity of the victim. However, they have the disadvantage of increasing size and cost of the products, which restrains their application, especially in portable equipments. Moreover, those methods, just fighting the generated interference, can't prevent the generation of EMI at the source. Hence, more efficient and economic techniques are desired.

In recent years, the spread-spectrum technique, which can reduce EMI at the source by spreading the spectra of input and output signals over a wide frequency band without changing the total energy, has received great research interest. Periodic carrier frequency modulation, randomized carrier frequency modulation and chaotic carrier frequency modulation (CCFM) are commonly used spread-spectrum techniques. The chaotic and randomized modulation techniques are more effective for EMI suppression than the periodic one. Moreover, as a nonlinear deterministic system to generate pseudo-random signals, a chaotic system is easier to control and manufacture than a random system, posing promising potentials in industrial applications. So far, the study on CCFM was focused on theoretical analyses, simulations, and experimental verifications, lacking of a practical consideration of applying CCFM in real power supplies, which will be main concern of this dissertation.

First, for power supplies with standard PWM ICs, a CCFM module is proposed to serve as a plug-in component for suppressing EMI, without changing the original circuit, thus, saving the development process and cost caused by the redesign of the product. The module is used to modulate the switching frequency of the standard PWM ICs by providing a chaotically dithering current for the frequency setting component. It is noted that the CCFM module is adjustable via its parameters to reach a trade-off between EMI suppression and ripples caused by chaotic modulation.

Secondly, for designing a chaotic frequency PWM IC, it is necessary to integrate a chaotic frequency oscillator into the standard PWM IC, which is to be realized both in analogue and digital manners for various practical applications. The oscillator of the traditional analogue PWM ICs is normally implemented by a sawtooth generator, of which the produced signal circularly vibrates between two threshold voltages. Therefore, an analogue chaotic driver of a PWM IC is designed to dither either of the threshold voltages chaotically. The digital PWM IC sets the switching frequency by a counter, which counts from 0 to a pre-assigned value at a certain rate during each switching period. Hence, a chaotic switching period counter is designed for the digital CCFM IC by modulating the pre-assigned value chaotically. Chaotic frequency PWM ICs provide an efficient and economical solution for EMI suppression in power supplies, and enable real industrial applications.

Keywords: Chaotic Carrier Frequency Modulation Module, Electromagnetic Interference, Switching Mode Power Supply, Chaotic Frequency Pulse-Width Modulation Integrated Circuit

1 Introduction

1.1 Power Supply

A power supply plays an important role in electrical and electronic devices, because it outputs the demanded electrical energy and affects the reliability, performance and cost of associated electronic equipments.

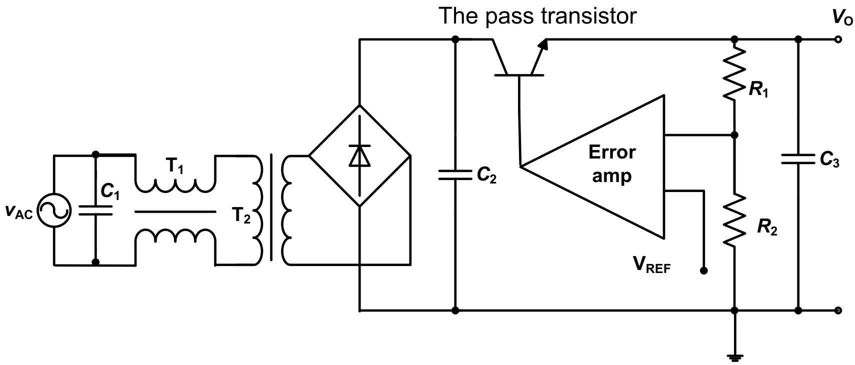

Figure. 1.1: The diagram of a linear power supply

There are two basic power supply configurations [1]: linear and switching-mode power supplies (SMPS). As shown in Fig.1.1, a pass transistor, which operates in a linear region, regulates the input power to a stable output voltage in the linear power supply. In contrary, the transistor in the switching-mode power supply (see Fig.1.2), namely a power switch, which is rapidly switched, works in the saturation region when it is on and in the cut-off region when it is off. Then the input electric energy of the power supply is transferred to the output device through the switching converter at a high frequency. Because the transistor working in the linear region takes more power consumption from the supply's input power than that working in a switching state, the input and output energy efficiency, a key index of the power supply quality, is higher in the SMPS. Additionally, compared with the linear supply, the SMPS has many advantages, including smaller size, lighter weight and the ability to boost output voltage above input voltage. As a result, SMPS has been applied growingly widely, especially in the field of household electrical and electronic appliances, communication equipments and industrial electronics.

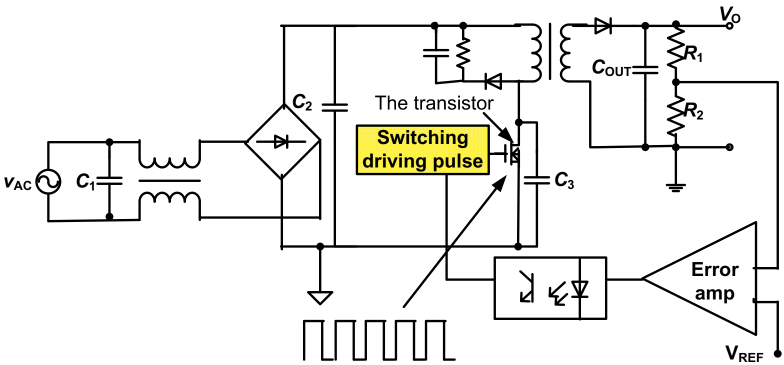

Figure. 1.2: The diagram of a typical SMPS

On the other side of the coin, the high-frequency switching action of the transistor, however, leads to high change rates of voltage and current and makes SMPS to generate unwanted electromagnetic interference (EMI), which is not such severe in the linear power supply. The generated EMI causes interference and possible operating faults to other equipments, and thus makes it difficult to satisfy the increasingly stringent international standards [2], restraining the application of SMPS. Even more, some sensitive devices have to adopts the linear power supply with a loss of energy efficiency. Consequently, the suppression of EMI is one of the most difficult challenges in the design of SMPS products.

1.2 EMI and EMC

EMI [3] is a disturbance caused by an electromagnetic field, which impedes the performance of an electrical device. As shown in Fig.1.3, an interference is generated by a source emitter and detected by a susceptible victim via a coupling path. In terms of the frequency bands, EMI is categorized into the conducted EMI (frequency band: 150kHz $\sim$ 30MHz) and the radiated EMI (frequency band: 30MHz $\sim$ 300MHz). The conducted EMI is caused by physical contact of the conductors. In contrary, the radiated EMI for higher frequencies is caused by induction (without physical contact of the conductors).

Normally, EMI can be estimated by measuring the power spectral density (PSD) [4], which describes how the power of a signal or time series is distributed with frequency. For example, the switching voltage, namely the voltage on the drain electrode of the transistor, and its spectrum are illustrated in Fig.1.4. Obviously, the transistor in SMPS always works with rapidly changing electrical current and voltage, and there are large spectrum peaks locating at the multiples of the fundamental frequency. The harmonic components of input and output signals may corrupt the power source and interfere with the operation of other equipments. As a result, the switching converter becomes interference source of SMPS. Generally, only conducted EMI is concerned in practice, because the transistors usually operate in the low and middle frequency band. Once the frequency of transistor operation exceeds 1GHz, radiated EMI should be taken into account.

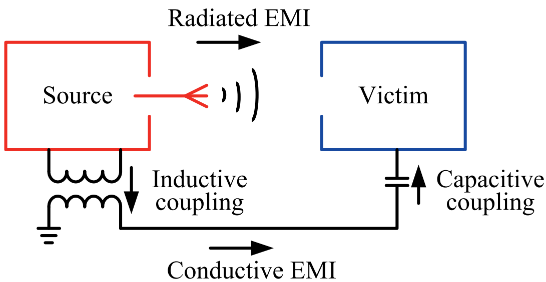

Figure. 1.3: EMI coupling modes

Because of the generation of unwanted EMI, it becomes a serious problem for the engineers to improve the electromagnetic compatibility (EMC) of SMPSs. The goal of EMC is to ensure the correct operation of different equipments in a common electromagnetic environment [5]. EMC requirements concern two basic concepts: emissions and susceptibility. Emission is the generation of electromagnetic disturbances by some sources, which may influence other electrical products. EMC is concerned with the unwanted emission and its reduction countermeasures. Susceptibility or immunity issue, in contrast, refers to the correct operation of electrical equipments (victims) in the presence of EMI. In a word, EMC is to suppress EMI and improve EMI immunity of electronic and electrical products, so that they can work as intended in its environment and the generated electromagnetic disturbances will not influence other devices. To define the specific EMC requirements that products must meet, EMC standards are established in many countries. For example, the electronic and electrical products sold to European Union (EU) countries have to meet the standard of EN550XX series, while the standards of Federal Communications Commission (FCC) Part 15 are employed in America. And EMC standards formulated by International Special Committee on Radio Interference (CISPR) are adopted in many countries [6].

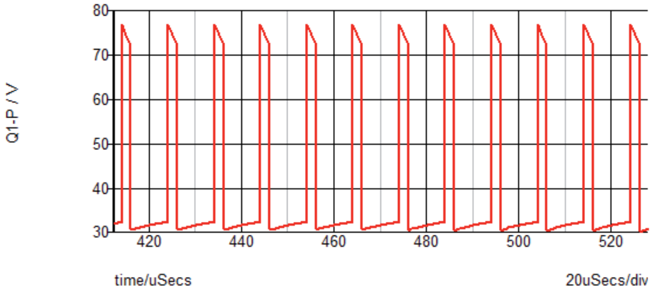

(a) Waveform of the switching voltage

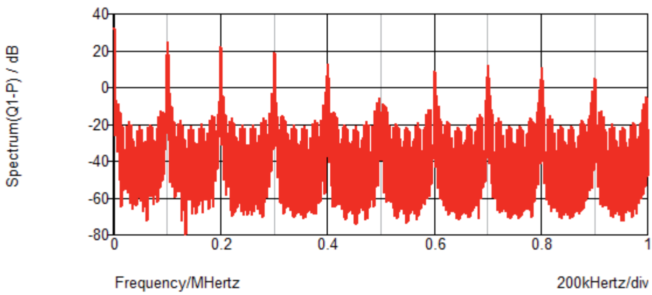

(b) Spectrum of the switching voltage

Figure. 1.4: The switching voltage and its spectrum

1.3 EMI Suppression Techniques

EMI can be suppressed by taking measurements on interference source, victim and the coupling path. The most commonly used methods are shielding and EMI filtering, which are mainly to cut off the coupling path and enhance the interference immunity victim [2]. However, they only reduce the generated disturbance, and their applications have to rely on the experience of the designer without the standard solutions for various products. Conversely, the EMI reduction techniques working on the interference source, such as the techniques of soft switching, spectrum-spread and optimizing the gate circuitry, became popular in recent years. These methods will be briefly reviewed as following.

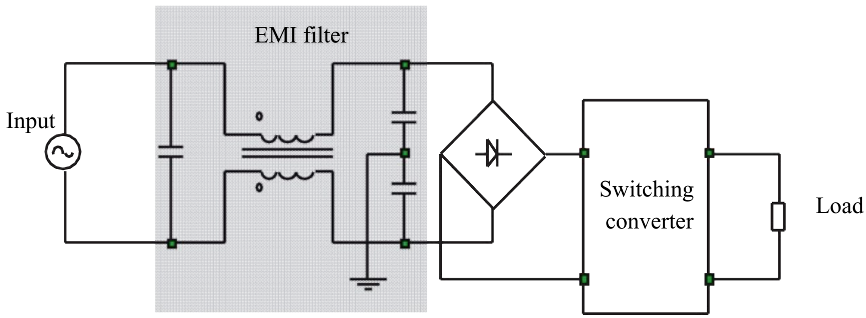

Figure. 1.5: EMI filter

(1)Shielding

Electromagnetic shielding [7, 8] is to reduce the electromagnetic field in a space by blocking the field with barriers made of conductive or magnetic materials. Shielding is typically applied to enclosures, separating electrical devices from the "outside world", and to cables, separating wires from its environment. Hence, shielding, which is noninvasive and does not affect high-speed operation, works for both emissions and susceptibility. It is also important to note that shielding usually can be installed after the design is completed. In contrast, the other suppression techniques generally can't be added easily once the device has gone beyond the prototype stage.

However, it is worth to notice that electromagnetic shielding is an expensive solution, which needs extra material, e.g. stripline, enclosure, and cable shield.

In addition, there may exist many leak sources, such as intake, display window, socket in real shield, degrading the effectiveness of EMI reduction.

(2)EMI Filtering

EMI filtering [9] is the most popular approach. As shown in Fig.1.5, the filters are normally appended at the input side of the converter to filter the noise either coming from or flowing to the power grid. Each EMI filter is only designed for a special narrow frequency band, so that it takes a lot of time to tune multiple discrete filters to reduce the noise on the whole frequency band. Moreover, not only the noise but also the useful signals may be suppressed. Hence, EMI filtering has the disadvantages of large size, high cost and long design process.

(3)Gate Circuitry Optimization

Gate circuitry optimization is to alter the voltage and current changing rates of the transistor, and a convenient way is to increase the equivalent gate driver resistance [10]. Additionally, the changing rates of voltage and current can be decreased by multi-step control and intelligent control on the switching action [11–14]. Owing to the increasing switching loss and its realization with digital processor, optimizing the gate circuitry is not suitable for the commonly used analogue SMPSs.

(4)Soft Switching

The main goal of soft switching technique is to reduce the switching loss when converters operate at high frequencies by turning the transistor on and off at zero current or zero voltage [15]. Consequently, the high change rates of voltage and current of the transistor are alleviated, thus EMI can be reduced.

Soft switching technique has its own limitations in improving EMC. Firstly, the effect to reduce EMI focuses on the frequency band 150kHz - 30MHz, but it almost does not work on the frequency band 10kHz - 150kHz. Secondly, more components are needed, such as resonant inductors, resonant capacitors, auxiliary diodes and even auxiliary switches. Moreover, when the converters are designed with some topologies, the EMI of the soft switching converters may be more severe than that of the hard switching ones [16, 17].

(5)Spread-Spectrum

As shown in Fig.1.6 [4], spread-spectrum technique was proposed to fight EMI by spreading the biggish spectrum peaks at the switching frequency and its multiples over a wide frequency band. Spread-spectrum can be implemented just by attaching a modulation circuit for the PWM controlled circuit, without considering other issues such as the supply's power rate, the transistor's working characteristics, the converter topology, etc. Hence, the spread-spectrum technique, an approach not only high-efficient but also convenient [18, 19], became a hot issue in recent years. The state-of-the-art of the spread-spectrum technique will be discussed in the following section.

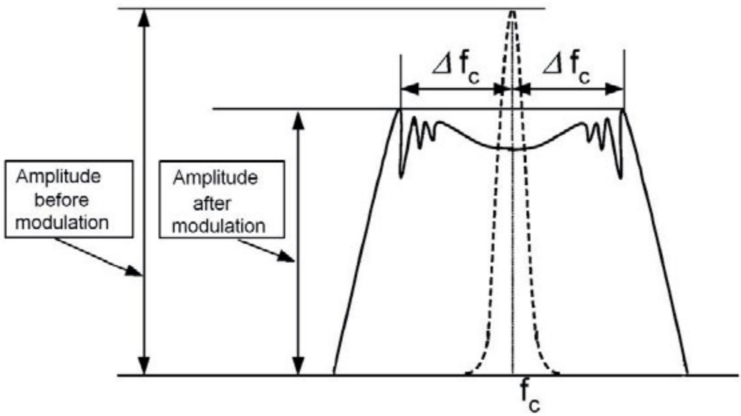

Figure. 1.6: The principle of the spread-spectrum technique

1.4 Spread-Spectrum Techniques

Periodic modulation, randomized modulation and chaotic modulation are commonly used spread-spectrum techniques.

1.4.1 Periodic Carrier Frequency Modulation

The periodic carrier frequency modulation is to modulate the switching frequency with periodic signals [20–22]. For example, the frequency modulated by a sinusoidal wave can be expressed as

$$f = f_c + \Delta f_s \cos(2\pi f_m t), \tag{1.1}$$

where f_c is a fixed reference switching frequency, f_m is the frequency of the modulation signal and Δf_s is the frequency modulation range.

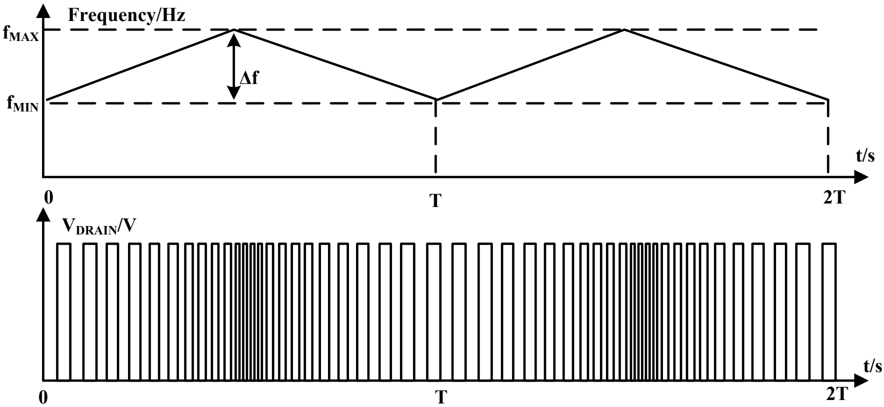

Figure. 1.7: The principle of the frequency jitter

Among the frequency modulation techniques, only frequency jitter, which is one of the periodic carrier frequency modulation techniques, has been witnessed in the commercial products [23]. As shown in Fig.1.7, under the control of frequency jitter [24], the switching frequency is modulated between f_{MIN} and f_{MAX} periodically. For example, TOPGX series are the PWM ICs with an internal frequency jitter module [24], which make the switching frequency changing from 128kHz to 136kHz at a speed of 4ms.

The original discrete spectrum peaks of the switching voltage can be reduced by using the periodic carrier frequency modulation, but are still discrete and distributed on certain frequency band [20, 21, 25]. Because the effectiveness of frequency modulation technique on EMI suppression is limited by the statistical characteristics of the modulation signal [25], the modulation signal should be non-periodic, in order to obtain a better EMI suppression effect. Consequently, randomized and chaotic modulation have been proposed.

1.4.2 Randomized Carrier Frequency Modulation

Randomized modulation is to modulate the switching frequency with random signal. Hence, the discrete harmonic power that usually exists in classical PWM schemes becomes continuous and is spread over a wide frequency range, resulting in EMI reduction. Randomized modulation was used to modulate PWM signal for DC/AC converters in [26] firstly. The same idea was pursued in a

DC/DC converter in [27]. Thereafter, randomized modulation has been widely studied [28–36].

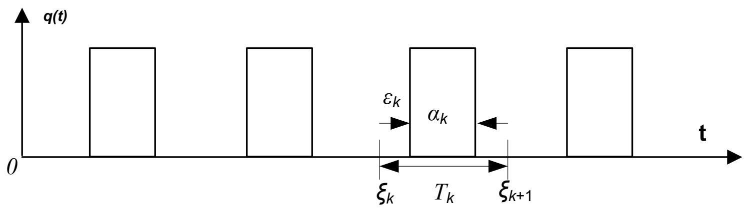

Figure. 1.8: The switching function $q(t)$

Randomized modulation schemes can be implemented in various ways [37]. As shown in Fig.1.8, the switching scheme for the transistor in a power converter can be described as a switching function $q(t)$, which is equal to 1 when the transistor is turned on, otherwise 0. ξ_k is the instant, at which the k-th switching cycle starts, T_k is the duration of the k-th cycle, a_k is the duration of the on-state and ε_k is the delay to the turn-on within the cycle. Note that the duty ratio is $d_k = a_k/T_k$. In general, ε_k, d_k and T_k can be dithered individually or simultaneously. The commonly used methods are as follows:

1) randomized pulse position modulation (RPPM): ε_k changes;

2) randomized pulse width modulation (RPWM): a_k changes; $\varepsilon_k = 0$;

3) randomized carrier frequency modulation with variable duty cycle (RCFMVD) [38]: T_k changes;

4) randomized carrier frequency modulation with fixed duty cycle (RCFMFD) [27]: T_k changes; $\varepsilon_k = 0$.

Among the four methods, RCFMFD is regarded as the best one for EMI suppression [39, 40], because the harmonic peaks of the switching voltage can be sharply reduced and the ripple increment of the output voltage is the smallest.

Compared with the periodic one, the randomized carrier frequency modulation is not only more effective for EMI reduction, but also more flexible to set the modulation range due to the variable randomness [25, 41–43]. The application of the randomized carrier frequency modulation, however, is restrained by its disadvantages, such as circuit complexity, debugging difficulty, high manufacture cost, and the generation of low frequency noise [42–45].

1.4.3 Chaotic Carrier Frequency Modulation

Chaotic system [46] is a deterministic system governed by the nonlinear rule, which can generate pseudo-random signal. The system has no "noise", randomness, or probabilities involved, and the apparent disorder arises from an extreme sensitivity to initial conditions. Therefore, owing to the features of pseudo-randomness and continuous spectrum, chaotic modulation can take place of randomized modulation. Furthermore, many benefits are brought by making use of CCFM. First of all, compared with the randomized one, the chaotic signal generator is more practical, because it is lower in circuitry complexity, debugging difficulty and manufacture cost [44, 45]. Besides, the utilization of CCFM can avoid the risk of inducing low frequency noise, which exists under randomized modulation [42, 43]. Hence, chaotic carrier frequency modulation technique has attracted more and more interest.

Plenty of work [47–52] based on the idealized and simplified models has been done to propose chaotic modulation schemes for EMI reduction, and even more, some of the latest research has proposed CCFM solutions to reduce EMI in a few of commercial power supplies [53–57]. As a result, it has been proven, over and over again, that CCFM is a superior technique for EMI suppression. For example, the spectra of the switching voltage under the traditional PWM control, periodic carrier frequency modulation and chaotic carrier frequency modulation are shown in Fig.1.9 [20], respectively. The spectrum under the traditional PWM control (see Fig.1.9a) is discrete, and then with periodic carrier frequency modulation, the harmonic peaks are reduced but the spectrum is still discrete (Fig.1.9b). The peaks are further spread to a continuous spectrum with CCFM as shown in Fig.1.9c.

Unfortunately, the previously proposed CCFM schemes have never been seen in commercial products, owing to the drawbacks of design complexity, high cost, and non-universality. Actually, in practice, only a fraction of commercial power supplies adopt the spread-spectrum technique to reduce EMI by employing the frequency jitter based IC to modulate the switching frequency periodically. Even only a tiny part of the dedicated PWM ICs have integrated the frequency jitter so far, and most of PWM ICs, the "normal" ones, drive the transistor operating at a fixed switching frequency, leading to severe EMI problem. Undoubtedly, there is a broad prospect to apply CCFM for EMI reduction in the commercial SMPS, so that the dissertation is to propose the CCFM schemes, which can solve the EMI problem to real products.

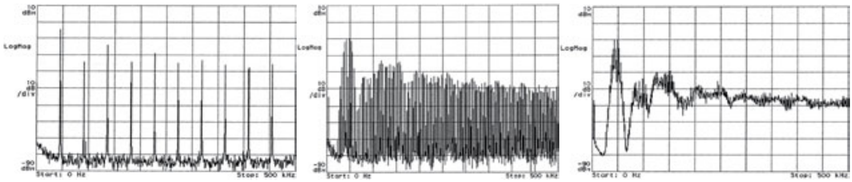

(a) Traditional PWM control (b) PWM control with periodic carrier frequency modulation (c) PWM control with chaotic carrier frequency modulation

Figure. 1.9: Power spectra of the switching voltage

1.5 Motivations and Innovations

Owing to the continuous spectrum feature of chaos, chaotic carrier frequency modulation is quite effective to reduce EMI by spreading the harmonics of the input and output signals over the whole frequency band. The power supply with chaotic modulation, however, has not yet been seen on the market, so that the thesis is concerned with the application of chaos to suppress EMI in commercial SMPSs.

Real products, which have to satisfy the demands of low cost, system stability and low circuit complexity, always make use of an IC, instead of a circuit composed of separate components, to control the system. Hence, the key point to implement CCFM on commercial SMPS is to integrate chaotic modulation into PWM IC. A PWM IC can be divided into a fixed switching frequency IC and a switching frequency programmable IC. In the fixed switching frequency IC, the clock circuit, namely the oscillator, which is to generate the clock signal determining the switching frequency, is completely integrated inside IC, and the switching frequency can't be modulated by the peripheral circuit any more. Conversely, for the frequency programmable IC, the switching frequency can be set by an external timing capacitor. The timing capacitor is charged and discharged periodically and its charging time plus discharging time are defined as a switching period. Consequently, once a chaotic modulation signal dithers the charging current of the timing capacitor, CCFM is realized.

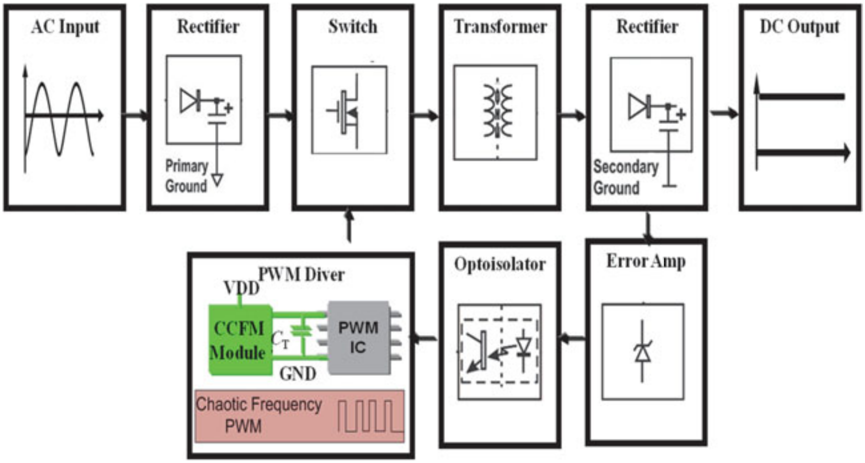

Figure. 1.10: The application of CCFM module in SMPS

Thus, as shown in Fig.1.10, a module circuit is designed to implement CCFM on various products, for which the only requirement is that they should be controlled by the frequency programmable PWM ICs without considering any other issues such as the supply's power range, the transistor's working characteristics, the converter topology, etc. The CCFM module, working on the interference source to suppress EMI, is more efficient than the conventional EMI filtering and electromagnetic shielding. Meanwhile, due to the features of low cost, easily debugging and universality to the SMPSs controlled by standard PWM ICs, the module overcomes the disadvantages of the previous CCFM schemes, and is potential in real applications. Moreover, it is a "plug-in" device, because the module can be easily installed on an end product. Most importantly, EMI reduction effectiveness can be estimated and improved by mathematical analysis, whereas most of the other techniques are to optimize EMC performance relying on the experts' experience.

Furthermore, analogue chaotic frequency PWM IC will be designed to facilitate the application of chaotic modulation. An analogue chaotic driver of a PWM

IC is designed to implement chaotic modulation on SMPS for EMI suppression, and it can be used widely in all kinds of PWM ICs. As shown in Fig.1.11, by using chaotic frequency PWM IC, CCFM will be realized without modifying the original circuit.

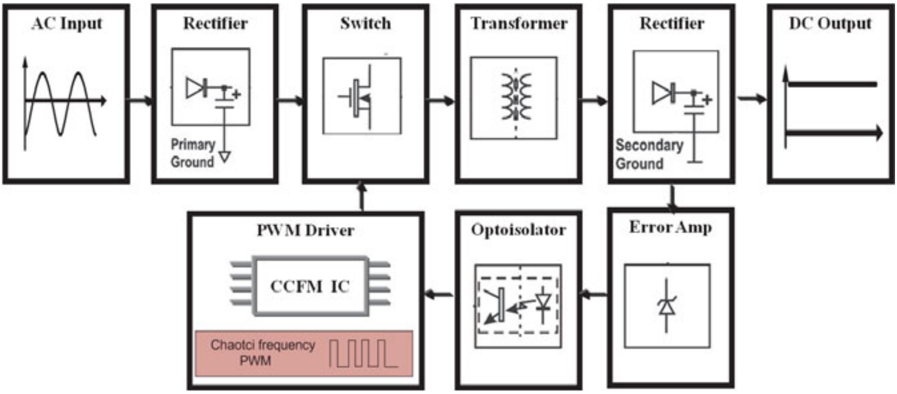

Figure. 1.11: Analogue chaotic frequency PWM IC controlled SMPS

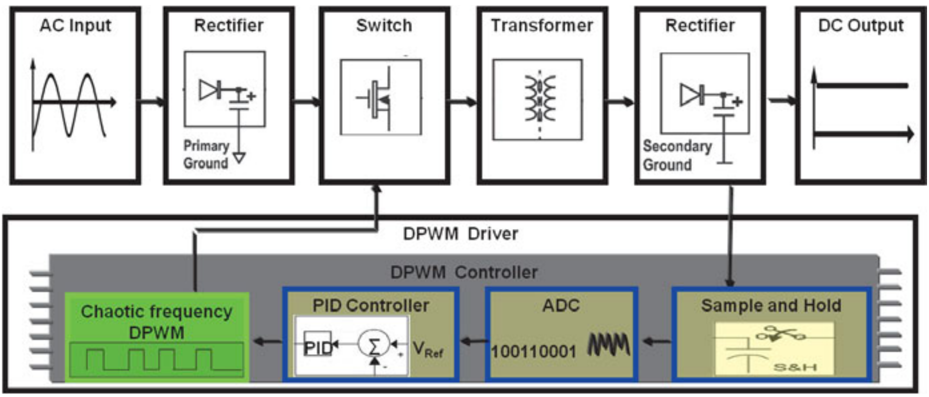

Figure. 1.12: Digital chaotic frequency PWM IC controlled SMPS

Most of the research on frequency modulation so far is carried on analogue SMPS, which is much more commonly used than the digital one, because the application of digital SMPS is limited by some constraints, such as high cost and slow response time caused by the discrete feature of the digital signal. However, with the development of electronic technique, the problems mentioned will be solved step by step. Moreover, owing to the features of the digital-control techniques, such as programmability, robustness and options for more advanced controls [58, 59], the digital system can satisfy the increasing demand for flexibility, multi-function, high portability, and intellectuality. Therefore, the digitally controlled SMPS will become more and more popular, and it is significant to develop digital chaotic frequency PWM IC for EMI suppression in digital systems. Fig.1.12 illustrates the SMPS controlled by a digital chaotic frequency PWM IC, whose design is based on a Field Programmable Gate Array (FPGA), and thus the CCFM scheme on the digitally controlled SMPS can be realized by chaotically dithering the pre-assigned value of the switching period counter. Simulations and experiments will be conducted to verify the effectiveness of the proposed method on EMI suppression in the digitally controlled SMPS.

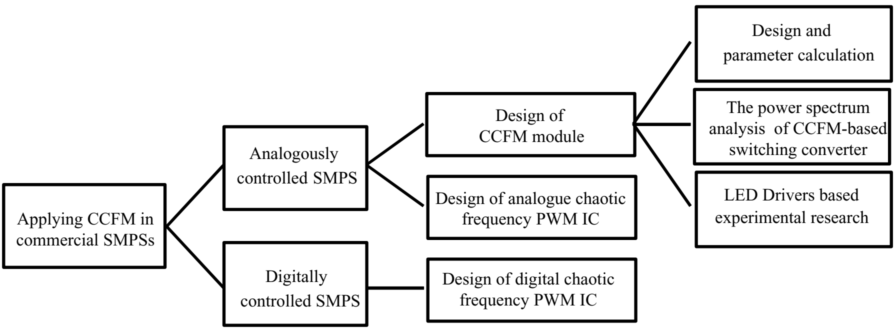

Figure. 1.13: Content of the dissertation

Hence, the dissertation is concerned with the application of CCFM to suppress EMI in commercial power supplies, which will be implemented both in analogue and digital ways, as illustrated in Fig.1.13.

1.6 About the Dissertation

The dissertation is sketched out as following:

In chapter 1, the research background, motivations, innovations and the content of the thesis are stated.

Chapter 2 is to propose a CCFM module with the features of low cost, simple connection ports, flexibility, and universality, aiming for commercial applications. Because the commercial SMPSs are normally controlled by a PWM IC, to make the module universal, it is designed to chaotically dither the switching frequency of the frequency programmable PWM IC. To make the module practicable, the circuit complexity of the module is low with just three connection ports, with one connecting to the timing capacitor while the others serving as the inputs of the power supply and ground wire, respectively. Furthermore, to improve the flexibility of the module, the switching frequency can be modulated within a desired range by a resistor.

In chapter 3, to investigate the EMI suppression effectiveness of chaotic carrier frequency modulation, the power spectral characteristics of a switching converter with CCFM will be studied. EMI is estimated by formulating and analyzing the power spectral density of the switching signals with CCFM, and it is found that the effectiveness on EMI reduction depends on the probability density function (PDF) and the modulation degree of the switching period. Consequently, EMI reduction effectiveness of the module can be improved in the instruction of mathematical analysis.

To investigate the feasibility of applying CCFM in SMPS, an experimental research on the CCFM module, taking two LED drivers as examples, will be carried out in chapter 4. Because the flyback topology is most commonly used in medium-low power SMPS, a flyback converter based LED driver, which is controlled by a typical current control mode (CCM) IC (UC3842), is chosen as one example. Meanwhile, the push-pull converter, which is often applied in a high power (more than 100W) LED driver, is selected as the other example, and it is controlled by TL494, the most commonly used IC of voltage control mode (VCM). EMI test, output voltage ripple measurement and efficiency measurement have been conducted on the CCFM-based SMPSs, leaving the influence of chaotic modulation on the whole system performance to be further investigated. For this purpose, the tests on the electrical characteristic, the key element's working condition and EMC performance of the LED drivers will be carried out.

To facilitate the design of chaos-modulated SMPS, an analogue chaotic frequency PWM IC will be designed in chapter 5. Chaotic frequency oscillator will be designed with Chua's circuit and integrated inside the analogue PWM IC, so that CCFM is realized without modifying the original circuit of a power supply. A CCM IC and a VCM&CCM IC will be taken as examples, which are used to control a flyback converter and a shift-phased full bridge converter, respectively. Simulations will be done to verify the effectiveness of the proposed method on EMI reduction.

Chapter 6 is to design a chaotic digital PWM (CDPWM) IC to reduce EMI of the digitally controlled power supplies, which are in a rapidly growing need. To realize CCFM on the digital systems, the emphasis is focused on the design of a chaotic switching period counter, and Logistic map, Shift map and Tent map are used to modulate the switching frequency of digitally controlled SMPS, respectively. The simulations and experiments will be conducted to investigate the effect of CCFM on the EMI reduction and output voltage ripple. Meanwhile, the comparison of the effect under various chaotic maps will be provided, so that the optimization decision can be made for different situations.

Chapter 7 is to summarize this dissertation, outline the contributions and point out the further research directions.

2 Chaotic Carrier Frequency Modulation Module

Although a lot of chaotic modulation schemes have been proposed to suppress EMI of SMPS, their drawbacks of design complexity, high cost, and non-universality prevent them from being marketable. Consequently, a CCFM module, which overcomes the mentioned disadvantages and can reduce EMI of the commercial power supplies controlled by standard PWM ICs, will be proposed in this chapter.

2.1 Introduction

Plenty of efforts have been given to apply chaotic carrier frequency modulation technique for EMI suppression in SMPS, but the SMPS with chaotic modulation has not yet been seen on the market.

On one hand, most of the work on CCFM was focused on theoretical study [4, 25, 47–52], and utilized idealized and simplified models, instead of the more complicated commercial products. To implement CCFM, the whole control circuit containing chaotic modulation circuit was designed with separate components. However, to meet the requirements of low cost, system stability and low circuit complexity, the control circuit of the actual products should be composed of a control IC and its peripheral circuit.

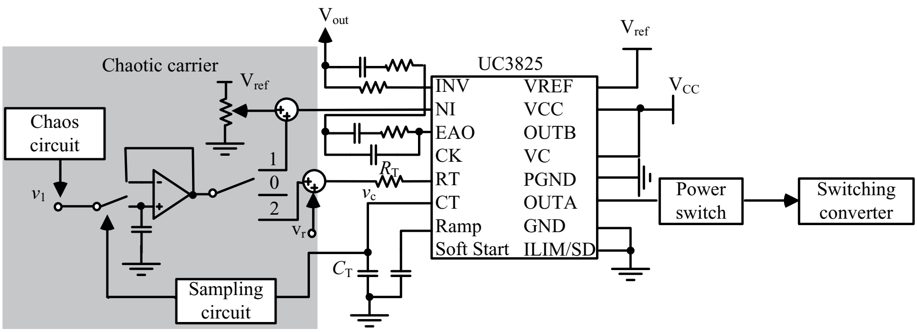

Figure. 2.1: The circuit design of CCFM scheme based on PWM IC

On the other hand, some of the latest research, combining chaotic modualtion with some PWM ICs, has proposed solutions to apply CCFM in a few of commercial power supplies [53–57]. Most of the schemes adopt the same PWM IC, i.e. UC3825, and are designed in the same circuit structure. As shown in Fig.2.1, the chaotic carrier is composed of a sampling circuit, an auxiliary circuit and a chaos circuit. Under the control of the sampling circuit, v_1, which is a chaotic voltage generated by the chaos circuit, is conducted to the auxiliary circuit at the beginning of each switching period. And then v_1 added to a reference voltage v_r is equal to v_c. v_c supplies a chaotic charging current to the timing capacitor C_T, dithering the switching frequency chaotically. Those solutions can be adopted by some commercial products, but the designed circuit is complex and only works on the PWM ICs with a programmable resistor, lacking of universality.

In general, owing to the drawbacks of design complexity, high cost, and non-universality, the previously proposed chaotic modulation solutions have rarely been seen in the commercial products. A CCFM module, which overcomes the mentioned disadvantages, is designed in this chapter to fill the gap. The module can work on SMPSs, which are controlled by the frequency programmable PWM ICs, and its application is so universal that it is unnecessary to consider any other issues such as the supply's power range, the transistor's working characteristics, the converter topology. The simulations are conducted to verify the effectiveness of the designed circuit on EMI reduction.

2.2 Oscillator of PWM IC

Generally, the oscillator of frequency programmable PWM IC makes use of an external timing capacitor and an external timing resistor (or only a timing capacitor) to set the switching frequency. As shown in Fig.2.2, a typical oscillator, used in UC3842 [60], is composed of the internal circuit (inside the dotted line) and the peripheral components, C_T and R_T. Initially, the voltage of C_T (v_C) is zero and $v_\mathrm{C} < \mathrm{V_{low}} < \mathrm{V_{upp}}$. Then, the switch S_1 is turned off, the oscillator is equivalent to the circuit in Fig.2.3a, and C_T will be charged by a reference voltage $\mathrm{V_{REF}}$ through R_T. Once v_C arrives at or exceeds $\mathrm{V_{upp}}$, S_1 is turned on, the oscillator is equivalent to Fig.2.3b, and C_T begins to be discharged through a current source $\mathrm{I_{discharge}}$ until $v_\mathrm{C} \leq \mathrm{V_{low}}$. Thereafter, C_T is charged and discharged circularly between $\mathrm{V_{low}}$ and $\mathrm{V_{upp}}$.

Hence, v_C exhibits the periodic sawtooth wave, and the period of the oscillator is the summation of the charging time t_c and the discharging time t_d of C_T. As shown in Fig.2.3, since the charging and discharging circuit are both the first order circuit [61], t_c and t_d can be calculated as

$$t_\mathrm{c} = R_\mathrm{T} C_\mathrm{T} \ln \frac{\mathrm{V_{low}} - \mathrm{V_{REF}}}{\mathrm{V_{upp}} - \mathrm{V_{REF}}}, \tag{2.1}$$

$$t_\mathrm{d} = R_\mathrm{T} C_\mathrm{T} \ln \frac{\mathrm{V_{upp}} + R_\mathrm{T} \mathrm{I_{discharge}} - \mathrm{V_{REF}}}{\mathrm{V_{low}} + R_\mathrm{T} \mathrm{I_{discharge}} - \mathrm{V_{REF}}}. \tag{2.2}$$

Because the discharging current $\mathrm{I_{discharge}}$ is normally much larger than the charging one, the discharging time is approximately 0. Therefore, the oscillator's period, namely the switching period of the converter, can be expressed as

$$T = t_\mathrm{c} + t_\mathrm{d} \approx t_\mathrm{c}. \tag{2.3}$$

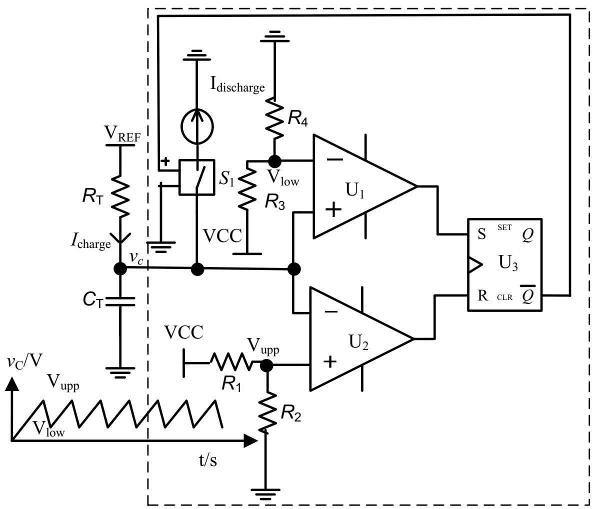

Figure. 2.2: Oscillator of PWM IC

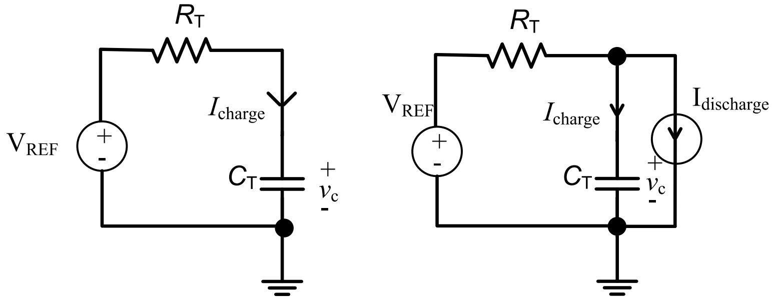

(a) The charging circuit (b) The discharging circuit

Figure. 2.3: The charging and discharging circuit of the timing capacitor

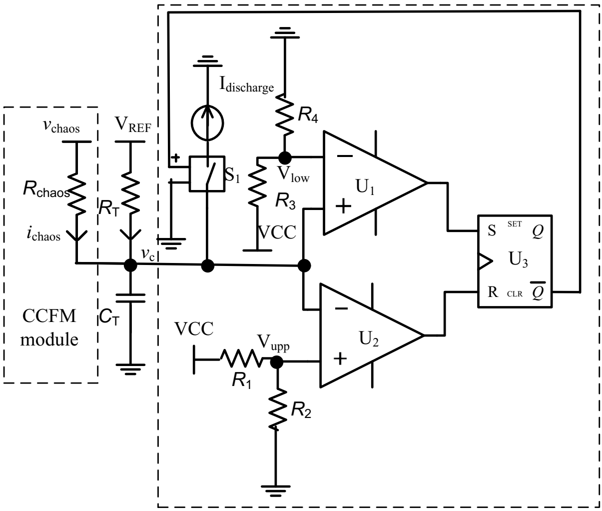

Figure. 2.4: The chaotic frequency oscillator

2.3 Implementation of CCFM

2.3.1 Operation Principle of CCFM

The frequency of the oscillator can be modulated by making the charging current of C_T changing chaotically. As shown in Fig.2.4, CCFM can be implemented by inducing a chaotic charging current to C_T, which is provided by a chaotic voltage v_{chaos} through R_{chaos}. Consequently, as shown in Fig.2.5, the chaotic carrier can be designed as a module with three ports, which are a power port (VDD), the ground port, and CT, the only one direct connection between the chaotic carrier and the control circuit. As a result, it is convenient to connect the module to the target products.

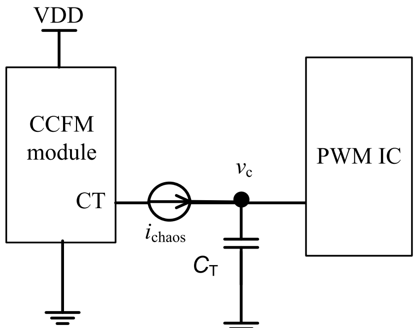

Figure. 2.5: Interface of the CCFM module

2.3.2 Chua's Circuit

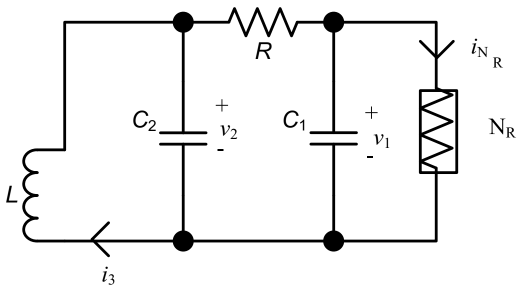

Figure. 2.6: Chua's Circuit

Chua's circuit [62] is used to generate the chaotic voltage. Fig.2.6 illustrates the famous Chua's circuit, which consistes of Chua's diode N_R, an inductor L, a resistor R, and the capacitors C_1 and C_2. $i_{\mathrm{N_R}}$ is the current through $\mathrm{N_R}$, the voltages of C_1 and C_2 are v_1, v_2, and $i_{\mathrm{N_R}}$ vs v_1 satisfies the relationship shown in Fig.2.7. Hence, Chua's circuit can operate in three regions, namely, region "D_{-1}" for $v_1 < -E$, region "D_0" for $-E \leq v_1 \leq E$, and region "D_1" for $v_1 > E$. In each region, the admittance of $\mathrm{N_R}$ is G_b, G_a and G_b respectively, so that $i_{\mathrm{N_R}}$ can be described by three sets of state equations:

$$i_{\mathrm{N_R}} = f(v_1) = \begin{cases} G_\mathrm{b}v_1 + (G_\mathrm{b} - G_\mathrm{a})\mathrm{E}, & v_1 < -\mathrm{E}, \\ G_\mathrm{a}v_1, & -\mathrm{E} \leq v_1 \leq \mathrm{E}, \\ G_\mathrm{b}v_1 + (G_\mathrm{a} - G_\mathrm{b})\mathrm{E}, & v_1 > \mathrm{E}. \end{cases} \tag{2.4}$$

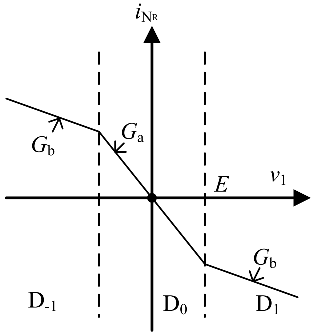

Figure. 2.7: Typical $i_{\mathrm{N_R}}$-v_1 characteristics of Chua's diode

The practical circuit of $\mathrm{N_R}$ is shown in Fig.2.8, where $\mathrm{V_{DD}}$ is the power supply of the operational amplifiers $\mathrm{U_1}$ and $\mathrm{U_2}$, and R_1-R_5 are the resistors. Hence, G_a, G_b and E are expressed as

$$\begin{cases} G_\mathrm{a} = -\dfrac{R_2}{R_1R_3} - \dfrac{R_5}{R_4R_6}, \\ G_b = \dfrac{1}{R_3} - \dfrac{R_5}{R_4R_6}, \\ E = \dfrac{\mathrm{V_{DD}}R_1}{R_1 + R_2}. \end{cases} \tag{2.5}$$

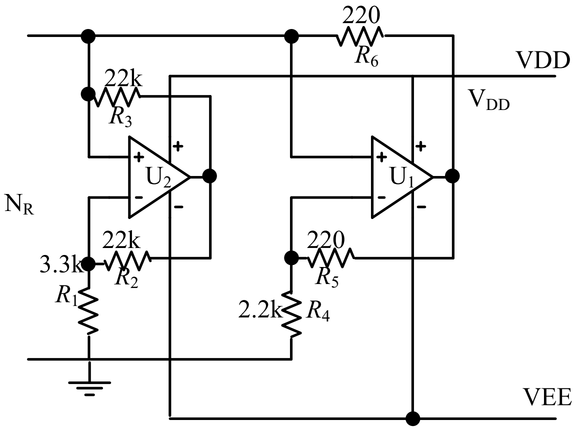

Figure. 2.8: The schematic of Chua's diode

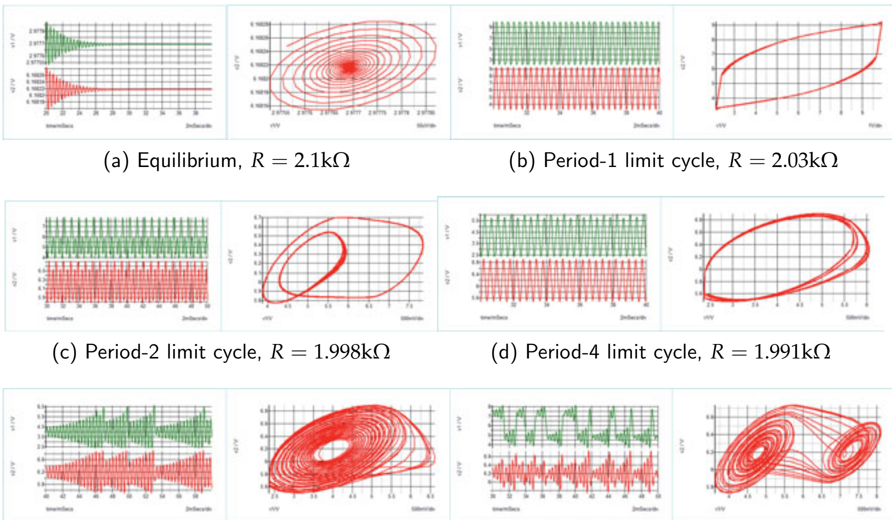

(a) Equilibrium, $R = 2.1\text{k}\Omega$

(b) Period-1 limit cycle, $R = 2.03\text{k}\Omega$

(c) Period-2 limit cycle, $R = 1.998\text{k}\Omega$

(d) Period-4 limit cycle, $R = 1.991\text{k}\Omega$

(e) Spiral chaos, $R = 1.98\text{k}\Omega$

(f) Double-scroll chaos, $R = 1.9\text{k}\Omega$

Figure. 2.9: Waveforms and the phase portraits of $v_1 - v_2$

Then Chua's circuit is described as

$$\begin{cases} \dfrac{dv_1}{dt} = \dfrac{1}{C_1}[(v_2 - v_1)G - f(v_1)], \\ \dfrac{dv_2}{dt} = \dfrac{1}{C_2}[(v_1 - v_2)G + i_3], \\ \dfrac{di_3}{dt} = -\dfrac{1}{L}v_2, \end{cases} \tag{2.6}$$

where $G = \dfrac{1}{R}$.

As $L = 23\text{mH}$, $C_1 = 100\text{nF}$, and $C_2 = 10\text{nF}$, v_1 and v_2 exhibit the waveforms of Fig.2.9, and the phase portraits of $v_1 - v_2$ show that Chua's circuit works under various dynamical behaviors with different values of R.

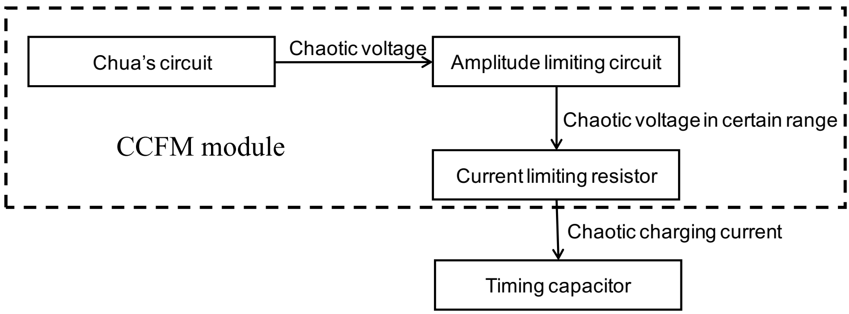

Figure. 2.10: The diagram of the CCFM module

2.3.3 CCFM Module

Because Chua's circuit only outputs the chaotic voltage, the generated chaotic voltage should be processed further to get the desired chaotic current. Therefore, the chaotic carrier is designed as Fig.2.10, which is composed of Chua's circuit, an amplitude-limiting circuit and a current-limiting resistor. The schematic of the CCFM module is given by Fig.2.11. The amplitude-limiting circuit is composed of R_1-R_4 and the amplifier U_1, and R_I is the current-limiting resistor. First of all, a chaotic voltage, v_2, is generated by Chua's circuit, and $v_2 \in [0, \text{VDD}]$. Second, because the chaotic voltage for charging the timing capacitor C_T, namely v_chaos, should be larger than the high threshold voltage of

C_T, V_{upp}, the amplitude-limiting circuit linearlly transforms v_2 to v_{chaos}. Thus v_{chaos} can be expressed as

$$v_{chaos} = \frac{(R_3 + R_4)R_2 v_2}{(R_1 + R_2)R_3}. \quad (2.7)$$

By adjusting R_1-R_4, v_{chaos} is set to above V_{upp}, and thus provides a chaotic charging current to C_T through R_I.

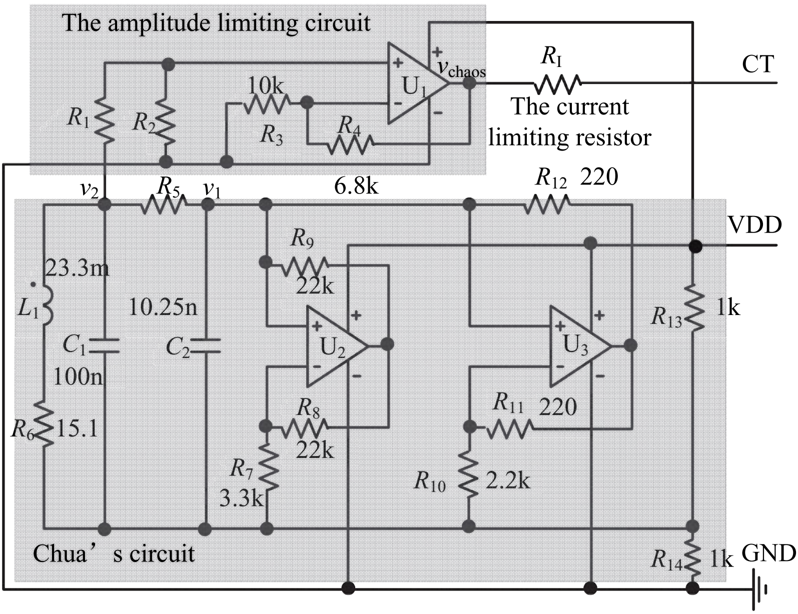

Figure. 2.11: The schematic of the CCFM module

Consequently, once the module shown in Fig.2.11 is used to drive the oscillator of PWM IC (see Fig.2.4), the k-th switching period can be expressed as

$$T_{\mathrm{k}}(v_{\mathrm{chaos}}, R_{\mathrm{I}}) \approx t_{\mathrm{c}_k}(v_{\mathrm{chaos}}, R_{\mathrm{I}}) = \frac{R_{\mathrm{T}}R_{\mathrm{I}}}{R_{\mathrm{T}}+R_{\mathrm{I}}} C_{\mathrm{T}} \ln \frac{\mathrm{V_{low}} - \dfrac{R_{\mathrm{I}}\mathrm{V_{REF}} + R_{\mathrm{T}}v_{\mathrm{chaos}}}{R_{\mathrm{T}}+R_{\mathrm{I}}}}{\mathrm{V_{upp}} - \dfrac{R_{\mathrm{I}}\mathrm{V_{REF}} + R_{\mathrm{T}}v_{\mathrm{chaos}}}{R_{\mathrm{T}}+R_{\mathrm{I}}}}. \quad (2.8)$$

The switching frequency of power supplies is also related to v_{chaos} and R_{I}, and can be calculated by

$$f(v_{\mathrm{chaos}}, R_{\mathrm{I}}) = \frac{1}{T_k(v_{\mathrm{chaos}}, R_{\mathrm{I}})} = \frac{1}{t_{\mathrm{c}_k}(v_{\mathrm{chaos}}, R_{\mathrm{I}})}. \quad (2.9)$$

The frequency of the oscillator can be fixed, periodically modulated and chaotically modulated respectively, corresponding to that v_{chaos} is constant, periodic and chaotic.

Denote v_{min} and v_{max} as the minimum and maximum of v_{chaos}. Then the switching frequency is minimized to $f(v_{\mathrm{min}}, R_{\mathrm{I}})$ and maximized to $f(v_{\mathrm{max}}, R_{\mathrm{I}})$, and its range from the minimum to the maximum is $\triangle \mathrm{F} = f(v_{\mathrm{max}}, R_{\mathrm{I}}) - f(v_{\mathrm{min}}, R_{\mathrm{I}})$. Therefore, $\frac{\triangle \mathrm{F}}{\mathrm{F}}$ is the modulation ratio of the oscillator frequency, defined by

$$\frac{\triangle \mathrm{F}}{\mathrm{F}} = \frac{f(v_{\mathrm{max}}, R_{\mathrm{I}}) - f(v_{\mathrm{min}}, R_{\mathrm{I}})}{f(v_{\mathrm{min}}, R_{\mathrm{I}})}. \quad (2.10)$$

Hence, it is deduced that the modulation range of the switching frequency can be set by R_{I}.

Here, take the oscillator of UC3842 as an example, and assume $\mathrm{V_{upp}} = 2.8\mathrm{V}$, $\mathrm{V_{low}} = 1.2\mathrm{V}$, $\mathrm{V_{REF}} = 5\mathrm{V}$, $R_{\mathrm{T}} = 30\mathrm{k}\Omega$, $C_{\mathrm{T}} = 1\mathrm{nF}$, and $4.5\mathrm{V} \leq v_{\mathrm{chaos}} \leq 5.5\mathrm{V}$. $\frac{\Delta \mathrm{F}}{\mathrm{F}}$ with different values of R_{I} is shown in Fig.2.12, and it is observed that $\frac{\Delta \mathrm{F}}{\mathrm{F}}$ becomes larger as R_{I} decreasing.

There are different oscillators in various frequency programmable PWM ICs, of which, however, almost all adopt the timing capacitor to set the switching frequency. They are to circularly charge and discharge the timing capacitor, and the sum of its charging and discharging time is the switching frequency. The only major difference for the oscillators is the ultilization of various charging circuits. Some ICs charge the timing capacitor by a reference voltage through an external resistor (see Fig.2.2), and some [63–65] do by an internal current source. Nevertheless, the module can be attached to almost all the frequency programmable PWM ICs to dither the switching frequency chaotically.

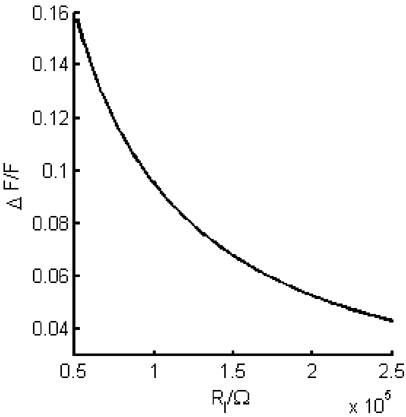

Figure. 2.12: The oscillator frequency modulation range vs R_I

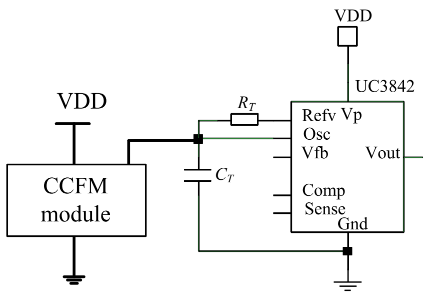

Figure. 2.13: The CCFM module used to drive UC3842

2.4 Simulations

2.4.1 Implementation of UC3842-based CCFM

The CCFM module shown in Fig.2.11 is used to drive UC3842, whose oscillator is the same as that in Fig.2.2 and makes use of a timing capacitor (C_T) and a timing resistor (R_T) to set the switching frequency. As illustrated in Fig.2.13, the charging current of C_T is dithered by the module, resulting in the switching frequency modulated chaotically.

Both the periodic and chaotic carrier frequency modulations are to be realized.

The spectra of the timing capacitor's voltage are given by Fig.2.14, where the spectrum with fixed frequency is drawn in red and otherwise in blue. It is obvious that there are harmonic peaks in the spectrum as the switching frequency is fixed, resulting in severe EMI. As shown in Fig.2.14a, under periodic modulation, the harmonic peaks are spread, but still concentrated on certain frequency band. The harmonic peaks under CCFM (see Fig.2.14b) are further spread and become continuous, indicating that the spread-spectrum effect of chaotic modulation is much better than that of periodic modulation.

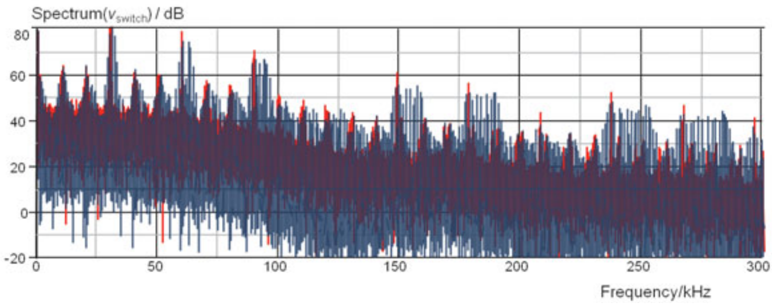

(a) Blue: periodic carrier frequency modulation, red: fixed frequency

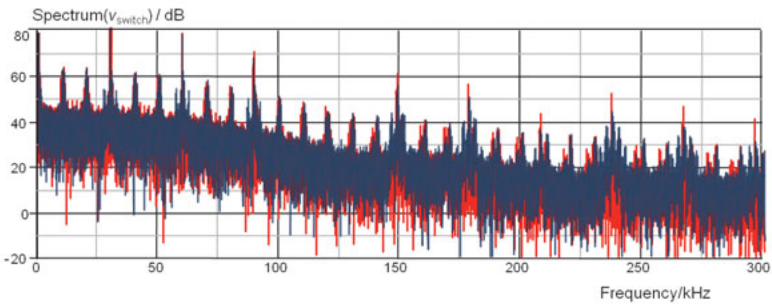

(b) Blue: chaotic carrier frequency modulation, red: fixed frequency

Figure. 2.14: Spectra of the switching voltage

The spectra of the switching voltage under chaotic modulation with various R_{I} are given by Fig.2.15, and Tab.2.1 shows the detailed reduction values of the harmonic peak. It is remarked that the harmonic peaks, especially those on the high-frequency band, are reduced more obviously with the decrease of R_{I}, resulting in EMI suppression.

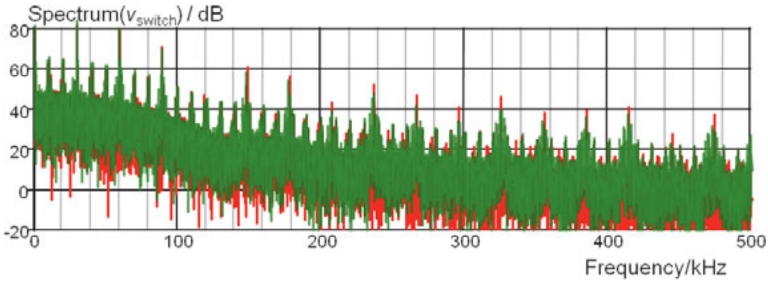

(a) $R_{\mathrm{I}} = 140\mathrm{k}\Omega$ (green: with CCFM, red: without CCFM)

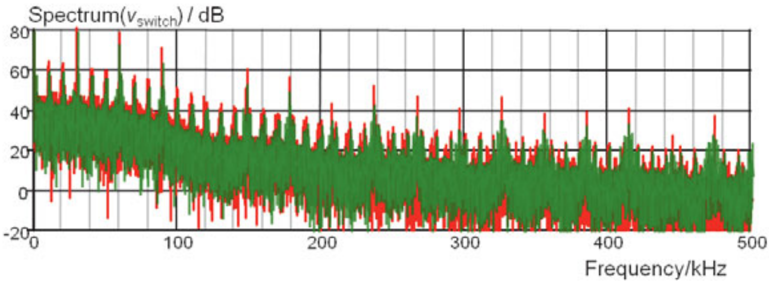

(b) $R_{\mathrm{I}} = 100\mathrm{k}\Omega$ (green: with CCFM, red: without CCFM)

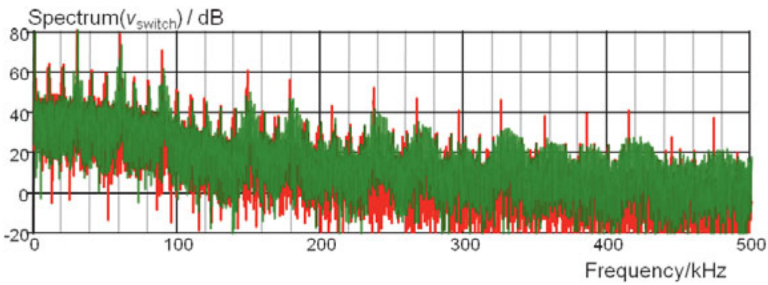

(c) $R_{\mathrm{I}} = 60\mathrm{k}\Omega$ (green: with CCFM, red: without CCFM)

Figure. 2.15: Spectra of the switching voltage driven by UC3842

Table 2.1: The harmonics peak reduction of the switching voltage driven by UC3842

Harmonic order		1	2	3	4	5	6	7	8	9	10
Reduction(dB)	$R_I = 140\text{k}\Omega$	0	1	2	3	3	5	5	8	7	8
	$R_I = 100\text{k}\Omega$	1	1	2	3	5	7	7	9	9	10
	$R_I = 60\text{k}\Omega$	2	6	8	2	10	10	6	11	12	13

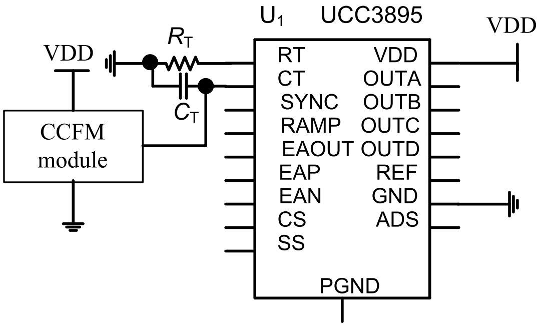

Figure. 2.16: The CCFM module used to drive UCC3895

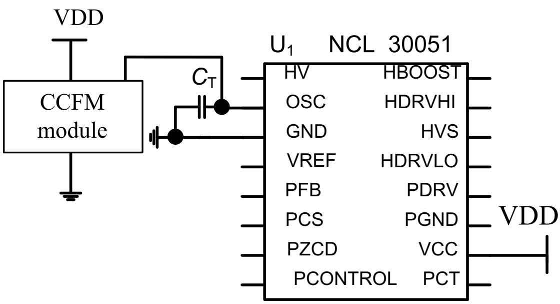

Figure. 2.17: The CCFM module used to drive NCL30051

2.4.2 Implementation of UCC3895 and NCL30001 based CCFM

The CCFM module can work on all the frequency programmable PWM ICs, which adopt the timing capacitor to set the oscillator frequency. For example, the module is used to drive UCC3895 [66], a phase-shift full bridge PWM IC, which makes use of a different oscillator from that of UC3842. As shown in Fig.2.16, for UCC3895, the timing capacitor C_T is charged by an internal current which is determined by a resistor connected with the RT pin. As the CCFM module is linked to C_T, both the internal current and the extra chaotic current charge the capacitor, so that the switching frequency is modulated chaotically. Further more, the modulation range of the switching frequency can be set by adjusting the current limiting resistor R_I. The spectra of the switching voltage under CCFM with various values of R_I are given by Fig.2.18, and the reduction of the harmonic peak is given by Tab.2.2. The simulations show that the module is effective to reduce EMI of the UCC3895-based SMPS.

Table 2.2: The harmonics peak reduction of the switch voltage driven by UCC3895

Harmonic order		1	2	3	4	5	6	7	8	9	10
Reduction (dB)	$R_I = 200k\Omega$	0	1	1	0	1	1	1	1	2	2
	$R_I = 150k\Omega$	0	1	0	1	1	2	3	4	5	6
	$R_I = 80k\Omega$	0	2	3	7	9	12	13	15	14	17

Table 2.3: The harmonics peak reduction of the switch voltage driven by NCL30051

Harmonic order		1	2	3	4	5	6	7	8	9	10
Reduction (dB)	$R_I = 200k\Omega$	0	0	0	0	2	3	4	4	4	4
	$R_I = 150k\Omega$	0	2	1	4	6	7	8	8	7	7
	$R_I = 80k\Omega$	1	4	6	6	10	10	12	12	12	12

As another example, the module is employed to drive NCL30051 [64] (see Fig.2.17), which uses only one timing capacitor to set the switching frequency. The spectra of the switching voltage and the reduction of the harmonic peak, provided in Fig.2.18 and Tab.2.2, vertify that the proposed module can work on various PWM ICs to reduce EMI.

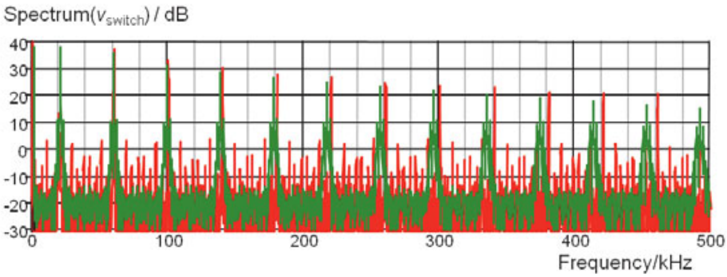

(a) $R_I = 200\text{k}\Omega$ (green: with CCFM, red: without CCFM)

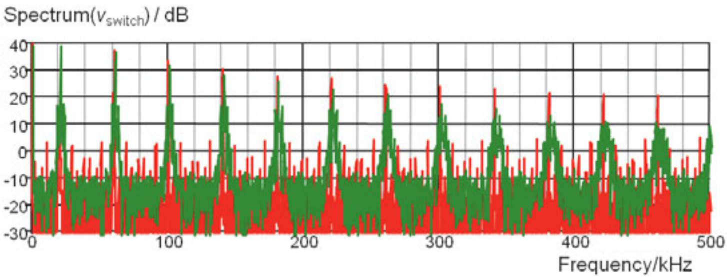

(b) $R_I = 150\text{k}\Omega$ (green: with CCFM, red: without CCFM)

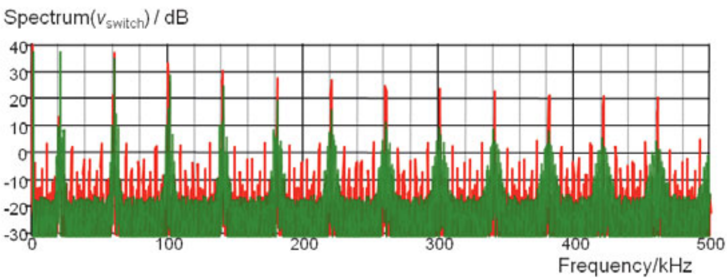

(c) $R_I = 80\text{k}\Omega$ (green: with CCFM, red: without CCFM)

Figure. 2.18: Spectra of the switching voltage driven by UCC3895

2.5 Summary

This chapter is concerned with a chaotic modulation module, which works on standard PWM IC to implement CCFM on commercial SMPSs. The module, containing three connection ports, is composed of the standard components. It can set the switching frequency modulation range with an adjustable resistor, and is suit to all the frequency programmable PWM ICs. In terms of the simulations, the CCFM module is effective to spread the spectrum of the switching voltage of SMPS. As a result, the module, with the features of low cost, low circuit complexity, flexibility and universality, can be well applied in real products for EMI suppression.

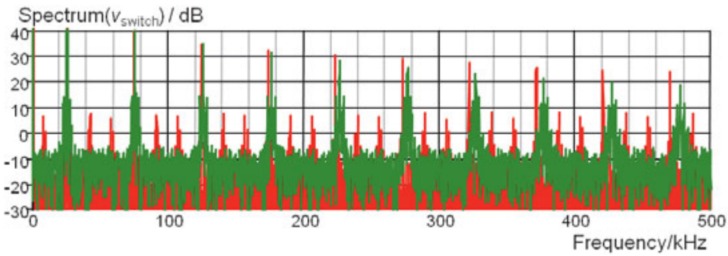

(a) $R_{\mathrm{I}} = 200\mathrm{k}\Omega$ (green: with CCFM, red: without CCFM)

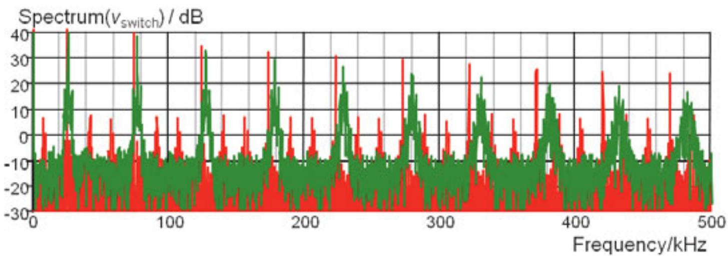

(b) $R_{\mathrm{I}} = 150\mathrm{k}\Omega$ (green: with CCFM, red: without CCFM)

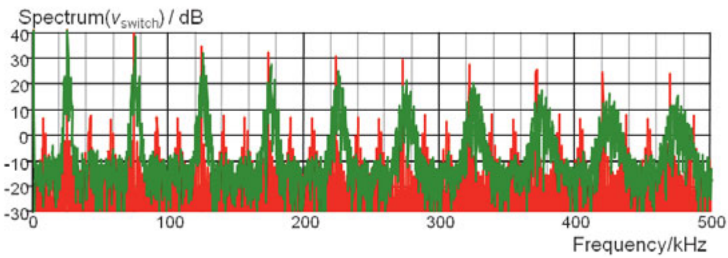

(c) $R_{\mathrm{I}} = 80\mathrm{k}\Omega$ (green: with CCFM, red: without CCFM)

Figure. 2.19: Spectra of the switching voltage driven by NCL30051

3 Power Spectral Characteristics of CCFM-based Switching Converters

Since EMI can be estimated by measuring the PSD of the switching signal in the converter, the power spectral characteristics of the chaotic frequency PWM signal will be studied in this chapter to investigate the effectiveness of the proposed CCFM module on EMI suppression of SMPS. As a result, it is revealed that the effectiveness of EMI reduction depends on the PDF and the randomness, called modulation degree, of the switching period, which both can be set by adjusting certain parameters of the module.

3.1 Introduction

The power spectral density describes how the power of a signal or time series is distributed with frequency [4], so that PSD of the PWM signal (namely the switching sequence or pulse) that controls the switching actions of the transistor of power supplies, can be used to estimate EMI of SMPS [67].

The power spectral characteristics of the CCFM-based switching converter has been studied in [18, 43, 55, 68, 69], which were normally based on the basic theoretical analysis for the randomized controlled switching converter described in [67]. Based on the previous research, the mathematical analysis on the PSD of switching pulses will be carried out to verify the effectiveness of the designed module on EMI reduction.

Firstly, the probability density function (PDF) of the chaotically changed switching period will be discussed in detail. It is found that the modulated switching period follows different probability distributions, when Chua's circuit operates in various state. Secondly, by analyzing the power spectral characteristics of the CCFM-based switching signal, it is revealed that the modulation degree and PDF of the switching period determine the effectiveness of chaotic modulation on EMI suppression. Coincided with the calculation results, the simulations show that increasing the modulation degree or using the uniform distribution will improve the effectiveness of EMI reduction. The study in this chapter provides a guideline for the product design and can be used to optimize the circuit parameters of the CCFM module.

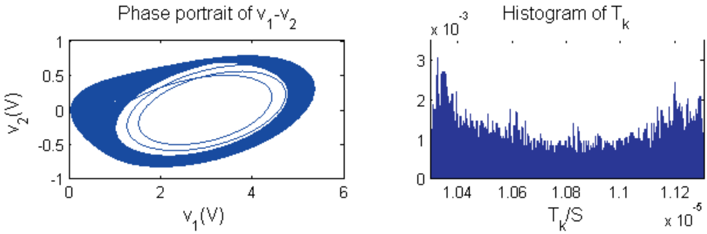

(a) $R = 1.988\text{k}\Omega$

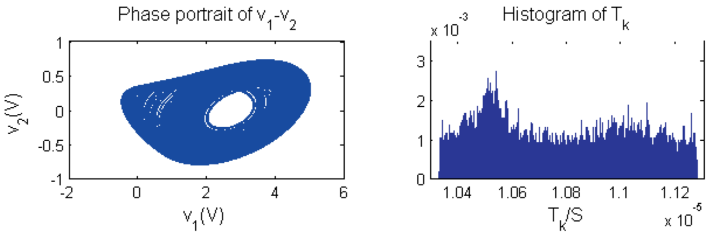

(b) $R = 1.978\text{k}\Omega$

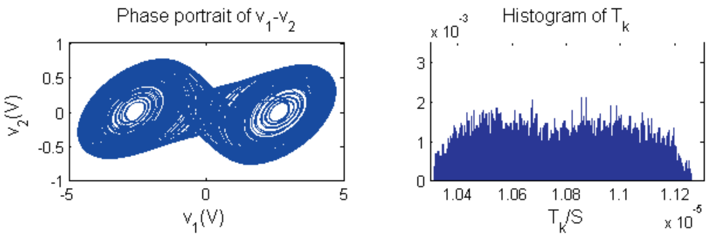

(c) $R = 1.95\text{k}\Omega$

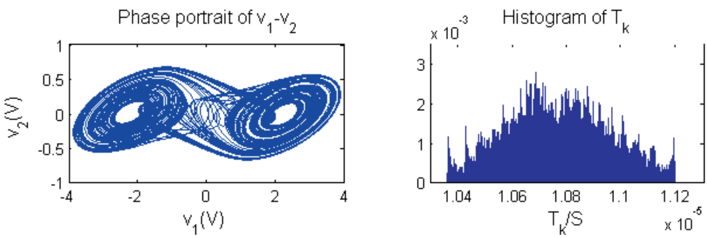

(d) $R = 1.80\text{k}\Omega$

Figure. 3.1: Histogram of the switching period

3.2 Statistical Characteristics of Switching Period

In [18, 43, 70], the chaotic signal generated by Chua's circuit was used to modulate the switching period, which was treated as a triangular distributed stochastic variable. However, it is observed that the switching period obeys different distributions, when Chua's circuit works under different conditions.

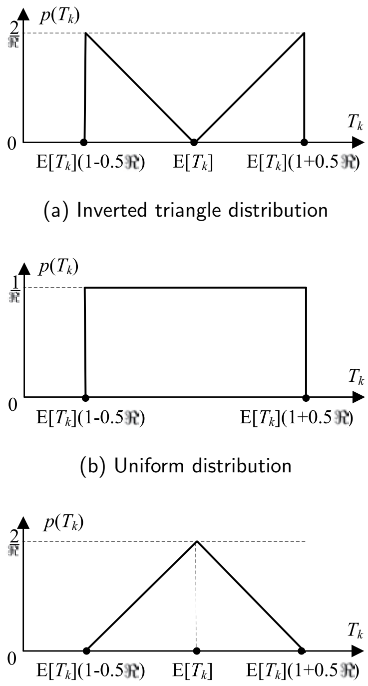

(c) Triangle distribution

Figure. 3.2: Probability distributions of the switching period

As the CCFM module discussed in Chapter 2 is employed to modulate the switching frequency, the statistical histograms of the k-th switching period T_k with different values of R (see Fig.2.6) are illustrated as Fig.3.1. As $R = 1.988\text{k}\Omega$, the values are distributed on the both sides. With the decrease of R, the values are gradually distributed towards the mean value. In this dissertation, T_k is regarded to follow the inverted triangle, the uniform and the triangle distribution, respectively.

Therefore, the PDFs of T_k, called $p(T_k)$, are illustrated Fig.3.2a, Fig.3.2b and Fig.3.2c, where $E[\bullet]$ is the expectation operator, and the maximum of T_k, namely $\mathrm{T_{max}}$, is expressed as $E[T_k](1+\Re)$, and the minimum of T_k, namely $\mathrm{T_{min}}$, is expressed as $E[T_k](1-\Re)$. Here, to study the effect of the variation range of T_k on the spread-spectrum performance, $\Re$, which is equal to $\frac{\mathrm{T_{max}}-\mathrm{T_{min}}}{E[T_k]}$, is defined as the modulation degree (called the randomness in [43]) of T_k. As T_k obeys inverted triangle distribution,

$$p(T_k)=\begin{cases} |\frac{4}{\Re^2}(T_k-E[T_k])|, & E[T_k](1-0.5\Re)\leqslant T_k\leqslant E[T_k](1+0.5\Re),\\ 0, & \text{otherwise.}\end{cases} \tag{3.1}$$

While T_k follows uniform distribution,

$$p(T_k)=\begin{cases} \frac{1}{\Re E[T_k]}, & E[T_k](1-0.5\Re)\leqslant T_k\leqslant E[T_k](1+0.5\Re),\\ 0, & \text{otherwise.}\end{cases} \tag{3.2}$$

As T_k obeys triangle distribution,

$$p(T_k)=\begin{cases} |\frac{4}{\Re^2}(T_k-E[T_k]+0.5\Re)|, & E[T_k](1-0.5\Re)\leqslant T_k\leqslant E[T_k](1+0.5\Re),\\ 0, & \text{otherwise.}\end{cases} \tag{3.3}$$

As using the designed CCFM module (Fig.2.11) to modulate switching period, its modulation degree is adjustable, because the variation range of the switching period can be set by R_I (see Equ.(2.9)). Hence, $\Re$ can be expressed as

$$\Re = 2\frac{T_k(v_{\min},R_{\mathrm{I}})-T_k(v_{\max},R_{\mathrm{I}})}{T_k(v_{\min},R_{\mathrm{I}})+T_k(v_{\max},R_{\mathrm{I}})}. \tag{3.4}$$

Furthermore, $\Re$ vs R_{I} can be described as Fig.3.3.

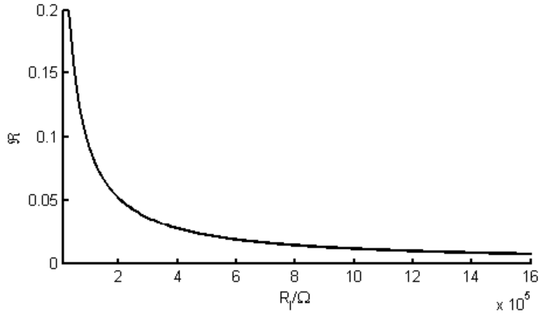

Figure. 3.3: $\Re$ vs R_{I}

3.3 Power Spectrum of Switching Signal with Chaotic Frequency

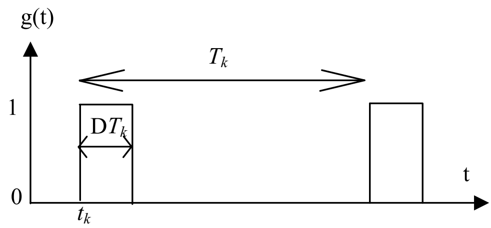

Figure. 3.4: Switching function

Fig.3.4 shows the waveform of the switching function $g(t)$. $g(t)$ has two discrete levels, which is 1 as the switch is on, and 0 as the switch is off. The k-th switching cycle $g_k(t - t_k)$ can be expressed as

$$g_k(t - t_k) = \begin{cases} 1, & t_k \leqslant t \leqslant \mathrm{D}T_k + t_k, \\ 0, & \text{otherwise}, \end{cases} \tag{3.5}$$

where D is the duty cycle, $\mathrm{D}T_k$ is the duration of on-state, and t_k is the beginning time of the k-th switching period.

Hence, $g(t)$ can be expressed as

$$g(t) = \lim_{N\to\infty} \sum_{k=1}^{N} g_k(t - t_k). \tag{3.6}$$

Then, the autocorrelation of $g(t)$ [43] is defined as

$$R_g(\tau) = E\left[\lim_{T\to\infty} \frac{1}{T} \int_0^T g(t)g(t+\tau)dt\right]. \tag{3.7}$$

By using Wiener-Khintchine theorem [71], the PSD of $g(t)$, namely $S_g(f)$, is the fourier transform of its autocorrelation, so it can be expressed by

$$S_g(f) = \int_{-\infty}^{\infty} R_g(\tau)e^{-j2\pi f\tau}d\tau. \tag{3.8}$$

To follow the methodology in [72–74], as $Re(\bullet)$ is the real part of the operation and $(\bullet)^*$ is the complex conjugate of the operation, $S_g(f)$ can be described as

$$S_g(f) = \frac{1}{E\left[T_k\right]}\left\{E\left[|G(f)|^2\right] + 2Re\left(\frac{E\left[G(f)e^{j2\pi f T_k}\right]E\left[G^*(f)\right]}{1 - E\left[e^{j2\pi f T_k}\right]}\right)\right\}, \tag{3.9}$$

where

$$G(f) = \int_0^{DT_k} e^{-j2\pi f t}dt = \frac{j}{\pi f}(e^{-j2\pi f DT_k} - 1). \tag{3.10}$$

For the simplification of the calculation, it is assumed that D$E\left[T_k\right]$ is constant and $E\left[T_k\right] = 1$, and then $G(f)$ [75] can be rewritten as

$$G(f) = \int_0^{\mathrm{D}} e^{-j2\pi f t}dt = \frac{j}{2\pi f}(e^{-j2\pi f\mathrm{D}} - 1). \tag{3.11}$$

As $P(f) = \int_{1-\frac{\Re}{2}}^{1+\frac{\Re}{2}} p(T_k)e^{j2\pi f T_k}dT_k$, $S_g(f)$ can be rewritten as

$$S_g(f) = \frac{sin^2(\pi f\mathrm{D})}{(\pi f)^2}\left[1 + 2Re(\frac{P(f)}{1 - P(f)})\right]. \tag{3.12}$$

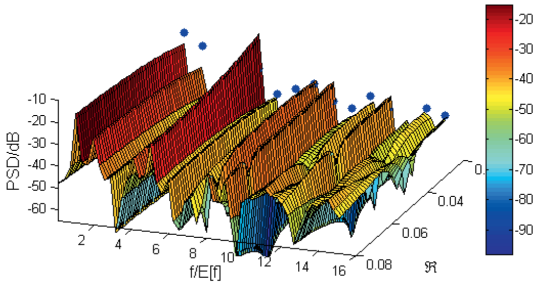

(a) Inverted triangle distribution

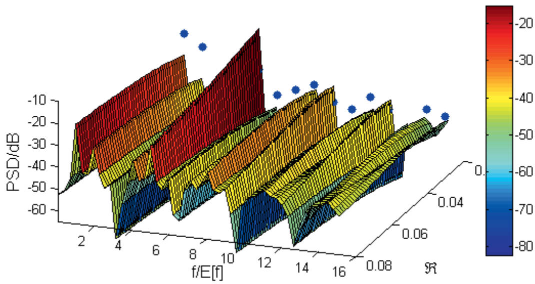

(b) Uniform distribution

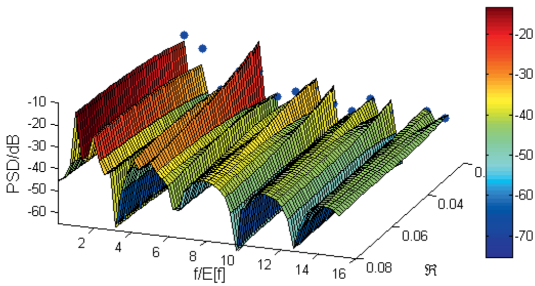

(c) Triangle distribution

Figure. 3.5: PSDs of chaotic frequency PWM signal

3.4 Evaluation of EMI Reduction

According to Equ.(3.12), it is remarked that $S_g(f)$ is determined by $P(f)$, which is related to the PDF and the modulation degree of the switching period.

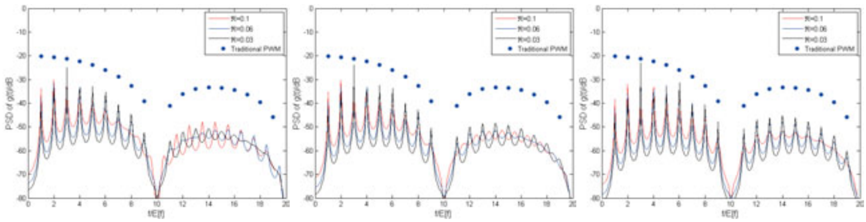

(a) Inverted triangle distribution, D = 0.1 (b) Uniform distribution, D = 0.1 (c) Triangle distribution, D = 0.1

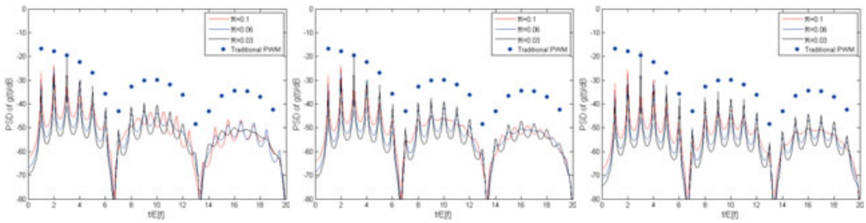

(d) Inverted triangle distribution, D = 0.15 (e) Uniform distribution, D = 0.15 (f) Triangle distribution, D = 0.15

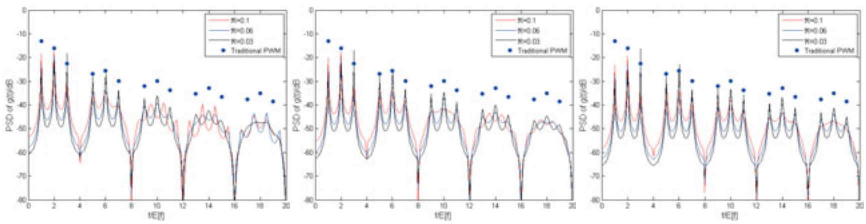

(g) Inverted triangle distribution, D = 0.25 (h) Uniform distribution, D = 0.25 (i) Triangle distribution, D = 0.25

Figure. 3.6: PSDs of chaotic frequency PWM signal

3.4.1 Effect of Switching Period's Modulation Degree on EMI Reduction

Fig.3.5 shows the calculated PSDs of $g(t)$, as T_k obeys different distributions with various modulation degree. Under the traditional PWM, there are power spectrum peaks (the blue point) at the switching frequency and its multiplications, resulting in a discrete spectrum. Those peaks, becoming continuous, are spread over a wide frequency band under CCFM.

The detailed PSDs of $g(t)$ with $\Re$ are given by Fig.3.6. It is obvious that the reduction of spectrum peak becomes larger and larger as $\Re$ increases. However, it is not right to set a large randomness in practice, because the large randomness leads to the large output ripple [18].

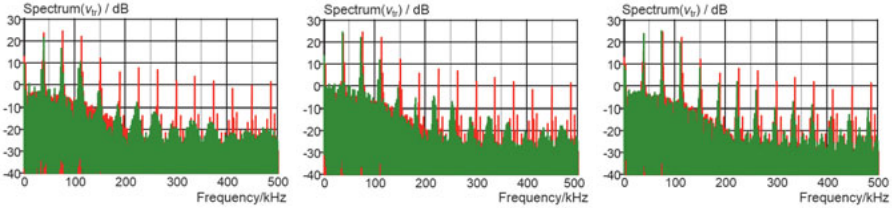

(a) Inverted triangle distribution, $\Re = 0.1$
(b) Inverted triangle distribution, $\Re = 0.06$
(c) Inverted triangle distribution, $\Re = 0.03$

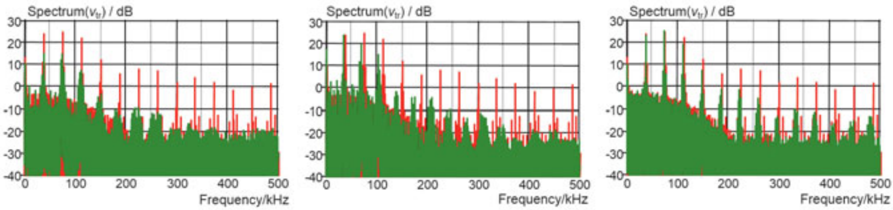

(d) Uniform distribution, $\Re = 0.1$
(e) Uniform distribution, $\Re = 0.06$
(f) Uniform distribution, $\Re = 0.03$

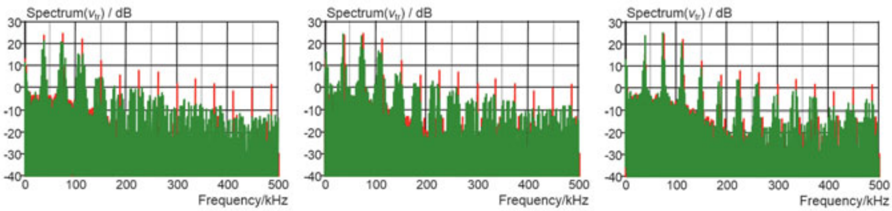

(g) Triangle distribution, $\Re = 0.1$
(h) Triangle distribution, $\Re = 0.06$
(i) Triangle distribution, $\Re = 0.03$

Figure. 3.7: As D = 0.1, spectra of the switching voltage (green: with CCFM, red: without CCFM)

3.4.2 Effect of Switching Period's PDF on EMI Reduction

As T_k obeys the triangle distribution, the effectiveness of EMI reduction is worst. The overall effects under uniform distribution and under inverted triangle distribution are equal roughly. However, there are extra power spectrum ledges on the high frequency band under inverted triangle distribution, resulting in a poorer result compared with that under uniform distribution.

3.5 Simulations

A flyback converter controlled by UC3842 is used as the test bed, and its switching period is modulated by the CCFM module. The spectra of the switching voltage are given by Fig.3.7 ($D = 0.1$) and Fig.3.8 ($D = 0.25$), and the reduction of the harmonic peak is shown in Tab.3.1. To make a comparison, the spectrum under the traditional PWM is drawn in red, and the spectrum under CCFM in green. The reduction of the harmonic peak becomes larger with the increase of the modulation degree of the switching period. The best effect of EMI suppression is achieved as using the uniform distribution, while the worst is obtained as the switching period follows the triangle distribution. The simulation results accord with the mathematical analysis in substance.

Table 3.1: The harmonics peak reduction of the switching voltage

Harmonic order	$D = 0.1, \Re =$									$D = 0.25, \Re =$								
	Inverted triangle distribution			Uniform distribution			Triangle distribution			Inverted triangle distribution			Uniform distribution			Triangle distribution		
	0.03	0.06	0.1	0.03	0.06	0.1	0.03	0.06	0.1	0.03	0.06	0.1	0.03	0.06	0.1	0.03	0.06	0.1
1	0	-1	2	1	0	7	0	-1	2	1	1	2	3	2	2	0	0	-2
2	-1	2	7	-1	5	10	-1	-1	3	0	0	3	0	0	5	0	0	0
3	2	10	12	2	7	13	2	1	6	2	3	1	3	3	2	0	0	-2
4	3	12	14	4	14	15	3	4	8	2	5	12	3	10	12	1	2	1
5	4	10	15	7	12	16	3	4	8	3	0	3	3	0	2	-2	1	0
6	6	12	16	9	13	18	4	3	8	2	9	14	5	11	15	1	5	4
7	8	13	19	12	17	19	4	5	10	2	0	5	3	2	7	0	2	0
8	11	14	20	14	15	20	4	7	11	5	12	18	12	14	20	4	8	5
9	11	16	19	13	16	20	4	8	11	1	3	7	4	0	6	0	4	0
10	12	17	18	13	19	20	5	8	10	9	11	18	13	14	19	4	10	8

3.6 Summary

By analyzing the power spectral characteristics of the CCFM-based switching converter, it is found that the effectiveness of chaotic modualtion on EMI reduction is related to the PDF and the modulation degree of the switching period. According to the calculations and simulations, a superior effectiveness of EMI reduction is obtained by increasing the modulation degree and using the uniform distribution. As the module proposed in Chapter 2 is used to modulate the switching frequency, both the PDF and the modulation degree of the switching period are adjustable via certain circuit parameters. Above all, the mathematic analysis, by which EMI reduction effect can be estimated and improved, provides a guideline for the design of the practical CCFM module.

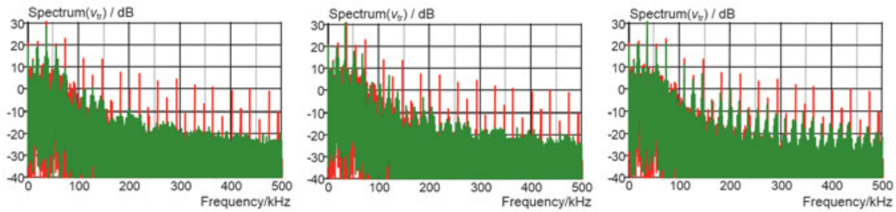

(a) Inverted triangle distribution, $\Re = 0.1$ (b) Inverted triangle distribution, $\Re = 0.06$ (c) Inverted triangle distribution, $\Re = 0.03$

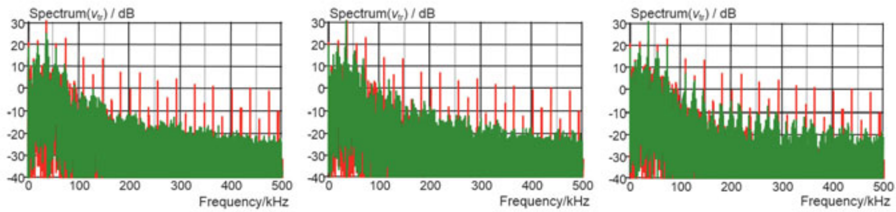

(d) Uniform distribution, $\Re = 0.1$ (e) Uniform distribution, $\Re = 0.06$ (f) Uniform distribution, $\Re = 0.03$

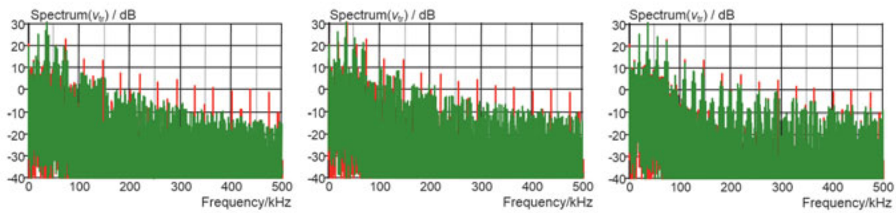

(g) Triangle distribution, $\Re = 0.1$ (h) Triangle distribution, $\Re = 0.06$ (i) Triangle distribution, $\Re = 0.03$

Figure. 3.8: As D = 0.25, spectra of the switching voltage (green: with CCFM, red: without CCFM)

4 Application of CCFM in LED Drivers

The commercial SMPS has to meet some basic requirements, which include 1) providing stable voltage or current for the output load, 2) satisfying EMC standards and 3) still operating stably after a long time of work. Until now, a lot of experimental research has been done on 1) and 2). Nevertheless, few work was done on 3) to investigate the impact of CCFM on the operating condition of the whole system. Therefore, to investigate the influence of the CCFM module on the whole system performance, the tests on the electrical characteristic, working condition and EMC performance of SMPS are carried out in this chapter. The experimental research verifies that the application of chaotic modulation in SMPS can reduce EMI without weakening the system performance.

4.1 Introduction

A lot of experimental research has been done to study the effect of chaotic modulation on the performance of SMPS. For example, the spectra of the switching voltage [25, 76, 77] and the conducted interference [51] with and without CCFM are compared to verify the effectiveness of chaotic modulation on EMI reduction. Furthermore, the comparison of the output voltage ripple with and without CCFM, which has been done in [40, 55, 56], indicates that the output ripple is increased slightly by chaotic modulation. More measurements, including the output characteristics, conducted interference, and input output power efficiency have been made in [45], which show that chaotic modulation technique is not only effective to suppress EMI but also of little influence on the overall electrical characteristics of the system.

However, whether chaotic modulation affects the operating condition of the system or not remains a question. The working condition of power supply is determined by the key elements, namely the transistor and the high-frequency transformer, which usually heat up as operating. Once their temperatures exceed the safe range, they may be out of order, resulting in a breakdown system. Hence, it is necessary to make the thermal test of the key elements, which has never been done before.

In this chapter, the feasibility of applying CCFM in SMPS will be investigated. The CCFM module is manufactured and applied in two typical LED drivers, CCM IC (UC3842) controlled flyback converter (20W) and VCM IC (TL494) controlled push-pull converter (150W). The tests on EMC, electrical characteristics and working condition will be done on the two power supplies, respectively.

According to the experimental research, the application of the CCFM module is effective to reduce the conducted interference and of little impact on the overall performance of power supplies. The experiments are significant for the marketization of the proposed module.

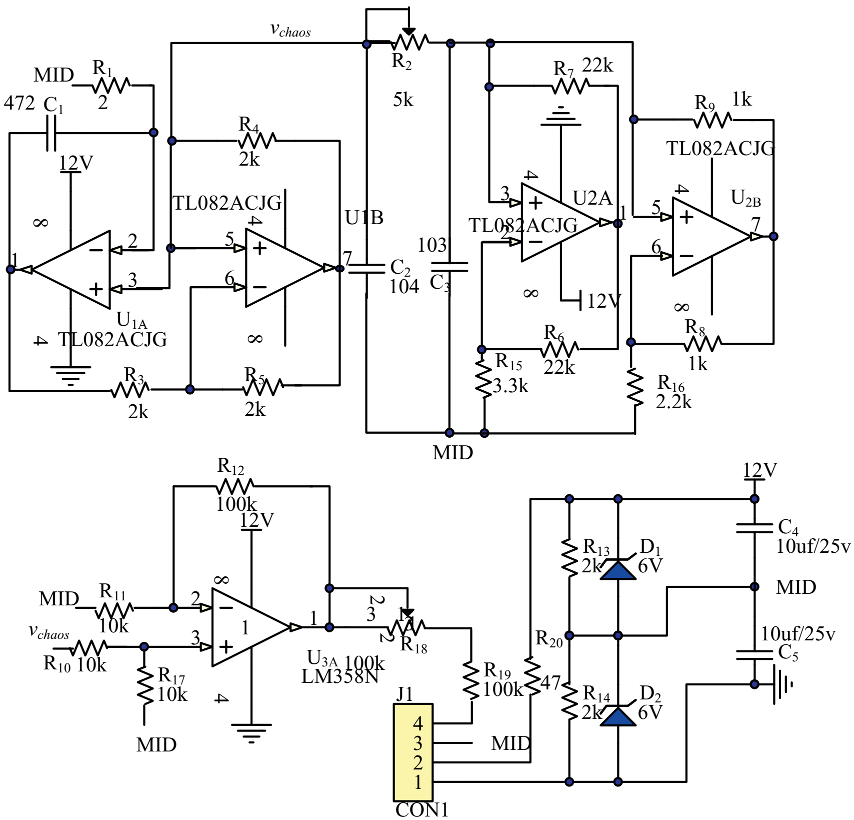

Figure. 4.1: The schematic of chaotic carrier frequency modulation module

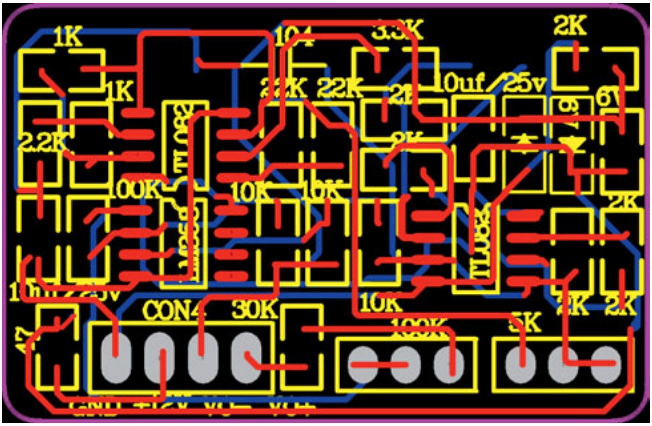

Figure. 4.2: Printed circuit board (PCB) diagram of the CCFM module

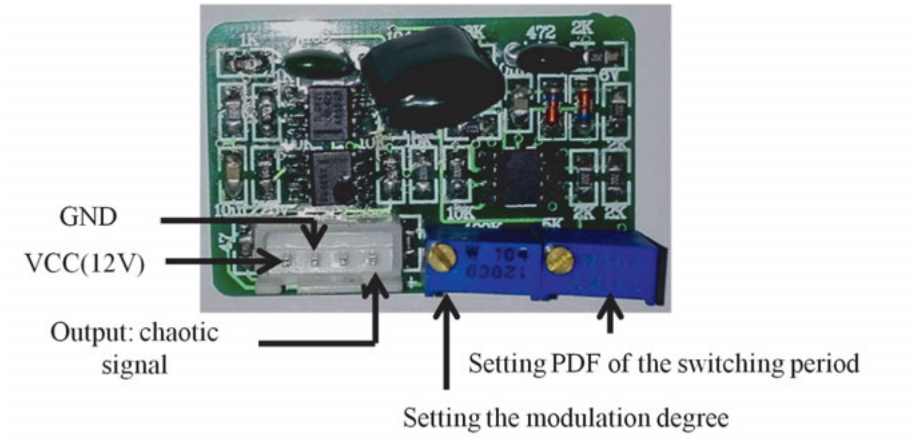

Figure. 4.3: The entity of the CCFM module

4.2 Implementation of CCFM Module

The schematic of the CCFM module is given by Fig.4.1, where the inductor in Chua's circuit is replaced by the circuit composed of C_1, R_1, R_3, R_4, R_5, U_{1B} and U_{1A}. Therein, CON1, the interface connected to PWM IC, has three pins, which are the power supply input port (the pin 1), ground port (the pin 2) and the pin 3 providing the chaotic charging current for the timing capacitor. Then, the printed circuit board (PCB), which is only 2.5cm long and 3.5cm wide, is designed as Fig.4.2. As shown in Fig.4.3, the entity circuit is composed of the standard components, and makes use of two adjustable resistors to set the modulation degree and the PDF of the switching frequency.

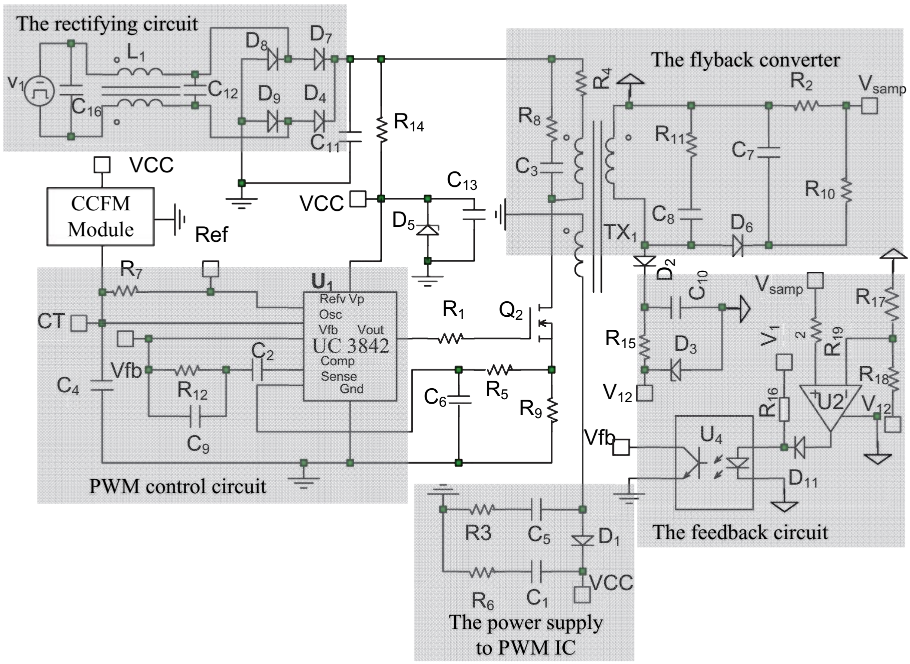

Figure. 4.4: The schematic of the flyback converter based LED driver

4.3 Flyback Converter-Based LED Driver

4.3.1 Working Principle

Due to the feature of low cost, the flyback converter is a mostly used choice in medium-low power (no more than 100W) supplies, so that a flyback based LED driver is chosen as an example. The LED driver, supplied by AC power of 220V and 50Hz, is a constant current source, of which the output current is 1A and the maximum rated power is 20W.

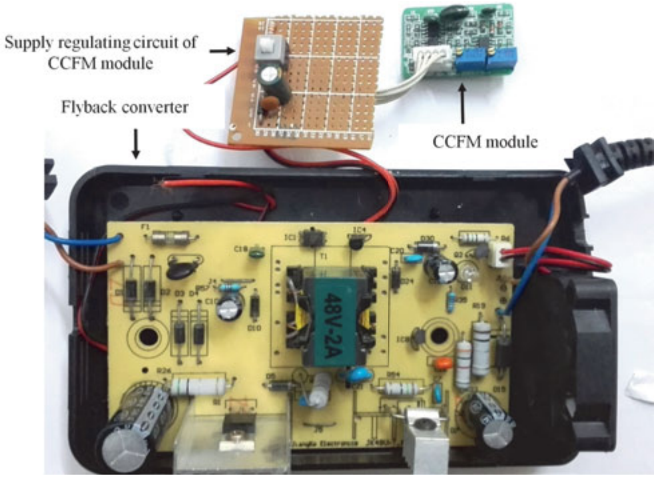

Figure. 4.5: The entity of the flyback converter based LED driver with CCFM

Figure. 4.6: Test environment

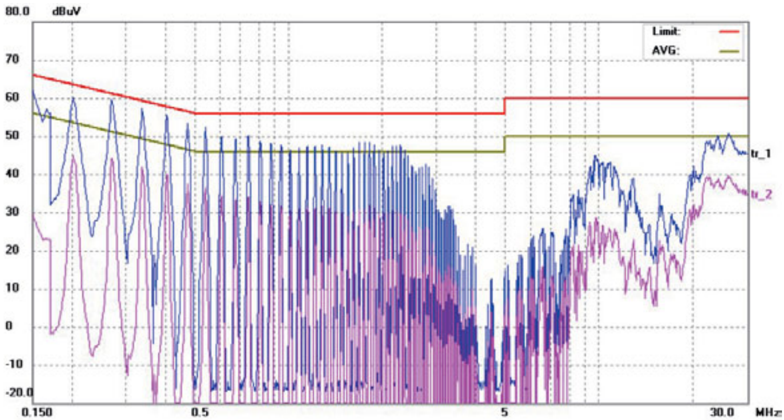

(a) Without CCFM

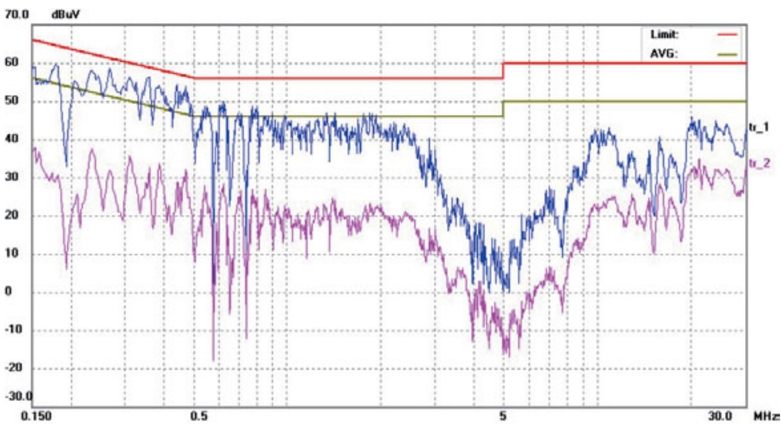

(b) With CCFM

Figure. 4.7: The EMI measurement results (blue: the peak value, pink: the average)

As shown in Fig.4.4, the rectifying circuit converts the alternating current (AC) input power to the direct current (DC) voltage of about 300V, which is periodically conducted to the primary side of TX_1. When the transistor Q_2 is turned on by PWM control circuit, the primary of the transformer is directly connected to the input voltage source. The primary current and magnetic flux in the transformer increase, storing energy in the transformer. The voltage induced in the secondary winding is negative, so the diode D_6 with a reverse voltage is off, and thus the capacitor C_7 supplies energy to the load. When the transistor is turned off, the primary current and magnetic flux drop. The secondary voltage is positive, turning on D_6, allowing current to flow from the transformer. The energy through the transformer core recharges C_7 and supplies the load. The output current is sampled, processed, sent to the PWM IC (UC3842) by the feedback circuit, and regulated to keep constant.

The CCFM module is attached to the LED driver, and the entity circuit is shown in Fig.4.5. Once a simple power processing circuit is attached to the module for its stable power supplying, CCFM is implemented. What follows is to investigate the influence of chaotic modualtion to electrical characteristics, EMC and the key elements working temperature of the LED driver. Except the EMC test which should be done in specific situation, the tests are done in the environment shown in Fig.4.6, a imitation of the real work environment.

4.3.2 EMI Test

The conducted interference of the LED driver is tested with Rohde&Schwarz instrument according to the standard of CISPR PUB.22 CLASS B. As shown in Fig.4.7, the upper red line is the quasi-peak (QP) limiting curve, and the green is the average value (AV) limiting curve.

By comparing Fig.4.7a with Fig.4.7b, it is obvious that both QP and AV peaks existing under the traditional PWM control are spread by chaotic modulation.

4.3.3 Electrical Characteristics Measurements

Firstly, the basic requirement for power supply is to provide the stable output voltage or output current for the load, so that the output voltage ripple is measured. Owing to the utilization of the linear load, the voltage ripple measurement can replace the current one, and is tested as the power operates with the max rate output voltage of 20V. As the LED driver works under the traditional PWM control, the ripple is 68mV. The ripple with chaotic modulation, increasing slightly, is 97mV, 78mV and 69mV, when R_I is 100kΩ, 150kΩ and 200kΩ, respectively. The ripple increment becomes larger as the modulation degree (R_I) decreases, but is still acceptable.

Secondly, the waveform and the spectrum of the switching voltage are tested. On one hand, the transistor, working at the turned-off state, is needed to endure the huge switching voltage, which is not allowed to exceed the rating to make sure the transistor not damaged. Therefore, its waveform is measured to detect whether there is an overvoltage on the transistor or not. On the other hand, because the switching action of the transistor is the underlying cause of EMI, the spectrum of the switching voltage is measured to observe the spread-spectrum effectiveness of the CCFM module. Hence, as shown in Fig.4.8, there is no obvious distinction between the switching voltage waveform with fixed frequency and that with chaotic frequency. Its harmonics peaks existing under the traditional PWM control are spread by chaotic modulation, and the EMI suppression effect is improved with a smaller R_I.

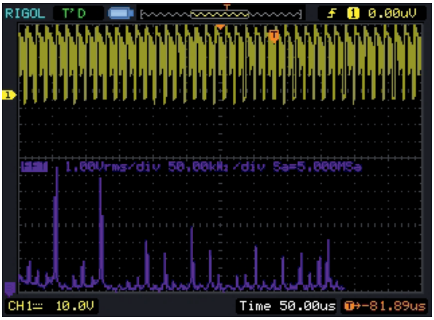

(a) Without CCFM

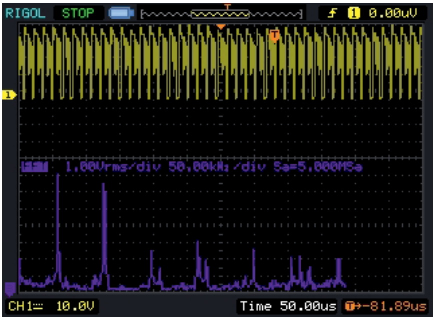

(b) With CCFM, $R_\mathrm{I} = 200\mathrm{k}\Omega$

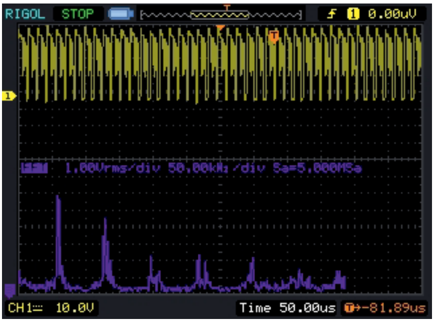

(c) With CCFM, $R_\mathrm{I} = 150\mathrm{k}\Omega$

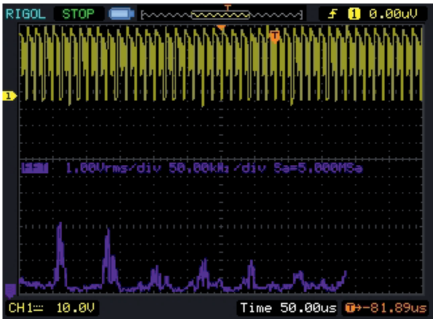

(d) With CCFM, $R_\mathrm{I} = 100\mathrm{k}\Omega$

Figure. 4.8: Waveforms and spectra of the switching voltage

Finally, the other indexes are given by Tab.4.1, while tests on CCFM-based power supply are carried out as $R_\mathrm{I} = 100\mathrm{k}\Omega$. The tests of the output stability indices, including input regulation rate, the load regulation rate and the output voltage star-up waveform, show that the power supply with CCFM can supply the load as stably as that without CCFM. The tests of power factor and the input and output power ratio are to survey the working efficiency of the SMPS. Because the LED driver supplies not only the original load but also the extra CCFM module, the supply's efficiency is impaired very slightly.

Table 4.1: The electrical characteristics measurments

Index	Parameter	Without CCFM			With CCFM		
The voltage regulation	Input voltage (V)	180	220	260	180	220	260
	Input current (A)	0.208	0.189	0.179	0.215	0.193	0.181
	Output voltage (V)	20	20	20	20	20	20
	Output current (A)	1	1	1	1	1	1
Power factor	Power factor	0.65	0.61	0.58	0.64	0.6	0.57
Efficiency (%)	Input Power (W)	24.8	25.4	26.5	25.1	25.6	26.8
	Output Power	20	20	20	20	20	20
	Efficiency (%)	80.6	78.7	75.4	79.7	78.1	74.6
Load regulation	Resistor load (Ω)	20	15	10	20	15	10
	Output current (A)	1	1	1	1	1	1
Start-up	Waveform of output voltage						

4.3.4 Test of Key Elements' Temperature

The transistor and high-frequency transformer, the necessary elements for SMPS, always work with a large current, resulting in the thermal problem. On one hand, the high-frequency transformer should work below 80°C, otherwise its saturation magnetic flux density falls to 70% of that at the normal temperature. It falls even more as the temperature increases, and thus the current and the power consumption of the transformer will rise sharply. Consequently, the overheat problem is exacerbated, resulting in a vicious circle, until the around elements are damaged by a huge current. On the other hand, the overheat of the transistor may impact the reliability of the switching action, leading to a breakdown system.

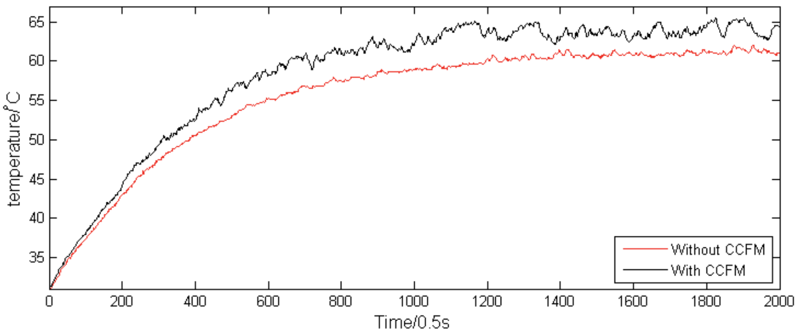

Figure. 4.9: The thermal curve of the transformer

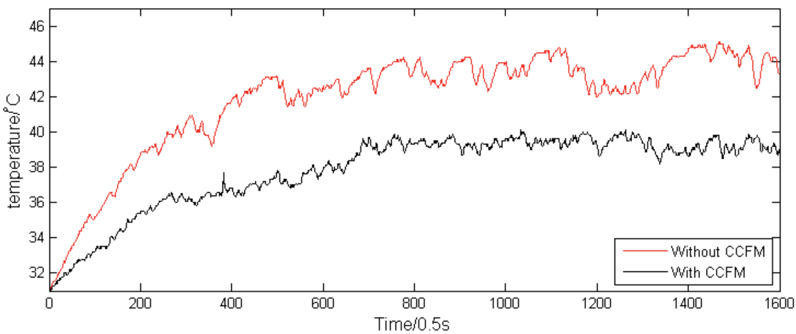

Figure. 4.10: The thermal curve of the transistor

Hence, it is necessary to perform thermal tests on the transistor and high-frequency transformer of SMPS. The thermal curves under the two situations given by Fig.4.9 show that the transformer's temperature under CCFM arises at a faster speed, and is about 4°C higher than that with fixed frequency. However, it is still within the safe range. As shown in Fig.4.10, the comparison of the transistor's thermal curves indicates that the transistor's temperature under CCFM is 4°C lower than that under the traditional PWM control.

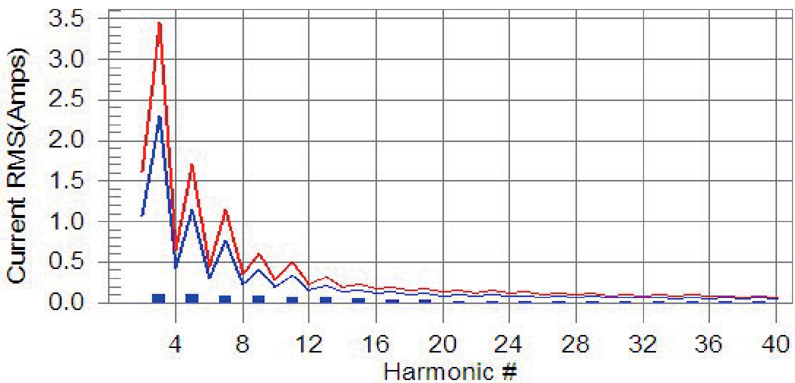

(a) Without CCFM

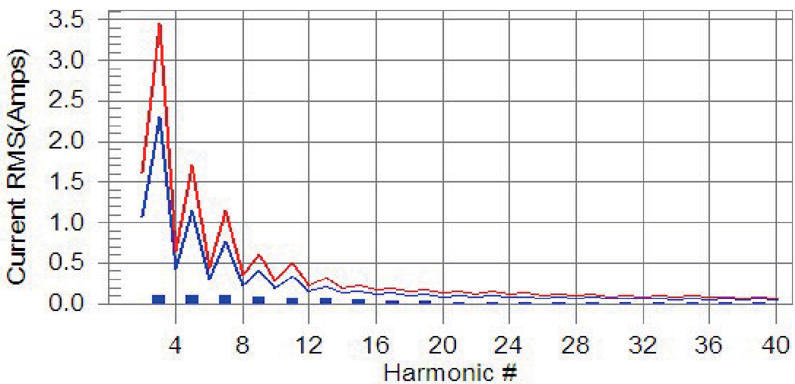

(b) With CCFM

Figure. 4.11: The measurement results of input current harmonic

4.3.5 Harmonics Current Measurement

The harmonic current of the electronic equipment may disturb the power grid, disorder the other devices on the grid, and even cause the grid overload and block the power transmission. Therefore, the standards, such as GB 17625.1 and IEC61000-3-2, are evolved to restrain the harmonic current. The harmonic current measurement is carried out, and the result under chaotic modulation (Fig.4.11b) is just as that under the traditional PWM control (Fig.4.11a).

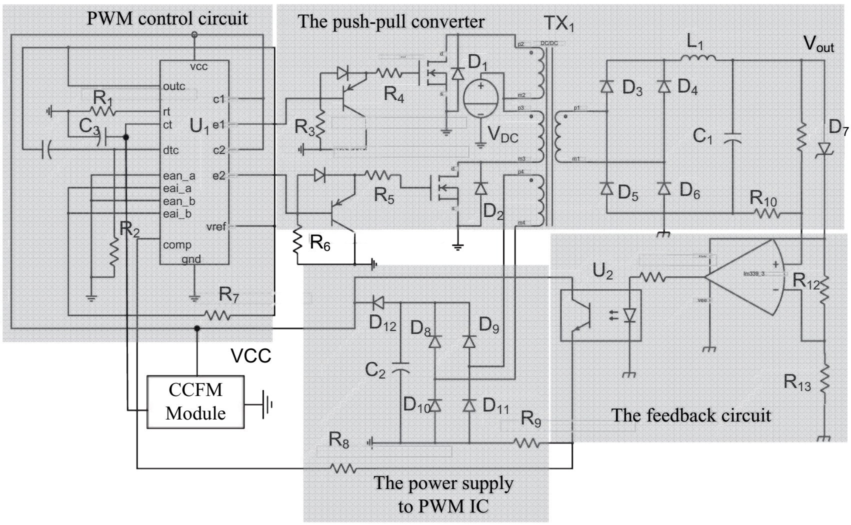

Figure. 4.12: The schematic of the push-pull converter based LED driver

4.4 Push-pull Converter-Based LED Driver

4.4.1 Working Principle

Because it is a good choice in the low voltage and large current situation, the push-pull topology is often applied in the high power (more than 100W) LED driver. Hence, a push-pull based LED driver is taken as the other example.

The LED drive, controlled by another typical PWM IC TL494, is also a constant current source, of which the output current is 3A and the maximum rated power is 150W. The schematic is shown in Fig.4.12. The transistors, Q_1 and Q_2, are alternately turned on and off, periodically reverse the current in the primary side of the transformer TX_1, and thus an AC voltage is coupled on the secondary side. Then, the voltage of the secondary side is rectified and filtered to the DC output voltage V_{out}. By the feedback circuit, the output current is regulated to keep constant.

The CCFM module is connected to the push-pull based LED driver, and the entity circuit is shown in Fig.4.13.

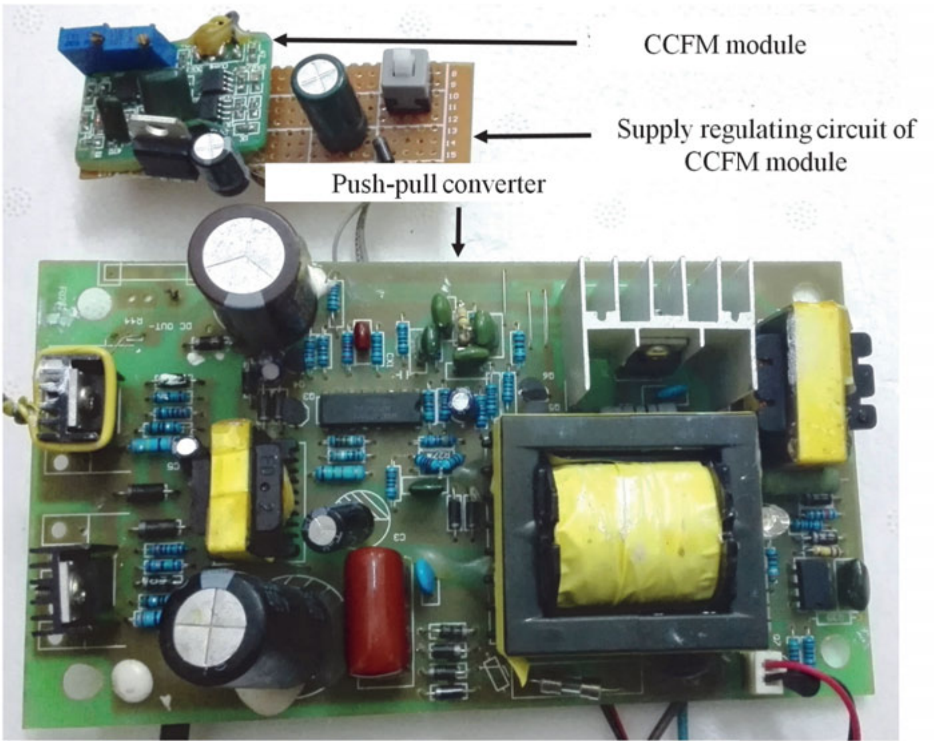

Figure. 4.13: The entity of the push-pull converter based LED driver with CCFM

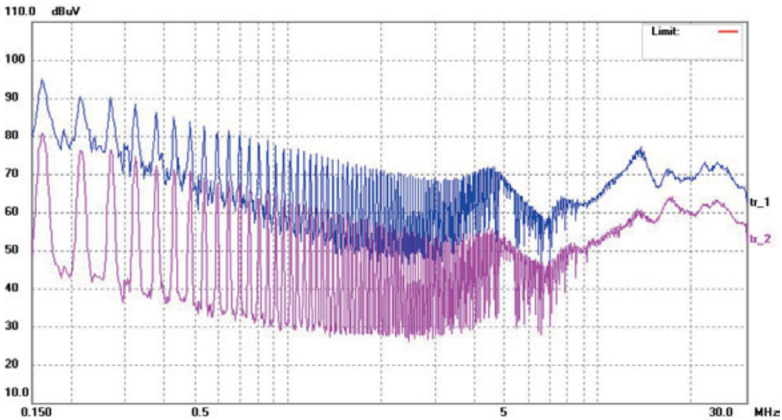

(a) Without CCFM

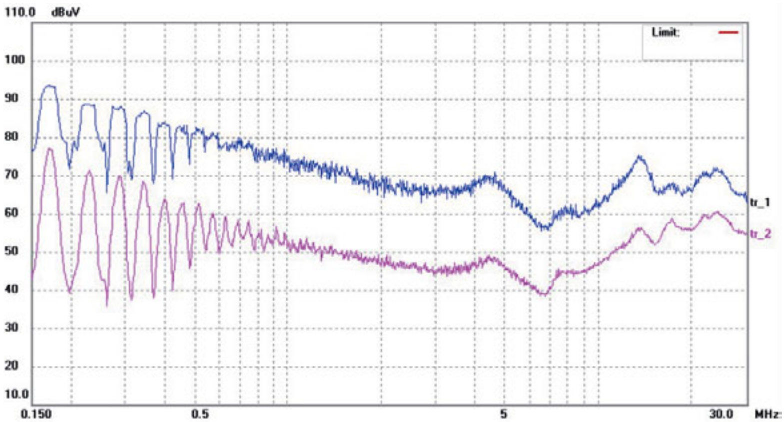

(b) With CCFM

Figure. 4.14: The EMI measurement results (blue: the peak value, pink: the average)

4.4.2 EMI Test

As shown in Fig.4.14, the conducted interference test under CCFM is much better than that under the traditional PWM control, just as same as the test result of the flyback converter based LED driver. It is verified that chaotic modulation is effective to reduce EMI of SMPS.

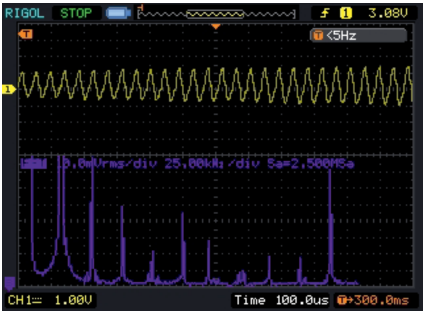

(a) Without CCFM

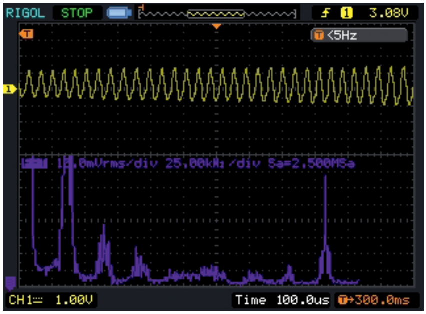

(b) With CCFM, $R_{\rm I} = 200\mathrm{k}\Omega$

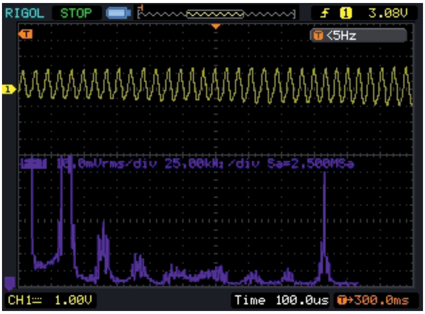

(c) With CCFM, $R_{\rm I} = 150\mathrm{k}\Omega$

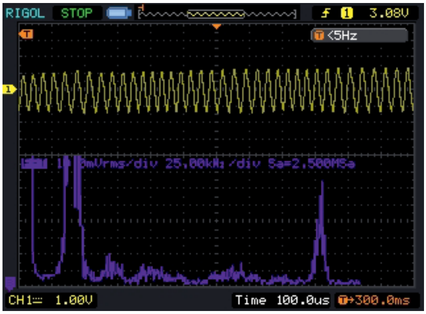

(d) With CCFM, $R_{\rm I} = 100\mathrm{k}\Omega$

Figure. 4.15: Waveforms and spectra of the switching voltage

4.4.3 Electrical Characteristics Measurements

The ripple of the output voltage is tested, when the power supply operates with the max rate output voltage of 48V. As the LED driver works with a fixed switching frequency, the ripple is 203mV. The ripple under chaotic modulation is 328mV, 225mV and 208mV, as $R_{\rm I}$ is 100kΩ, 150kΩ and 200kΩ respectively. With the increase of the modulation degree, the ripple becomes larger, but still within the acceptable range.

As shown in Fig.4.15, the switching voltage waveform with chaotic frequency is just as that with fixed frequency, and the peaks on the spectrum with fixed frequency are spread under chaotic modulation, and the EMI suppression effect is improved with a smaller $R_{\rm I}$.

Table 4.2: The electrical characteristics measurments

Index	Parameter	Without CCFM			With CCFM		
The voltage regulation	Input voltage (V)	180	220	260	180	220	260
	Input current (A)	1.45	1.27	1	1.51	1.2	1
	Output voltage (V)	48	48	48	48	48	48
	Output current (A)	3	3	3	3	3	3
Power factor	Power factor	0.61	0.58	0.64	0.6	0.61	0.63
Efficiency (%)	Input Power (W)	165	164	168	166	165	169
	Output Power	144	144	144	144	144	144
	Efficiency (%)	87.7	87.8	85.7	86.7	87.3	85.2
Load regulation	Resistor load (Ω)	16	10	4	16	10	4
	Output current (A)	3	3	3	3	3	3
Start-up	Waveform of output voltage						

The other electrical characteristics measurements are given by Tab.4.2. The only caveat is that a slight decrease of the efficiency of SMPS is caused by the utilization of the CCFM module.

4.4.4 Test of Key Elements' Temperature

As shown in Fig.4.16, the transformer's temperature under chaotic modulation is about 5°C higher than that under the traditional PWM control, but it does not affect the operation of the system. As illustrated in Fig.4.17, the transistor's temperature under chaotic modulation rises faster than that under the traditional PWM control, but there lies no difference in both cases as the working condition tends to be stable.

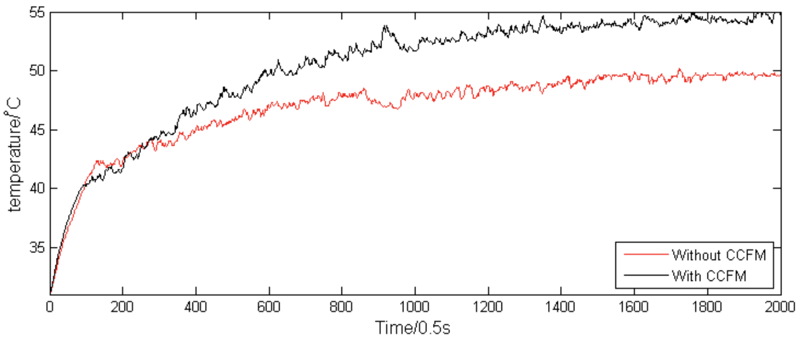

Figure. 4.16: The thermal curve of the transformer

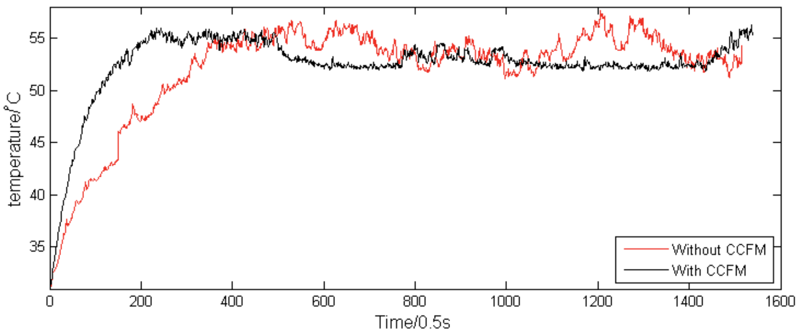

Figure. 4.17: The thermal curve of the transistor

4.4.5 Harmonics Current Measurement

The harmonic current measurements with and without CCFM, which are given by Fig.4.11, show that the application of CCFM does not impact the harmonic current, just as similar as that of the flyback-based supply.

4.5 Summary

To investigate the effect of chaotic modulation on the system performance, the CCFM module is applied in a flyback and a push-pull based LED drivers, and the tests of electrical characteristic, working condition and EMC performance are carried out.

First of all, the EMC test verifies that chaotic modulation is effective to reduce EMI of SPMS. Secondly, the electrical characteristics test shows that only the output ripple under CCFM will be increased slightly without any other different indexes from those under the conventional PWM control. Thirdly, the thermal test of the key elements indicates that the temperature of the high-frequency transformer increases several degrees under chaotic modulation, but it doesn't disturb the operation of the system.

The CCFM module designed in Chapter 2 can be applied in SMPSs controlled by standard PWM ICs to reduce the conducted interference, without weakening the overall performance of the power supplies. To sum up, it is feasible to apply CCFM in commercial SMPSs, and the experimental research lays the foundation of marketization of the proposed module.

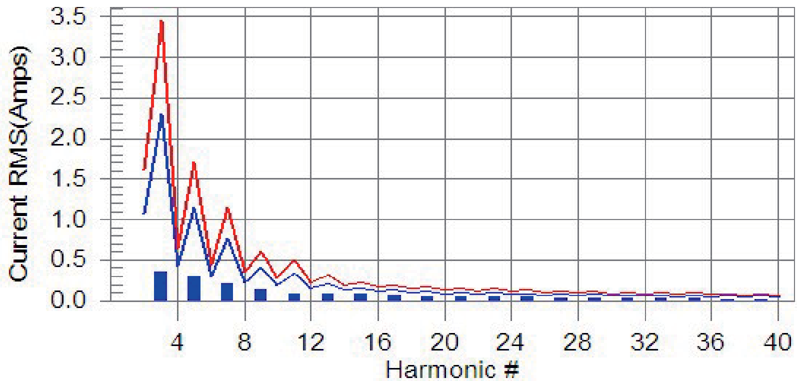

(a) Without CCFM

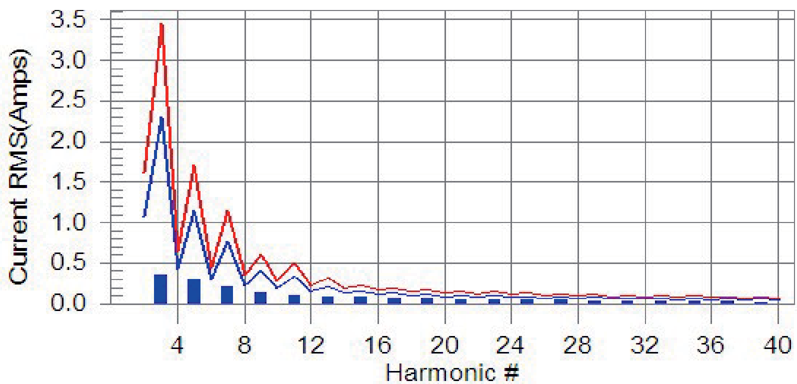

(b) With CCFM

Figure. 4.18: The measurement results of input current harmonic

5 Analogue Chaotic Frequency PWM IC

Owing to the lack of the chaotic frequency PWM IC, it is necessary to attach an auxiliary modulation circuit to the original product for implementing CCFM on SMPS, leading to the cost increase and inconvenience for production. Therefore, chaotic frequency PWM ICs will provide an efficient and economic solution for EMI suppression in power supplies. In this chapter, the analogue chaotic frequency PWM IC will be designed to facilitate the application of chaotic modulation, so that CCFM can be realized on SMPS for EMI suppression, without modifying the original circuit of power supplies.

5.1 Introduction

There are some restrictions in the application of the CCFM module. First, the chaotic modulation circuit has to be attached to PWM IC as a peripheral device, which is inconvenient for the development and the production of SMPS. Besides, the module can only work on the frequency programmable IC, while there are a lot of SMPSs controlled by the fixed frequency PWM ICs, of which the switching frequency can not be modulated. Hence, PWM IC with an internal chaotic frequency oscillator can facilitate the design of CCFM-based SMPS, providing an efficient and economic solution for EMI reduction.

A PWM IC can be divided into the analogue and digital PWM IC respectively. The analogue PWM ICs are more commonly used than the digital ones, due to its advantages of low cost, mature scheme, and most importantly, fast response time. For the analogously controlled SMPS, once the output voltage exceeds a reference voltage, the transistor is turned off immediately, resulting in a fast reaction system, whereas the digitally controlled SMPS is to sample the output voltage, quantify it, calculate the on-state duration of the transistor, and finally output the switching signal on the transistor.

Nevertheless, the analogue PWM IC has some disadvantages, such as fewer functions, more components, temperature sensitivity, and the lack of versatility and portability. In contrary, the digital IC has the attractive advantages such as programmability, robustness and options for more advanced control [58, 59, 78, 79]. Hence, for now, the analogue IC is much more commonly used, especially in the low-cost or fast-response applications, and the digital one, will become more and more popular for the increasing demand for flexibility, multi-function, high portability, and intellectuality.

Until now, there has been no chaotic frequency PWM IC of both the control mode on the market. Therefore, in this chapter, the analogue chaotic frequency PWM IC will be designed, and then the design of the digital one will be discussed in the next chapter. A chaotic frequency oscillator will be designed and embedded in analogue PWM ICs to implement chaotic modulation on SMPS for EMI suppression. A UC3842-based CCM and a UCC3895-based VCM&CCM IC with CCFM will be taken as two examples to control a flyback converter and a shift-phased full bridge converter, respectively. The simulations is conducted to verify the effectiveness of the proposed approach.

5.2 Analogue PWM IC

Pulse-width modulation is a commonly used SMPS controlled technique, which modulates the transistor's on-state duration during a switching period to regulate the output voltage or current. There are two PWM control modes of SMPS, namely current control mode (CCM) and voltage control mode (VCM), which adopt the sampling of the transistor's or transformer's current and the sampling of output voltage respectively to determine the duty cycle of the switching pulses. Correspondingly, there are CCM PWM IC (UC3842) [63], VCM PWM IC (TL494) [65] and CCM & VCM PWM IC [66].

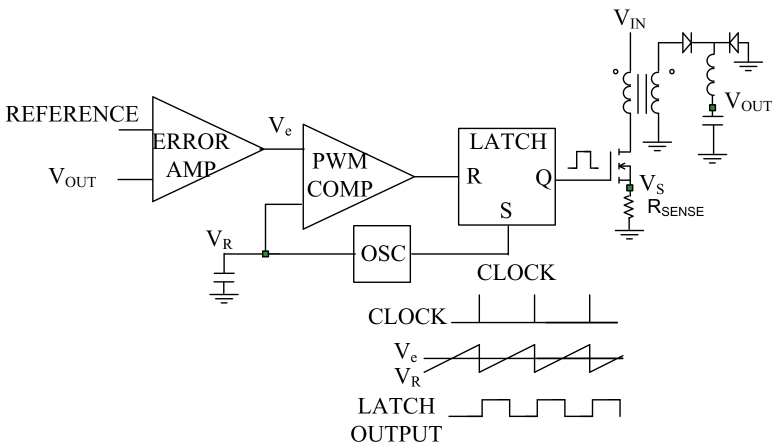

Figure. 5.1: The principle of voltage controlled mode

The schematic of the VCM PWM IC and its working principle are shown in Fig.5.1. At the beginning of each switching period, the transistor is turned on. Then, the output error voltage v_e, to which the sampling of output voltage v_{OUT} reduces a reference voltage, is compared with a sawtooth signal v_R. Once v_R exceeds v_e, the transistor is turned off until the end of the switching period.

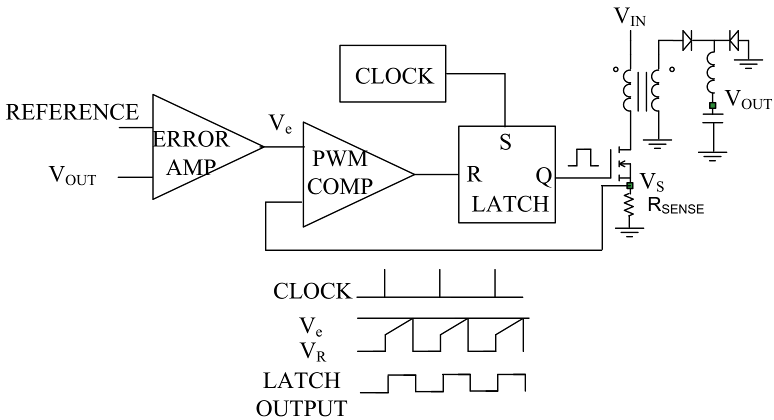

Figure. 5.2: The principle of current control mode

The schematic of the CCM PWM IC and its working principle are shown in Fig.5.2, where v_e is compared with the sampling of the transistor's or transformer's current to control the switching actions of the transistor.

No matter which control mode the PWM IC is, the sawtooth generator constitutes the oscillator and its frequency is exactly the switching frequency. The oscillator of PWM IC (see Fig.2.2), which has been analyzed in Chapter 2, is to periodically charge and discharge the timing capacitor between a low threshold voltage and a high threshold voltage. Therefore, the chaotic frequency PWM IC can be designed in the way of making either the charging current of the timing capacitor or the threshold voltage of the sawtooth changing chaotically.

A chaotic voltage generator and a current limiting resistor are necessary for the approach of dithering the charging current of the timing capacitor, which has been done in Chapter 2. Nevertheless, only a chaotic voltage generator is needed for the method of dithering the threshold voltage of the sawtooth, which will be studied in this chapter.

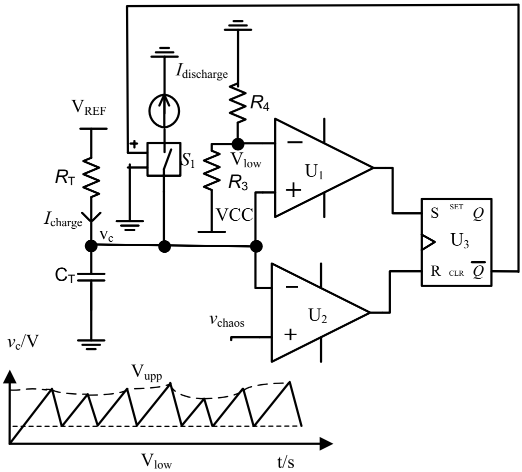

(a) Chaotic V_{upp}

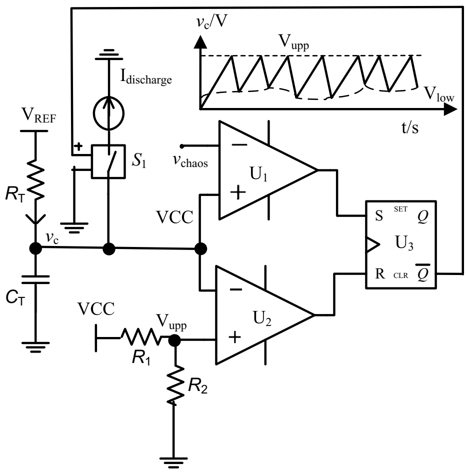

(b) Chaotic V_{low}

Figure. 5.3: The chaotic frequency oscillator

5.3 Design of CCFM-Based Oscillator

5.3.1 System Design

As shown in Fig.5.3, C_T is periodically charged and discharged between V_{low} and V_{upp}, and the switching period is equal to the sum of the charging and the discharging time. Thus, the switching frequency can be chaotically modulated by replacing V_{low} or V_{upp} with a chaotic voltage.

5.3.2 Chaotic Threshold Voltage

The chaotic threshold voltage can be generated by the schematic in Fig.5.4, where v_1, a chaotic voltage produced by Chua's circuit, is set to v_{chaos} within the certain range by the amplifying circuit. Then, v_{chaos} can be calculated as

$$v_{chaos} = \frac{\dfrac{V_{CC}R_4(R_5+R_6)}{R_3+R_4} - \dfrac{v_1 R_1 R_6}{R_1+R_2}}{R_5}, \tag{5.1}$$

where V_{CC} is the power supply of the chaos circuit, R_1-R_6 are resistors.

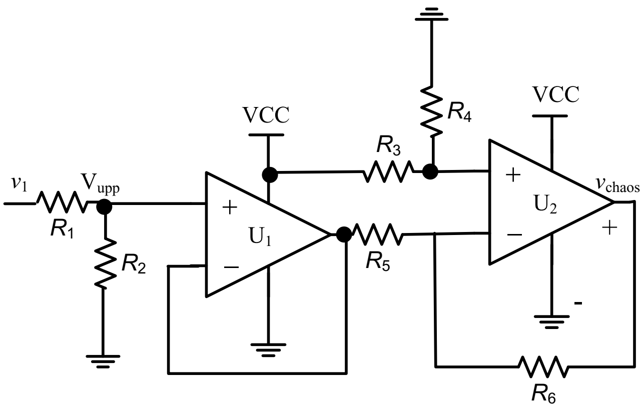

Figure. 5.4: Amplifying circuit for setting the chaotic threshold voltage

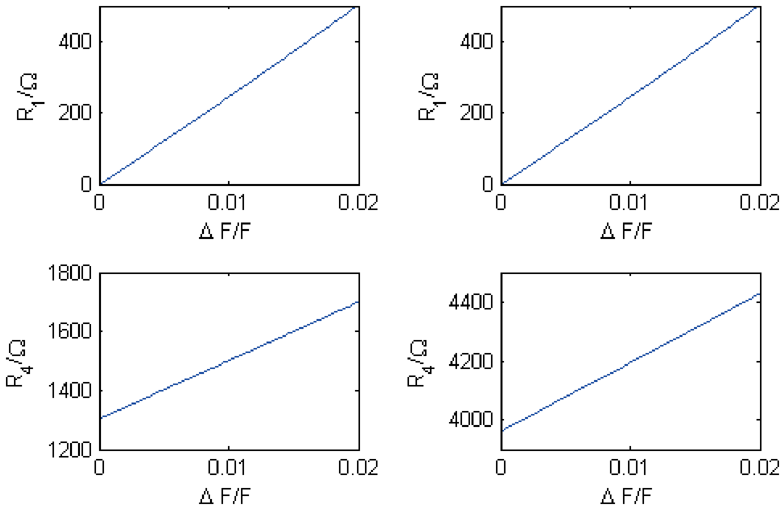

(a) Chaotic V_{low} (b) Chaotic V_{upp}

Figure. 5.5: $\frac{\triangle F}{F}$ vs the resistor parameter of the circuit

As the maximum and the minimum of v_{chaos} are v_{1max} and v_{1min}, v_{chaos} is maximized to $v_{chaosmax}$ and minimized to $v_{chaosmin}$ severally. Hence, the variation range of v_{chaos}, Δv, and its average value, $v_{chaosavg}$, can be expressed as

$$\Delta v = \frac{R_1 R_6 (v_{1max} - v_{1min})}{R_5 (R_1 + R_2)}, \tag{5.2}$$

$$v_{chaosavg} = \frac{(R_5 + R_6)\left[\frac{2V_{CC}R_4}{R_3 + R_4} - \frac{(v_{1min} + v_{1max})R_1 R_6}{R_1 + R_2}\right]}{2R_5}. \tag{5.3}$$

Therefore, Δv can be set by R_1, meanwhile, v_{chaos} can be adjusted by R_4. If V_{upp} is replaced by v_{chaos} to realize chaotic modulation, the charging and discharging time are expressed as [61]

$$t_c(v_{chaos}) = R_T C_T \ln \frac{V_{low} - V_{REF}}{v_{chaos} - V_{REF}}, \tag{5.4}$$

$$t_d(v_{\text{chaos}}) = R_{\text{T}}C_{\text{T}}\ln\frac{v_{\text{chaos}} + R_{\text{T}}\text{I}_{\text{discharge}} - \text{V}_{\text{REF}}}{\text{V}_{\text{low}} + R_{\text{T}}\text{I}_{\text{discharge}} - \text{V}_{\text{REF}}}. \tag{5.5}$$

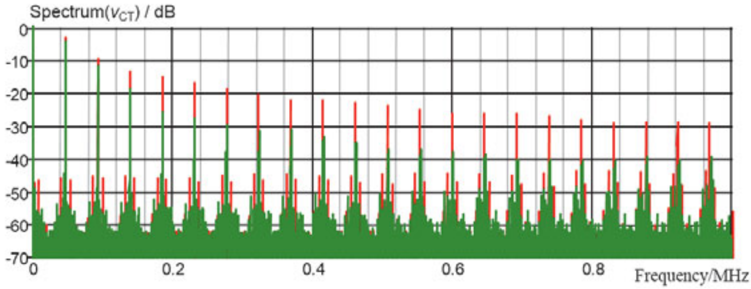

(a) $\frac{\triangle F}{F} = 0.5\%$ (green: with CCFM, red: without CCFM)

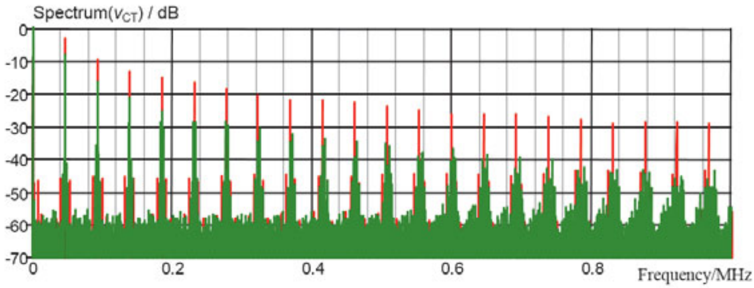

(b) $\frac{\triangle F}{F} = 1\%$ (green: with CCFM, red: without CCFM)

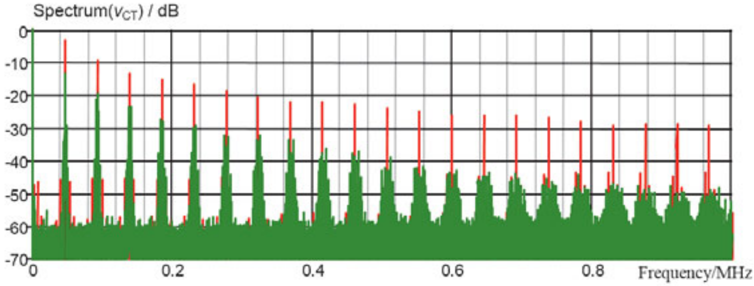

(c) $\frac{\triangle F}{F} = 2\%$ (green: with CCFM, red: without CCFM)

Figure. 5.6: Spectra of the C_{T} voltage

Because the discharging current $I_{discharge}$ is generally far larger than the charging current, the discharging time t_d is approximately 0. Therefore the switching period $T(v_{chaos})$ and frequency $f(v_{chaos})$ are

$$T(v_{chaos}) \approx t_c(v_{chaos}), \tag{5.6}$$

$$f(v_{chaos}) = \frac{1}{T(v_{chao})}. \tag{5.7}$$

According to Equ.(5.6) and Equ.(5.7), $T(v_{chaos}) \in [T(v_{chaosmax}), T(v_{chaosmin})]$ and
$f(v_{chaos}) \in [f(v_{chaosmin}), f(v_{chaosmax})]$, so that the variation range of $f(v_{chaos})$, $\Delta F = f(v_{chaosmax}) - f(v_{chaosmin})$, and the frequency modulation ratio can be described as

$$\frac{\triangle F}{F} = \frac{\ln \frac{v_{chaosmax} - V_{REF}}{v_{chaosmin} - V_{REF}}}{\ln \frac{V_{low} - V_{REF}}{V_{chaosavg} - V_{REF}}}, \tag{5.8}$$

where F is the average value, namely $\frac{f(v_{chaosmax}) + f(v_{chaosmin})}{2}$.

To sum up, F and $\triangle F$ can be adjusted by R_1 and R_4, thus, CCFM with a programmable frequency modulation range is realized.

Assume that $F = 24kHz$, $V_1 \in [5.5, 6.5]$, $R_2 = 10k\Omega$, $R_3 = 30k\Omega$, $R_5 = 30k\Omega$, $R_6 = 30k\Omega$, $V_{upp} = 1.2V$ and $V_{upp} = 2.8V$. $\frac{\triangle F}{F}$ vs R_1 and $\frac{\triangle F}{F}$ vs R_4 are shown in Fig.5.5a, while V_{low} is chaotic. When V_{upp} is chaotic, $\frac{\triangle F}{F}$ vs R_1 and $\frac{\triangle F}{F}$ vs R_4 are shown in Fig.5.5b. In case that V_{upp} is changed chaotically, the spectra of the timing capacitor's voltage are shown in Fig.5.6. The harmonics peaks under the traditional PWM control are spread within a wide frequency range obviously by CCFM. Moreover, the better effect of spread-spectrum can be obtained by increasing the modulation ratio of the switching frequency.

5.4 Simulations

5.4.1 Chaotic Frequency PWM IC Controlled Flyback Converter

As shown in Fig.5.7, a chaotic frequency PWM IC, which employs UC3842 as the prototype, is used to control a flyback-based constant current supply. The diagram of the PWM IC is shown in Fig.5.8. Under chaotic modulation, the clock

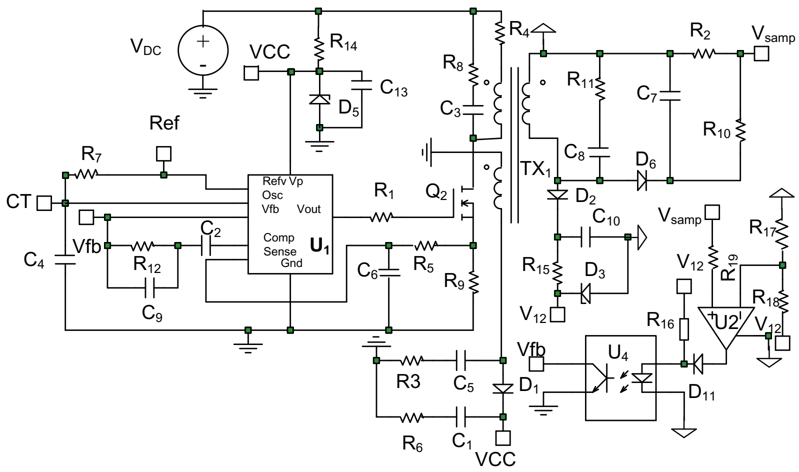

Figure. 5.7: The flyback converter

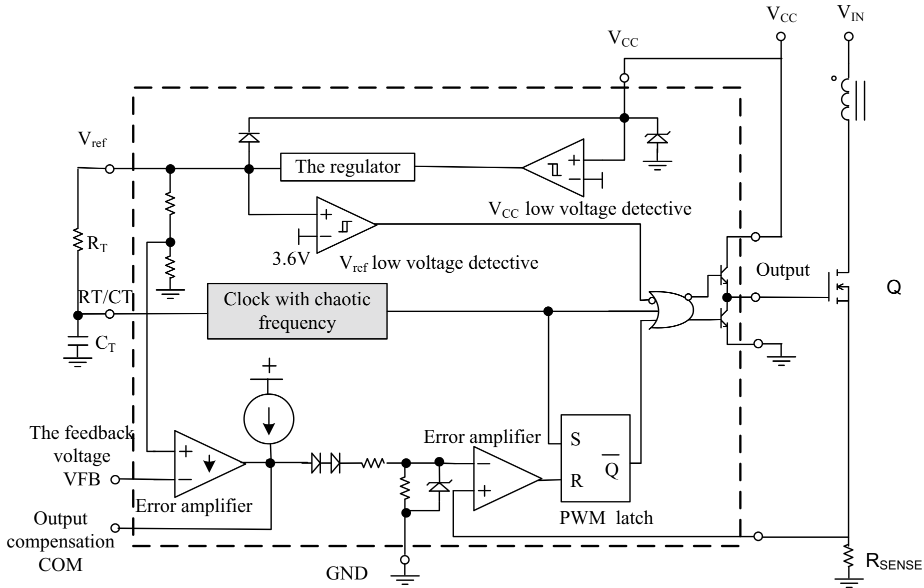

Figure. 5.8: The diagram of PWM IC with chaotic frequency

signals, such as the frequency of the sawtooth and the switching PWM signal, are chaotically modulated as shown in Fig.5.9.

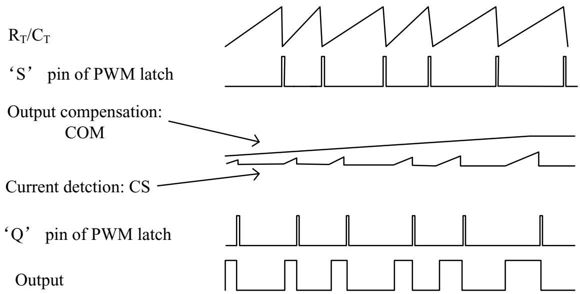

Figure. 5.9: The signals' waveforms with CCFM

The output current is 0.9A and the load is 10Ω. The output ripple is 85.21mV, 86.33mV, 86.43mV, 86.87mV, as $\frac{\triangle F}{F} = 0\%$, $\frac{\triangle F}{F} = 0.5\%$, $\frac{\triangle F}{F} = 1\%$ and $\frac{\triangle F}{F} = 2\%$, respectively. The output ripple is slightly increased under CCFM, which is acceptable. As shown in Fig.5.10, the spectra of the switching voltage show that the harmonic peaks existing under the traditional PWM control are spread by the application of the chaotic frequency PWM IC, and EMI reduction becomes larger with the increase of the modulation ratio of the switching frequency. The detailed reduction values of the harmonic peak are given by Tab.5.1.

Table 5.1: The harmonics peak reduction of the switching voltage in flyback converter

Harmonic order		1	2	3	4	5	6	7	8	9	10
Reduction (dB)	$R_I = 60k\Omega$	1	0	2	2	3	2	3	4	6	8
	$R_I = 100k\Omega$	1	0	2	3	2	3	4	7	9	9
	$R_I = 140k\Omega$	1	0	2	3	3	3	7	9	9	12

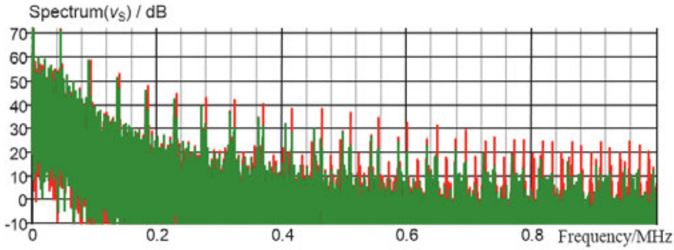

(a) $\frac{\triangle F}{F} = 0.5\%$ (green: with CCFM, red: without CCFM)

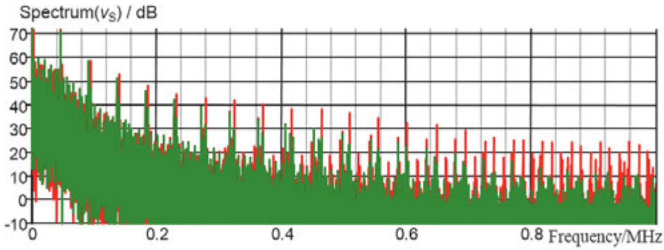

(b) $\frac{\triangle F}{F} = 1\%$ (green: with CCFM, red: without CCFM)

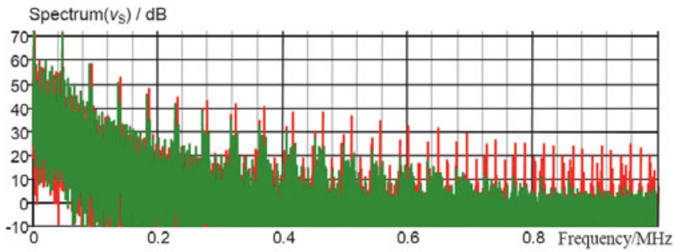

(c) $\frac{\triangle F}{F} = 2\%$ (green: with CCFM, red: without CCFM)

Figure. 5.10: The switching voltage spectra of the flyback converter

5.4.2 Chaotic Frequency PWM IC Controlled Shift-Phased Full Bridge Converter

A VCM& CCM PWM IC, UCC3895, is adopted as the other example to control a shift-phased full bridge converter as shown in Fig.5.12. The designed diagram of the PWM IC is given by Fig.5.12, and the waveforms of the chaotically modulated clock signals are shown in Fig.5.13.

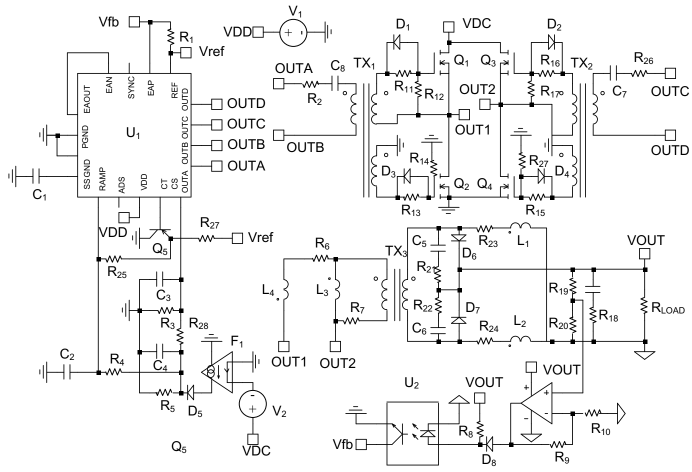

Figure. 5.11: The phase-shifted full bridge converter

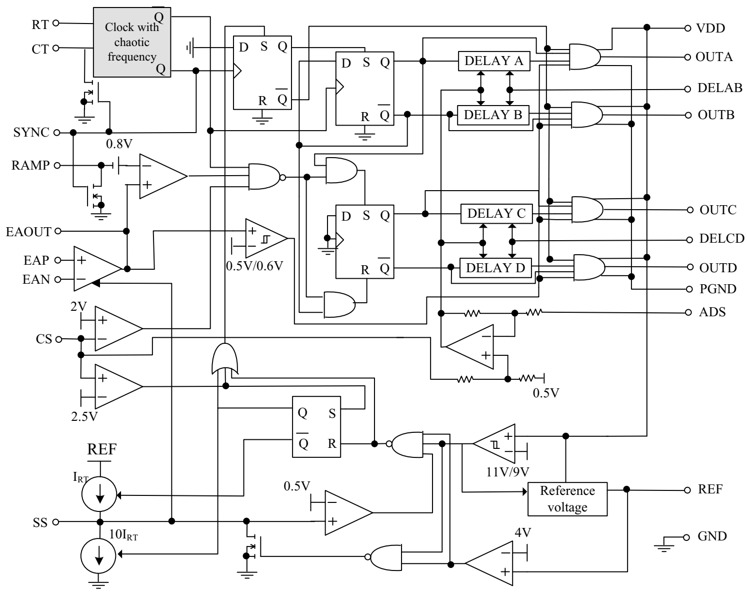

Figure. 5.12: The diagram of chaotic frequency PWM IC

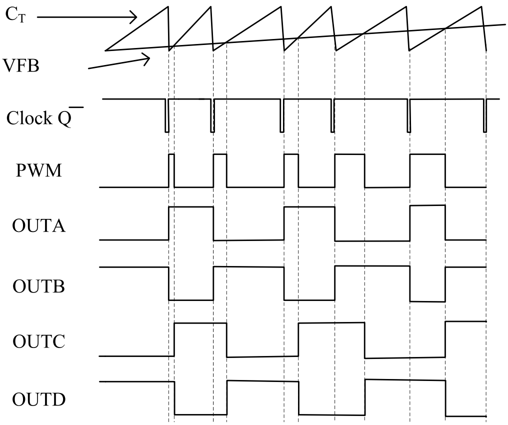

Figure. 5.13: The signals' waveforms with CCFM

The spectra of the switching voltage and the reduction values of the harmonic peak, which are given by Fig.5.14 and Tab.5.2, show that the CCFM IC is effective to reduce EMI of SMPS. The output ripple is 71.07mV, 86.43mV, 100mV, and 124mV as $\frac{\triangle F}{F} = 0\%$, $\frac{\triangle F}{F} = 0.5\%$, $\frac{\triangle F}{F} = 1\%$ and $\frac{\triangle F}{F} = 2\%$, respectively. In general, the designed chaotic frequency oscillator can be integrated in various PWM ICs.

Table 5.2: The harmonics peak reduction of the switching voltage in shift-phased full bridge converter

Harmonic order		1	2	3	4	5	6	7	8	9	10
Reduction (dB)	$R_I = 60k\Omega$	1	6	6	7	6	7	6	6	7	9
	$R_I = 100k\Omega$	4	9	9	7	9	10	10	12	10	11
	$R_I = 140k\Omega$	7	9	12	12	9	14	13	14	14	114

5.5 Summary

An analogue chaotic driver of a PWM IC is designed to implement chaotic modulation on SMPS for EMI suppression. A CCM IC (UC3842) and a VCM&CCM

IC (UCC3895), which are taken as examples, are used to control a flyback converter and a shift-phased full bridge converter respectively, and effectiveness of the proposed method on EMI reduction is verified by the simulations. Since the oscillators inside IC are similar in the construct, the designed CCFM oscillator can be used widely in all kinds of PWM ICs. Therefore, the application prospect of chaotic modulation is further expanded.

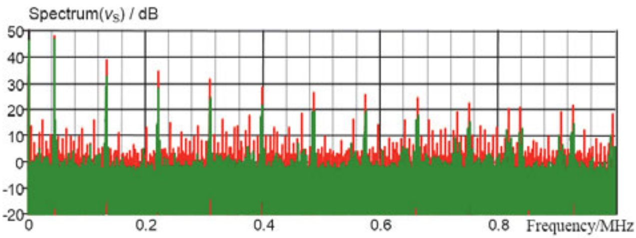

(a) $\frac{\triangle F}{F} = 0.5\%$ (green: with CCFM, red: without CCFM)

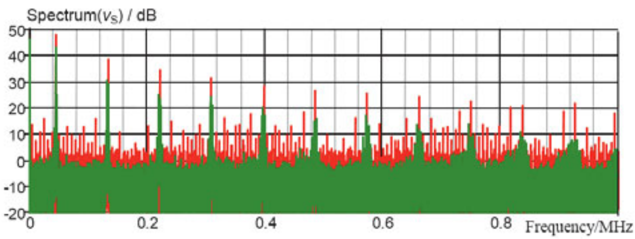

(b) $\frac{\triangle F}{F} = 1\%$ (green: with CCFM, red: without CCFM)

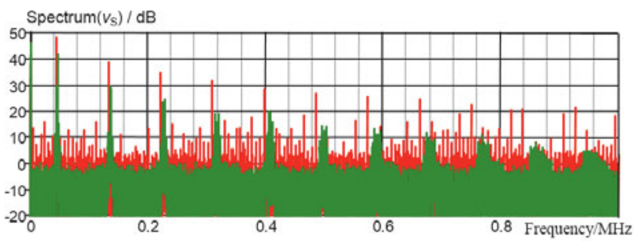

(c) $\frac{\triangle F}{F} = 2\%$ (green: with CCFM, red: without CCFM)

Figure. 5.14: The switching voltage spectra of the shift-phased full bridge converter

6 Digital Chaotic Frequency PWM IC

With the features of flexibility, multi-function, high portability, and intellectuality, the digitally controlled power supplies are in a rapidly growing need. To reduce EMI in the digital systems, a chaotic digital PWM (CDPWM) IC is designed based on FPGA, and its effect on EMI reduction and output voltage ripple will be investigated by simulations and experiments.

6.1 Introduction

With the development of electronic technique, the disadvantages of the digital processor such as high cost and slow response time will be solved step by step. Meanwhile, owing to the advantages of digital system, such as programmability, robustness and options for more advanced control, the digitally controlled SMPS becomes more and more popular.

It is noted that the CCFM solutions applied in the analogue system can not be extended to the digital one at all, because the control strategies for both the systems are totally different, which has been explained in Sec.5.1. Hence, this chapter is concerned with the application of CCFM in digital system. The CDPWM controller can be manufactured with DSP, MCU, MPU and FPGA, among which FPGA is selected as the control core in this dissertation due to the lower cost than DSP and MPU, the faster processing speed than MCU, and most importantly, its unique ability to design application specific integrated circuit (ASIC). To realize chaotic modulation on the digital systems, the emphasis is focused on the design of a chaotic switching period counter, and Logistic map, Shift map and Tent map are used to generate the pre-assigned value of the counter, respectively. The comparisons will be made on the effectiveness of CCFM on EMI suppression and output voltage ripple with the three chaotic maps to help the designer to optimize the product. The simulations and experiments on a buck converter are conducted to verify the effectiveness of CDPWM IC on EMI reduction in the digitally controlled SMPS.

6.2 Digitally Controlled SMPS

6.2.1 Diagram of Digitally Controlled SMPS

As shown in Fig.6.1 [80], the diagram of a typical digitally controlled SMPS is as similar as the analogue one, except the feedback and PWM control section, where the output voltage is sampled, converted from an analogue signal to a digital signal and sent to a PID operator to generate the switching signal.

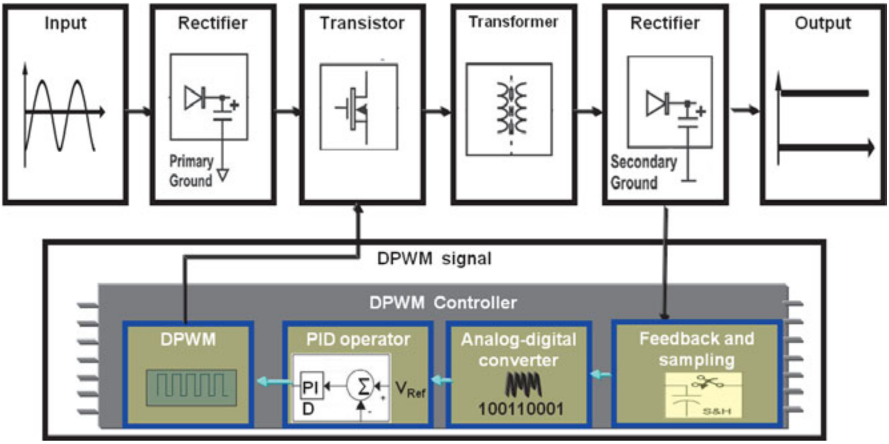

Figure. 6.1: The diagram of digitally controlled SMPS

6.2.2 DPWM

The working principle of DPWM is illustrated in Fig.6.2. First of all, a counter, C, whose pre-assigned value is N, is employed to calculate the switching period, called T. During one switching period, C counts from 0 to N at a counting frequency f_0, that is to say, C increases by 1 per $\frac{1}{f_0}$ second. Then the switching period can be expressed as $\mathrm{T} = \frac{\mathrm{N}+1}{f_0}$, and thus $f = \frac{1}{\mathrm{T}}$ is the switching frequency. By the digital PID operator, the output sampled voltage is converted to the on-state duration of a switching period, defined as D ($\mathrm{D} < \mathrm{N}+1$). At the beginning of the switching period, the transistor is turned on. As soon as $C > \mathrm{D}$, the transistor is turned off and lasts until the end of the switching period. Consequently, the schematic of DPWM is described in Fig.6.3.

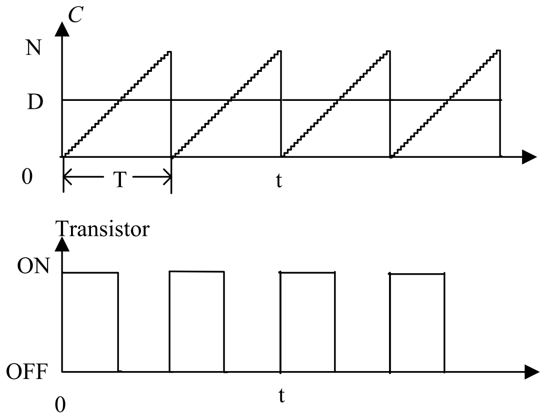

Figure. 6.2: The principle of DPWM

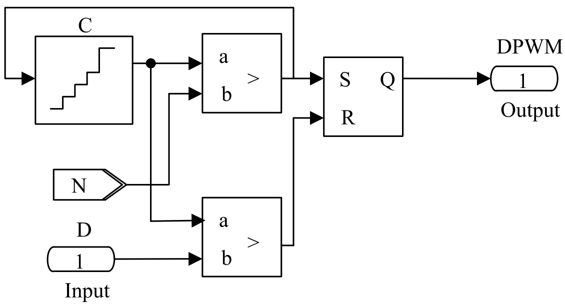

Figure. 6.3: The schematic of DPWM

6.3 DPWM with Chaotic Frequency

6.3.1 Working Principle of CDPWM

Normally, the switching period of the digital system is constant, leading to EMI problem. However, as shown in Fig.6.4, the switching period can be modulated by replacing the pre-assigned value of the switching period counter (N) with a chaotic sequence N_c. In the following sections, Logistics map, Tent map and Shift map will be used to generate N_c, respectively.

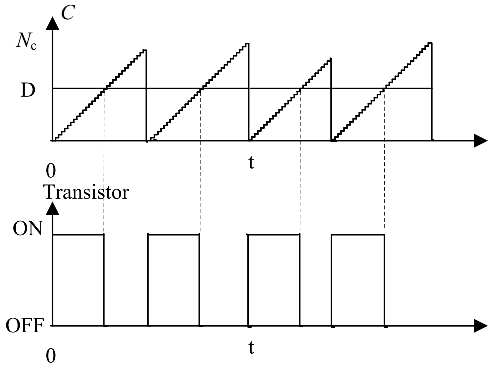

Figure. 6.4: The principle of chaotic frequency DPWM

6.3.2 Logistic Map Based Digital Chaotic Signal Generator

The chaotic sequence x_{n+1} of Logistic map [81] is defined as

$$x_{n+1} = \mu x_n(1 - x_n)(0 < x_n < 1), \tag{6.1}$$

where μ is the fractal parameter, and x_{n+1} is chaotic as $3.5699456... < \mu < 4$.

The schematic of Logistics map is illustrated in Fig.6.5. On the beginning of each switching period, a new chaotic number x_{n+1} will be generated and outputted, and the output chaotic sequence is shown in Fig.6.6.

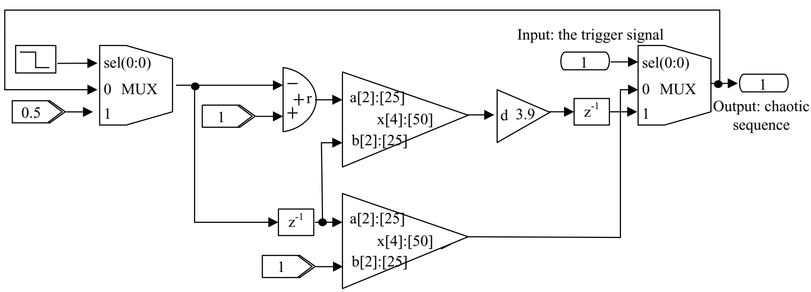

Figure. 6.5: The digital circuit of Logistic map

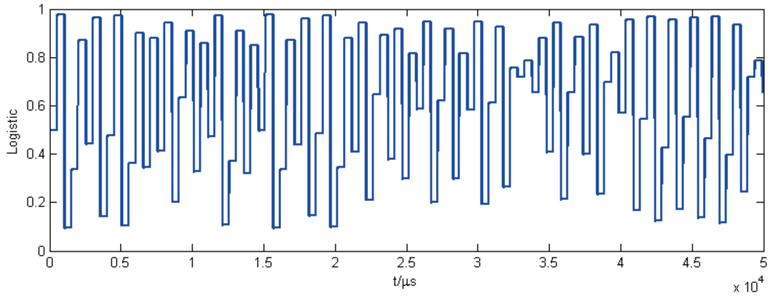

Figure. 6.6: Waveform of Logistic map sequence

6.3.3 Tent Map Based Digital Chaotic Signal Generator

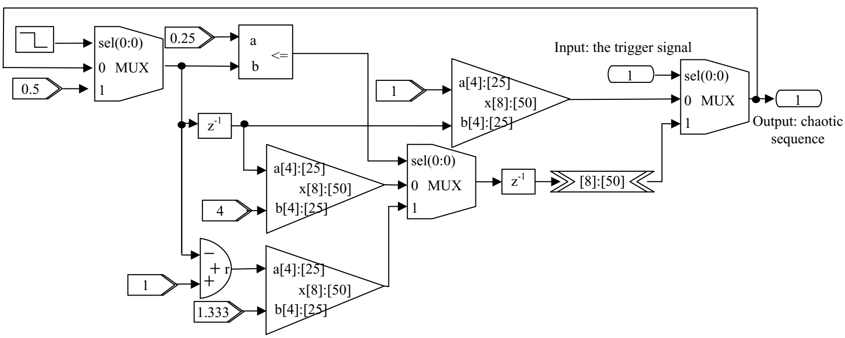

Figure. 6.7: The digital circuit of Tent map

Tent map [82] belongs to one-dimensional piecewise linear map, and is described as

$$x_{n+1} = \begin{cases} \dfrac{x_n}{\mu}, & 0 \leq x_n \leq \mu, \\ \dfrac{1 - x_n}{1 - \mu}, & \mu < x_n \leq 1, \end{cases} \tag{6.2}$$

where $\mu \in (0, 1)$, and x_{n+1} is chaotic as $x_1 \in (0, 1)$.

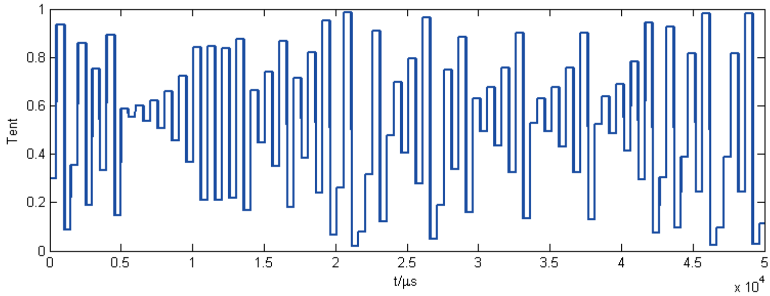

Figure. 6.8: Waveform of Tent map sequence

Its schematic is illustrated as Fig.6.7, and the output chaotic sequence is shown in Fig.6.8.

6.3.4 Shift Map Based Digital Chaotic Signal Generator

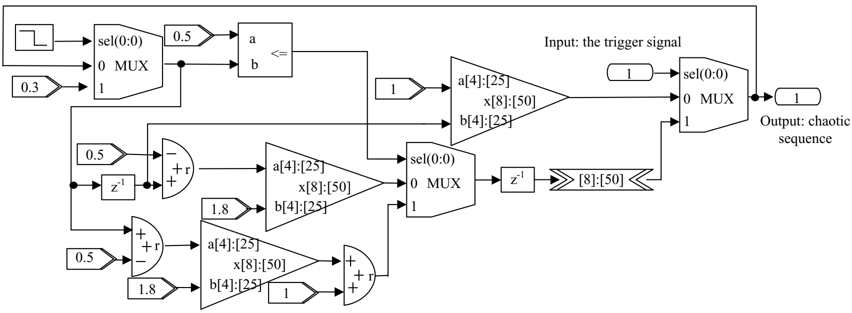

Figure. 6.9: The digital circuit of Shift map

Shift map is expressed as

$$x_{n+1} = \begin{cases} \mu(x_n - \frac{1}{2}) + 1, & 0 \leq x_n \leq \frac{1}{2}, \\ \mu(x_n - \frac{1}{2}), & \frac{1}{2} < x_n \leq 1, \end{cases} \tag{6.3}$$

where $\mu = 1.8$, and x_{n+1} is chaotic as $x_1 \in (0, 1)$.

The schematic of Shift map is shown as Fig.6.9, and the chaotic sequence is shown in Fig.6.10.

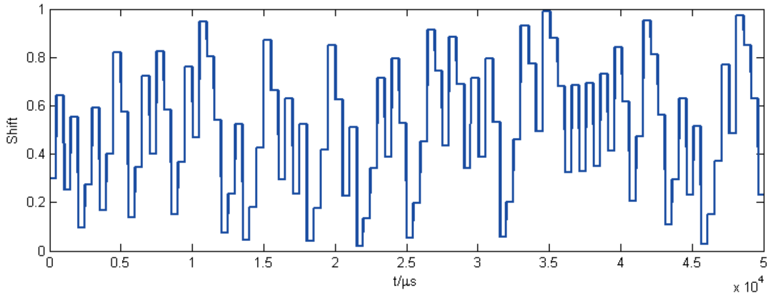

Figure. 6.10: Waveform of Shift map sequence

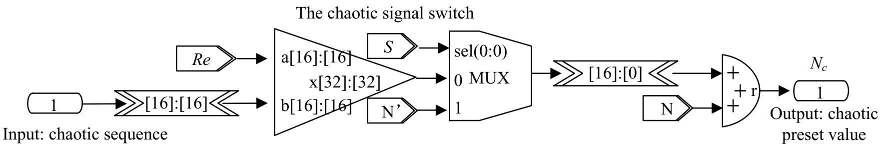

Figure. 6.11: The generation of PWM period counter pre-assigned value N_c

6.3.5 Circuit Design of CDPWM

Because $x_n \in (0,1)$, x_n should be further processed to get the integer N_c. A pre-assigned value processing circuit is designed as Fig.6.11. As the chaotic signal switch, S, is turned off, the switching period is fixed, and $N_c = \mathrm{N}' + \mathrm{N}$, where both N and N$'$ are constant. Otherwise, as S is turned on, the switching period is modulated by x_n, and $N_c = x_n Re + \mathrm{N}$. Here Re is defined as the modulation degree to transform the decimal x_n to an integer N_c within the desired range.

Therefore, N_c is maximized to $Re + \mathrm{N}$ and minimized to N. Assume that the switching frequency is f_c, $f_c \in (\mathrm{F} - \frac{\Delta f}{2}, \mathrm{F} + \frac{\Delta f}{2})$, where F is the desired mean frequency, and Δf is its desired range from the minimum to the maximum, then

$$\frac{f_0}{Re + \mathrm{N} + 1} = \mathrm{F} - \frac{\Delta f}{2}, \tag{6.4}$$

$$\frac{f_0}{\mathrm{N} + 1} = \mathrm{F} + \frac{\Delta f}{2}. \tag{6.5}$$

And for demanded F and Δf, N and Re can be calculated as

$$\mathrm{N} = \frac{f_0}{\mathrm{F} + \frac{\Delta f}{2}} - 1, \tag{6.6}$$

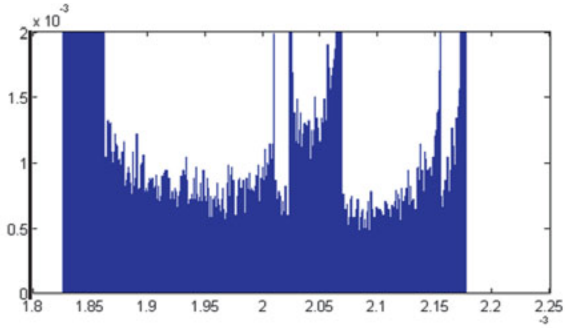

(a) Logistic map

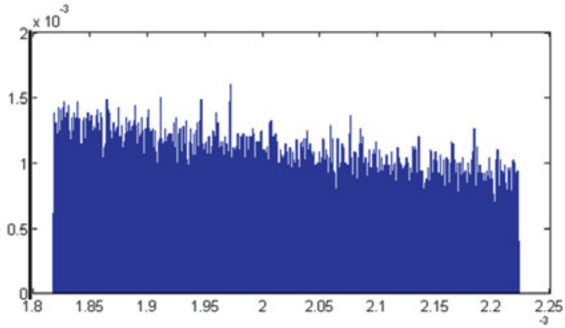

(b) Tent map

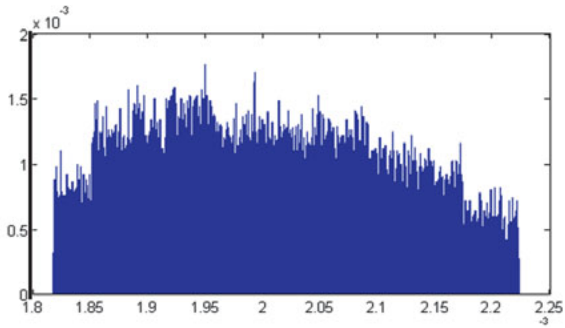

(c) Shift map

Figure. 6.12: Statistical histograms of of the switching period

$$Re = \frac{\Delta f f_0}{F^2 - (\frac{\Delta f}{2})^2}. \quad (6.7)$$

To make sure that the mean frequency under chaotic modulation is the same as that under the traditional PWM control, it is obtained that

$$N' = \frac{Re}{2} = \frac{2\Delta f f_0}{F^2 + \Delta f F}. \quad (6.8)$$

With different chaotic map, the distribution of the switching period differs. As shown in Fig.6.12, the statistical histogram of the switching period with Logistic map is concentrated upon certain areas. Then, it tends to obey the uniform distribution with Tent map. And it is distributed around the expectation with Shift map.

In general, because both the modulation degree and the distribution of the switching period can be adjusted, it is possible to optimize chaotic modulation circuit to improve the effectiveness of EMI reduction.

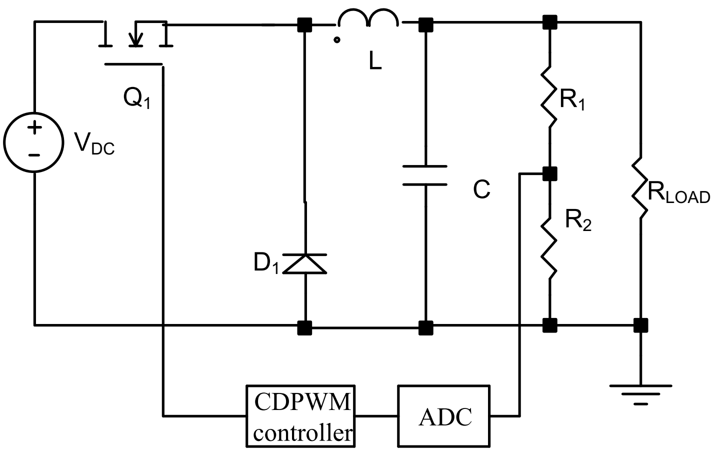

Figure. 6.13: The DPWM controlled buck converter

6.4 Simulations

CDPWM is adopted to control a buck converter shown in Fig.6.13, where R_{LOAD} is the load of the power supply. The analogue partial voltage of R_2 is converted to the digital signal and feedback to CDPWM controller to regulate the output voltage to a stable DC of 12V. CDPWM controller is designed as shown in Fig.6.3, and the chaotic integer N_c is generated by the circuit of Fig.6.11.

The spectra of the switching voltage with the three maps and different values of Re are exhibited in Fig.6.15, and the detailed reduction values of the harmonic peak are given by Tab.6.1. It is observed that EMI can be reduced no matter which chaotic map is used to modulate the switching frequency. And the effect of EMI suppression is improved with the increase of Re, however, the output voltage ripple is also increased (see Fig.6.15). Consequently, the value of Re is determined by the requirement for the output ripple.

Table 6.1: The harmonics peak reduction of the switching pulses

Harmonic	Logistic map, $Re =$			Tent map, $Re =$			Shift map, $Re =$		
order	10	20	30	10	20	30	10	20	30
1	0	1	1	0	1	1	0	1	2
2	1	3	2	1	2	2	1	3	3
3	2	2	4	3	3	4	4	6	6
4	1	3	4	2	4	3	3	5	7
5	1	5	6	2	4	6	3	5	9
6	2	4	6	3	3	7	5	7	9
7	4	7	9	3	3	9	5	9	10
8	3	7	8	4	6	9	6	10	10
9	3	8	9	2	7	8	6	9	11
10	3	8	10	4	8	8	6	9	11

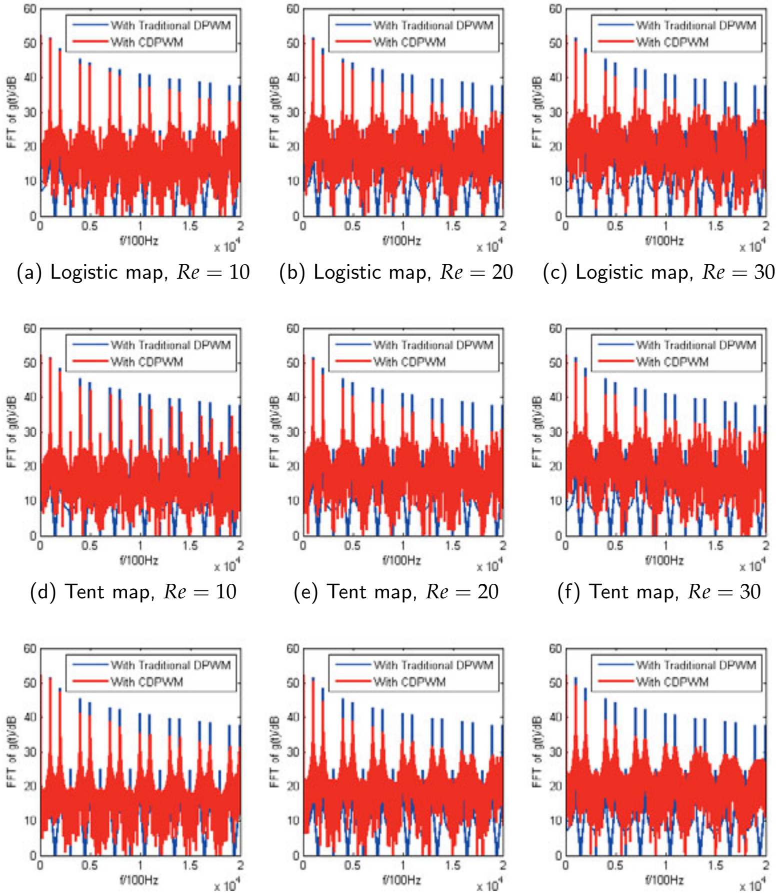

(a) Logistic map, $Re = 10$ (b) Logistic map, $Re = 20$ (c) Logistic map, $Re = 30$

(d) Tent map, $Re = 10$ (e) Tent map, $Re = 20$ (f) Tent map, $Re = 30$

(g) Shift map, $Re = 10$ (h) Shift map, $Re = 10$ (i) Shift map, $Re = 30$

Figure. 6.14: Spectra of the switching voltage

The effectiveness of EMI reduction with Shift map is best, while the ripple is largest. In contrary, the output ripple with Logistics map is lowest. Among the three maps, the Tent map is not worthy of application, because there are extra ledges on the high-frequency band and the output ripple is larger than that of Logistics map. To sum up, the Logistics map is fit for the systems with stringent requirement for the output ripple, and Shift map should be adopted by power supplies with severe EMI.

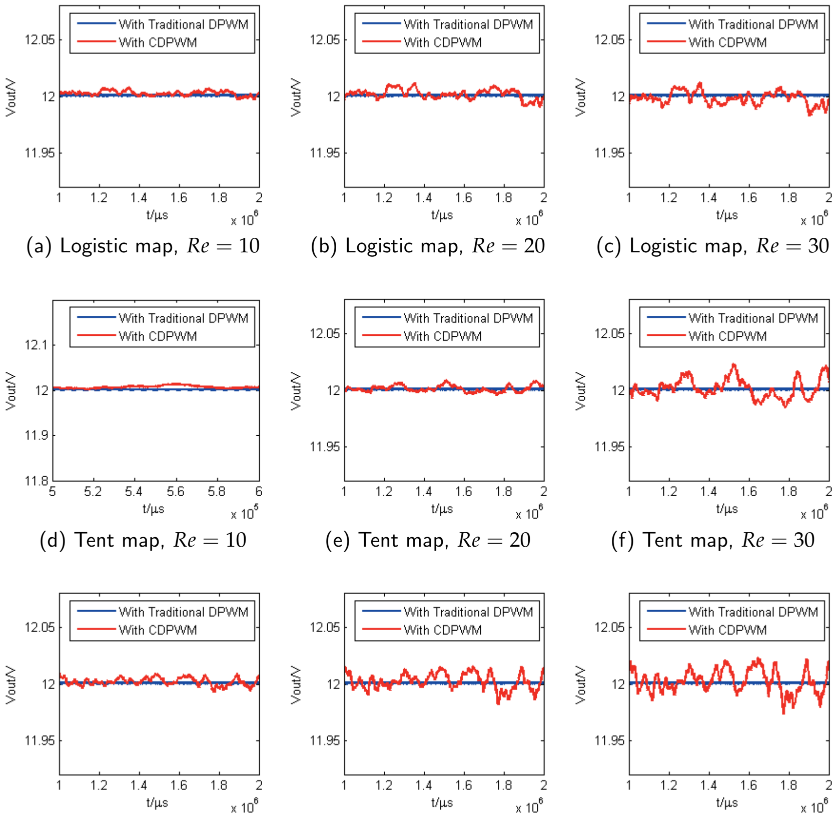

(a) Logistic map, $Re = 10$ (b) Logistic map, $Re = 20$ (c) Logistic map, $Re = 30$

(d) Tent map, $Re = 10$ (e) Tent map, $Re = 20$ (f) Tent map, $Re = 30$

(g) Shift map, $Re = 10$ (h) Shift map, $Re = 10$ (i) Shift map, $Re = 30$

Figure. 6.15: Waveforms of output voltage

6.5 Experiments

The experiments on the power supply shown in Fig.6.13 are also carried out. The spectra of the switching voltage (see Fig.6.16) show that increasing the modulation degree can suppress EMI more effectively, and the best effect of EMI reduction is obtained by using Shift map.

The waveforms of the output voltage are given by Fig.6.17, and the ripple under the traditional DPWM control is 440mV. It is obvious that the output ripple becomes larger as the modulation degree increases. As Re is 10, 20 and 30 separately, the ripples with Logistics map are 440mV, 480mV and 560mV, those with Tent map are 440mV, 480mV and 600mV, and those with Shift map are 480mV, 520mV and 640mV. The ripple is the lowest as using Logistic map, and the largest as using Shift map.

The experimental results are consistent with the simulations, and it is verified that the designed CDPWM IC is effective to reduce EMI of digitally controlled power supplies.

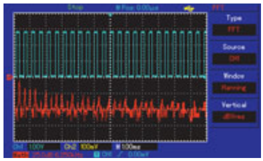

(a) Traditional DPWM

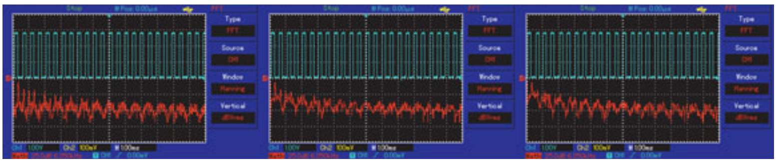

(b) Logistic map, $Re = 10$ (c) Logistic map, $Re = 20$ (d) Logistic map, $Re = 30$

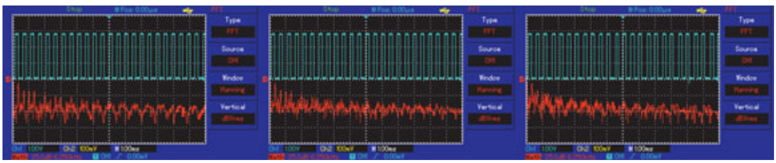

(e) Tent map, $Re = 10$ (f) Tent map, $Re = 20$ (g) Tent map, $Re = 30$

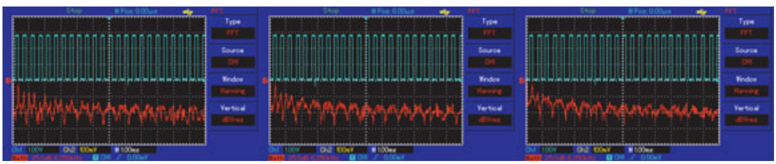

(h) Shift map, $Re = 10$ (i) Shift map, $Re = 10$ (j) Shift map, $Re = 30$

Figure. 6.16: Spectra of the switching voltage

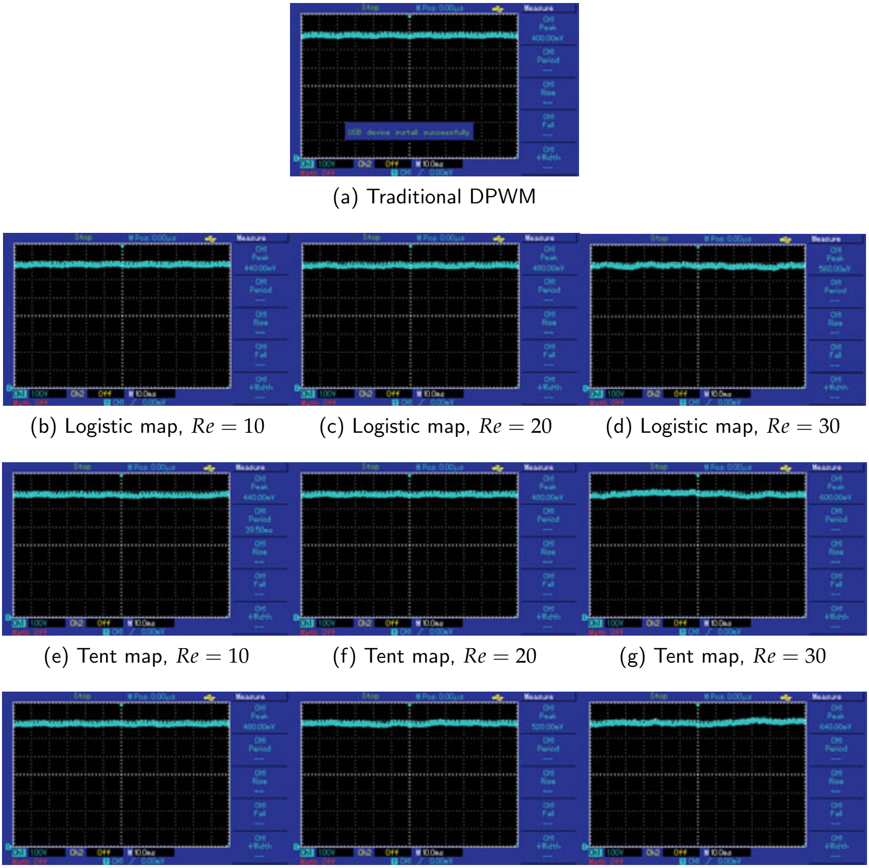

(a) Traditional DPWM

(b) Logistic map, $Re = 10$ (c) Logistic map, $Re = 20$ (d) Logistic map, $Re = 30$

(e) Tent map, $Re = 10$ (f) Tent map, $Re = 20$ (g) Tent map, $Re = 30$

(h) Shift map, $Re = 10$ (i) Shift map, $Re = 10$ (j) Shift map, $Re = 30$

Figure. 6.17: Waveforms of output voltage

6.6 Summary

CCFM scheme for the digitally controlled SMPS can be realized by making the pre-assigned value of the switching period counter changing chaotically. Therefore, the CDPWM IC is designed, and different chaotic maps, namely Logistics map, Shift map and Rent map, are used to modulate the switching frequency. A buck converter controlled by digital PID algorithm is employed as an example. According to simulations and experiments, EMI is suppressed more efficiently with the increase of the frequency modulation degree, while the output ripple is increased slightly in an acceptable range. With shift map, EMI is reduced most, but the output voltage ripple is increased most. Conversely, the ripple increment is lowest when using Logistic map. Hence, the Logistics map can be employed by the systems with stringent requirement for the output ripple, and Shift map is useful for the products with severe EMI problem. The digital chaotic frequency PWM IC will facilitate the application of chaotic modulation in the digitally controlled SMPSs.

7 Conclusion

The highly unpredictable and random-like features of chaotic signals are very useful for engineering applications. One of the successful applications is chaotic carrier frequency modulation technique, which has been utilized in EMI suppression of SMPS. By chaotically dithering the switching frequency around the nominal value, the discrete harmonic power that usually exists in classical PWM scheme becomes continuous and can be spread over a wide frequency range. Although CCFM has been proved effective to reduce EMI of SMPS, there has been no commercial CCFM-based power supply. Therefore, this dissertation is concentrated on the application of chaos in real products for EMI reduction. The contributions of the dissertation are as follows:

(1) With the advantages of low cost, low design complexity, flexibility and universality to the frequency programmable PWM IC, a chaotic carrier frequency modulation module has been designed to reduce EMI of commercial SMPSs.

(2) The power spectral characteristics of the switching converter with CCFM shows that the effectiveness of EMI suppression is determined by the probability distribution and the randomness of the switching period. When the proposed module is used to modulate the switching frequency, it is found that both the PDF and the randomness of the switching period can be set by adjusting certain circuit parameters. Therefore, the EMI reduction effectiveness can be estimated and improved basing on the power spectrum analysis.

(3) The electrical characteristics test, working condition test and EMC test have been done on two typical LED drivers. The test results show that the output ripple is increased a little and the temperature of the high-frequency transformer increases several degrees when working under chaotic modulation. However, that does not disturb the operation of the power system. As a conclusion, the CCFM module improves the EMC of SMPS without weakening the overall system performance, and the feasibility of applying the chaotic carrier frequency modulation in SMPSs is verified.

(4) The analogue chaotic frequency PWM IC was designed. CCFM was realized by making the certain parameter of the IC's oscillator changing chaotically. The designed oscillator can be employed in all kinds of PWM IC to improve EMC of SMPS without modifying the original circuit of power supply, providing an efficient and economic EMI reduction solution.

(5) The digital chaotic frequency PWM IC was designed. The switching frequency can be modulated by dithering the switching period counter chaotically. Tent map, Shift map and Logistic map have been used to generate the modulation signal, respectively. From the simulations and experimental results, it was found that EMI can be suppressed by CDPWM and the output ripple is increased slightly. With shift map, EMI is reduced most, whereas the output voltage ripple is increased most also. In addition, the ripple increment is least when using Logistic map. The designers can make an optimized choice based on the comparisons.

Although great efforts have been made on the application of chaotic modulation in real products, there are still some issues to be addressed in the future. Detailed as follows:

(1) The present theoretical study on the system stability under CCFM is not enough to guide the application of chaotic modulation. Consequently, the study on the SMPS stability with CCFM will be carried on, since the product's performance is determined by the system stability.

(2) Only Chua's circuit has been used to modulate the switching frequency of power supply so far. The other chaos oscillators will be adopted to generate the modulation signal. And the complexity of the circuit, the EMI suppression result and the effect of chaotic modulation on the system performance will be compared individually when using different chaos circuit. And then the CCFM module will be optimized.

(3) Chaotic frequency PWM IC will be made by Field Programmable Analog Array (FPAA) and FPGA. And the experimental research on the chaotic frequency PWM IC will be carried out to optimize the scheme and verify the effectiveness of the designed IC on EMI reduction.

(4) Chaotic modulation will be applied in other commercial switching systems, such as transverter and inverter.

References

[1] R. Lenk. *Practical Design of Power Supplies*. IEEE Press, 2005.

[2] M. R. Yazdani, H. Farzanehfard, and J. Faiz. Classification and Comparison of EMI Mitigation Techniques in Switching Power Converters–a Review. *Journal of Power Electronics*, 11(5):767–777, 2011.

[3] W. H. Parker. Electromagnetic interference: a tutorial. In *Aerospace Applications Conference, 1996. Proceedings., 1996 IEEE*, volume 3, pages 177–186, Feb 1996.

[4] H. Li. *Reducing Electromagnetic Interference in DC-DC Converters with Chaos Control*. Fortschritt-Berichte VDI / 21: Elektrotechnik. VDI-Verlag, 2009.

[5] T. C. Toh. *Electromagnetic Theory for Electromagnetic Compatibility Engineers*. CRC Press, 2005.

[6] M. R. Yazdani, H. Farzanehfard, and J. Faiz. Classification and comparison of emi mitigation techniques in switching power converters - a review. *Journal of Power Electronics*, 11(5):767–777, 2011.

[7] G. A. Jackson. Introduction to Electromagnetic Compatibility. *Introduction to Electromagnetic Compatibility John Wiley & Sons*, 93(7-8):1–12, 2006.

[8] Noise Reduction Techniques in Electronic Systems, author=Ott, Henry W., journal=A Wiley-Interscience Publication, New York: Wiley, 1976, year=1976,.

[9] D. Qu. EMI Characterization and Improvement of Bi-directional DC/DC Converters. *Virginia Tech*, 1999.

[10] A. A. Boora, F. Zare, and A. Ghosh. Efficient Voltage/current Spike Reduction by Active Gate Signaling. In *Electromagnetic Compatibility Symposium Adelaide, 2009.*, pages 59–64. IEEE, 2009.

[11] H. Mecke, R. Doebbelin, T. Winkler, and W. Fischer. Conducted Emission of Inverter Power Sources for Resistance Welding. *Journal of Power Electronics*, 2(2):124–129, 2002.

[12] M. Tsukuda, I. Omura, Y. Sakiyama, M. Yamaguchi, K. Matsushita, and T. Ogura. Critical IGBT Design Regarding EMI and Switching Losses. In *Power Semiconductor Devices and IC's, 2008. ISPSD'08. 20th International Symposium on*, pages 185–188. IEEE, 2008.

[13] N. Idir, R. Bausiere, and J. J. Franchaud. Active Gate Voltage Control of Turn-on di/dt and turn-off dv/dt in Insulated Gate Transistors. *Power Electronics, IEEE Transactions on*, 21(4):849–855, 2006.

[14] J. D. Kagerbauer and T. Jahns. Development of an Active dv/dt Control Algorithm for Reducing Inverter Conducted EMI with Minimal Impact on

Switching Losses. In *Power Electronics Specialists Conference, 2007. PESC 2007. IEEE*, pages 894–900. IEEE, 2007.

[15] M. Mahdavi and H. Farzanehfard. A New Zero Voltage Transition Bridgeless PFC with Reduced Conduction Losses. *Journal of Power Electronics*, 9(5):708–717, 2009.

[16] M. Yoshida, E. Hiraki, and M. Nakaoka. Actual Efficiency and Electromagnetic Noises Evaluations of a Single Inductor Resonant AC Link Snubber-Assisted Three-Phase Soft-Switching Inverter. In *Telecommunications Energy Conference, 2003. Intelec '03. the International*, pages 721 – 726, 2003.

[17] P. Caldeira, R. Liu, D. Dalal, and W. J. Gu. Comparison of EMI Performance of PWM and Resonant Power Converters. In *Power Electronics Specialists Conference, 1993. Pesc '93 Record., IEEE*, pages 134–140, 1993.

[18] W. Zhou and S. Qiu. Effect of Chaotic Spectrum-Spread on Output Voltage Ripple of Power Converter. *Electric Power Automation Equipment*, 12:52–55, 2008.

[19] T. Daimon. Spread-spectrum Clocking in Switching Regulators for EMI Reduction. *Ieice Trans Fundamentals*, 86(2):381–386, 2003.

[20] K. Tse, H. Chung, S. R. Hui, and H. So. A Comparative Study of Carrier-Frequency Modulation Techniques for Conducted EMI Suppression in PWM Converters. *Industrial Electronics, IEEE Transactions on*, 49(3):618–627, 2002.

[21] F. Lin and D. Chen. Reduction of Power Supply EMI Emission by Switching Frequency Modulation. In *Power Electronics Specialists Conference, 1993. PESC'93 Record., 24th Annual IEEE*, pages 127–133. IEEE, 1993.

[22] J. Balcells, A. Santolaria, A. Orlandi, D. Gonzalez, and J. Gago. EMI Reduction in Switched Power Converters Using Frequency Modulation Techniques. *Electromagnetic Compatibility, IEEE Transactions on*, 47(3):569–576, 2005.

[23] B. Zhang and X. Wang. *Chaos analysis and chaotic EMI suppression of DC-DC converters*. IEEE Press , Wiley, 2014.

[24] Q. Li. Reduce EMI by Spectrum Spreading. *International Electronic Elements*, 1(12):63–64, 2001.

[25] J. Jankovskis, D. Stepins, S. Tjukovs, and D. Pikulins. Examination of different spread spectrum techniques for EMI suppression in dc/dc converters. *Elektronika Ir Elektrotechnika*, 86(6):60–64, 2008.

[26] A. M. Trzynadlowski, S. Legowski, and R. Lynn Kirlin. Random Pulse-Width Modulation Technique for Voltage-Controlled Power Inverters. *International Journal of Electronics Theoretical and Experimental*, 68(6):1027–1037, 1990.

[27] T. Tanaka, T. Ninomiya, and K. Harada. Random-Switching Control in DC-to-DC Converters. In *Power Electronics Specialists Conference, 1989. PESC'89 Record., 20th Annual IEEE*, pages 500–507. IEEE, 1989.

[28] A. M. Stankovic, G. C. Verghese, and D. J. Perreault. Randomized Modulation of Power Converters via Markov Chains. *Control Systems Technology, IEEE Transactions on*, 5(1):61–73, 1996.

[29] M. M. Bech, J. K. Pedersen, F. Blaabjerg, and A. M. Trzynadlowski. A Methodology for True Comparison of Analytical and Measured Frequency Domain Spectra in Random PWM Converters. *Power Electronics, IEEE Transactions on*, 14(3):578–586, 1999.

[30] R. L. Kirlin, S. Kwok, S. Legowski, and A. M. Trzynadlowski. Power Spectra of a PWM Inverter with Randomized Pulse Position. *Power Electronics, IEEE Transactions on*, 9(5):463–472, 1994.

[31] K. Tse, H. Chung, S. R. Hui, and H. So. A comparative Investigation on the Use of Random Modulation Schemes for DC/DC Converters. *Industrial Electronics, IEEE Transactions on*, 47(2):253–263, 2000.

[32] F. Mihalic and M. Milanovic. Wide-Band Frequency Analysis of the Randomized Boost Rectifier. In *Power Electronics Specialists Conference, 2000. PESC 00. 2000 IEEE 31st Annual*, volume 2, pages 946–951. IEEE, 2000.

[33] R. L. Kirlin, J. Wang, and R. Dizaji. Study on Spectral Analysis and Design for DC/DC Conversion Using Random Switching Rate PWM. In *Statistical Signal and Array Processing, 2000. Proceedings of the Tenth IEEE Workshop on*, pages 378–382. IEEE, 2000.

[34] Y. Shrivastava and S. Hui. Analysis of Random PWM Switching Methods for Three-Level Power Inverters. *Power Electronics, IEEE Transactions on*, 14(6):1156–1163, 1999.

[35] R. L. Kirlin, M. M. Bech, and A. M. Trzynadlowski. Power Apectral Sensity Analysis of Randomly Switched Pulse Width Modulation for DC/AC Converters. In *Statistical Signal and Array Processing, 2000. Proceedings of the Tenth IEEE Workshop on*, pages 373–377. IEEE, 2000.

[36] M. M. Bech, F. Blaabjerg, and J. K. Pedersen. Random Modulation Techniques with Fixed Switching Frequency for Three-Phase Power Converters. In *Power Electronics Specialists Conference, 1999. PESC 99. 30th Annual IEEE*, volume 1, pages 544–551. IEEE, 1999.

[37] A. M. Stankovic and H. Lev-Ari. Randomized Modulation in Power Electronic Converters. *Proceedings of the IEEE*, 90(5):782–799, 2002.

[38] T. Tanaka, H. Kameda, and T. Ninomiya. Noise Analysis of DC-to-DC Converter with Random-Switching Control. *IEICE Transactions on Communications*, 75(11):1142–1150, 1992.

[39] K. Tse, H. Chung, S. R. Hui, and H. So. A comparative Investigation on the Use of Random Modulation Schemes for DC/DC Converters. *Industrial Electronics, IEEE Transactions on*, 47(2):253–263, 2000.

[40] J. Zhang, L. Zhang, and S. Qiu. An Experimental Investigation of EMI Suppression of Off-Line Switching Converter by Chaotic Modulation. *AerOspace Control*, 24(4):87–90, 2006.

[41] B. Wang and W. Haoxiong. Comparative Investigation of Randomized Modulation and Frequency Jitter in Restraining Conduct EMI. *Journal of China Three Gorges Univ.(Natural Sciences)*, 27(4):314–317, 2006.

[42] K. Tse, H. Chung, S. R. Hui, and H. So. A comparative Study of Carrier-Frequency Modulation Techniques for Conducted EMI Suppression in PWM Converters. *Industrial Electronics, IEEE Transactions on*, 49(3):618–627, 2002.

[43] K. Tse, R. Ng, H. Chung, and S. R. Hui. An Evaluation of the Spectral Characteristics of Switching Converters with Chaotic Carrier-Frequency Modulation. *Industrial Electronics, IEEE Transactions on*, 50(1):171–182, 2003.

[44] S. Callegari, R. Rovatti, and G. Setti. Spectral Properties of Chaos-Based FM Signals: Theory and Simulation Results. *Circuits & Systems I Fundamental Theory & Applications IEEE Transactions on*, 50(1):3 – 15, 2003.

[45] R. Yang. *Chaotification and EMI Suppression of Power Converter*. PhD thesis, South China University of Technology, 2007.

[46] E. N. Lorenz. *The Essence of Chaos*. University of Washington Press, 1993.

[47] J. Rodriguez Marrero, J. Font, and G. C. Verghese. Analysis of the Chaotic Regime for DC-DC Converters Under Current-Mode Control. In *Power Electronics Specialists Conference, 1996. PESC'96 Record., 27th Annual IEEE*, volume 2, pages 1477–1483. IEEE, 1996.

[48] S. Banerjee, D. Kastha, and S. SenGupta. Minimising EMI Problems With Chaos. In *Electromagnetic Interference and Compatibility, 2001/02. Proceedings of the International Conference on*, pages 162–167. IEEE, 2002.

[49] S. Callegari, R. Rovatti, and G. Setti. Chaotic Modulations Can Outperform Random Ones in Electromagnetic Interference Reduction Tasks. *Electronics Letters*, 38(12):543–544, 2002.

[50] S. Santi, R. Rovatti, and G. Setti. Advanced Chaos-Based Frequency Modulations for Clock Signals EMC Tuning. In *Circuits and Systems, 2003. ISCAS'03. Proceedings of the 2003 International Symposium on*, volume 3, pages 111–116. IEEE, 2003.

[51] H. Li, Z. Li, B. Zhang, F. Wang, N. Tan, and W. Halang. Design of Analogue Chaotic PWM for EMI Suppression. *Electromagnetic Compatibility, IEEE Transactions on*, 52(4):1001–1007, 2010.

[52] H. Li, Z. Li, B. Zhang, Q. Zheng, and W. Halang. The Stability of a Chaotic PWM Boost Converter. *International Journal of Circuit Theory and Applications*, 39(5):451–460, 2011.

[53] R. Yang, B. Zhang, F. Li, and J. Jiang. Experiment Research of Chaotic PWM Suppressing EMI in Converter. In *Power Electronics and Motion Control Conference, 2006. IPEMC 2006. CES/IEEE 5th International*, volume 1, pages 1–5. IEEE, 2006.

[54] Y. Song, Z. Li, J. Niu, G. Zhang, W. Halang, and H. Hirsch. Reducing EMI in a PC Power Supply with Chaos Control. In *Foundations and Applications of Intelligent Systems*, pages 231–241. Springer, 2014.

[55] Z. Li, S. Qiu, and Y. Chen. Experimental Study on the Suppressing EMI Level of DC-DC Converter with Chaotic Map. *Proceedings of the CSEE*, 5:012, 2006.

[56] Z. Li, S. Qiu, and L. Zhang. Research on the Enhanced Electromagnetic Compatibility of Switching Converter with Chaotic Frequency Modulation. *Acta Electronica Sinica*, 33(11):1983, 2005.

[57] Z. Li, S. Qiu, and Y. Chen. Experimental Study on the Effectiveness of EMI Suppression with Chaotic Modulation for Switching Converters. *Transactions of China Electrotechnical Society*, 21(8):97–102, 2006.

[58] D. Maksimovic, R. Zane, and R. Erickson. Impact of Digital Control in Power Electronics. In *Power Semiconductor Devices and ICs, 2004. Proceedings. ISPSD'04. The 16th International Symposium on*, pages 13–22. IEEE, 2004.

[59] B. J. Patella, A. Prodic, A. Zirger, and D. Maksimovic. High-Frequency Digital PWM Controller IC for DC-DC Converters. *Power Electronics, IEEE Transactions on*, 18(1):438–446, 2003.

[60] J. Zarębski and K. Górecki. Spice-aided modelling of the uc3842 current mode pwm controller with selfheating taken into account. *Microelectronics Reliability*, 47(7):1145–1152, 2007.

[61] C. Alexander, C. K. Alexander, and M. Sadiku. *Fundamentals of Electric Circuits*. Urban Media Comics, 2006.

[62] L. O. Chua, L. Kocarev, K. Eckert, and M. Itoh. Experimental Chaos Synchronization in Chua's Circuit. *International Journal of Bifurcation and Chaos*, 2(03):705–708, 1992.

[63] J. Niu. Application of Chaotic Carrier-Frequency Modulation in Phase-Shifted Full-Bridge Converters for Reducing EMI. *Journal of Shunde Polytechnic*, (2):22–27, 2014.

[64] J. Niu, Y. Song, Z. Li, and W. A. Halang. Reducing EMI in Half-Bridge Resonant LED Drivers with Chaos-Based PWM. In *Electromagnetic Compatibility (EMC EUROPE), 2013 International Symposium on*, pages 637–640.

IEEE, 2013.

[65] D. Liu, Y. S. Hang, L. U. Lin xiang, and Q. M. Zhou. The PWM Control System Made of TL494. *Telecom Power Technologies*, 24(6):39–41, 2007.

[66] Z. Zhang, C. Zhang, and H. Shen. Applications of Advanced Phase Shift PWM Controller UCC3895 in the ZVS-FB-PWM Converter. *Power Electronics*, 3:025, 2005.

[67] A. M. StankoviÄ. *Random Pulse Modulation with Applications to Power Electronic Converters*. PhD thesis, Massachusetts Institute of Technology, 1993.

[68] G. Li, X. Chen, and F. Liu. Analysis of Power Spectral Density of the Output Voltage in Chaotic PWM Inverter . *Proceedings of the CSEE*, 26(20):79–83, 2006.

[69] R. Yang and B. Zhang. Quantification Description of the Chaotic PWM Spectrum of the Switching Converter. *Acta Physica Sinica*, 11, 2006.

[70] G. Li, X. Chen, and F. Liu. Analysis of Power Spectral Density of the Output Voltage in Chaotic PWM Inverter. *Proceedings of the Chinese Society of Electrical Engineering*, 26(20):79–83, 2006.

[71] J. L. Doob. *Stochastic Processes*. New York Wiley, 1953.

[72] A. M. Stankovic, G. C. Verghese, and D. J. Perreault. Analysis and Synthesis of Randomized Modulation Schemes for Power Converters. *Power Electronics, IEEE Transactions on*, 10(6):680–693, 1995.

[73] M. M. Bech, J. K. Pedersen, F. Blaabjerg, and A. M. Trzynadlowski. A Methodology for True Comparison of Analytical and Measured Frequency Domain Spectra in Random PWM Converters. *Power Electronics, IEEE Transactions on*, 14(3):578–586, 1999.

[74] K. Tse, H. S. Chung, S. Huo, and H. So. Analysis and Spectral Characteristics of a Spread-Spectrum Technique for Conducted EMI Suppression. *Power Electronics, IEEE Transactions on*, 15(2):399–410, 2000.

[75] T. Tanaka, H. Kameda, and T. Ninomiya. Noise Analysis of DC-to-DC Converter with Random-Switching Control. *IEICE Transactions on Communications*, 75(11):1142–1150, 1992.

[76] K. Tse, W. Ng, H. S. Chung, and S. Hui. Evaluation of a Chaotic Switching Scheme for Power Converters. In *Power Electronics Specialists Conference, 2000. PESC 00. 2000 IEEE 31st Annual*, volume 1, pages 412–417. IEEE, 2000.

[77] J. Zhang, S. Qiu, and L. Chen. An Investigation of Chaotic Frequency Modulation for Improved EMC of Switching Mode Power Supply. *Electrical Applications*, 25(6):71–74, 2006.

[78] P. J. Shah, R. Saxena, and M. Chawla. Design and Modeling of a Digital Controller for SMPS. *International journal of power electronics and energy*, 1(1):1–9, 2012.

[79] V. Yousefzadeh. Advances in Digital Power Control. In *Telecommunications Energy Conference (INTELEC), 32nd International*, pages 1–8. IEEE, 2010.

[80] Y. Gao, S. Guo, Y. Xu, S. X. Lin, and B. Allard. FPGA-based DPWM for Digitally Controlled High-Frequency DC-DC SMPS. In *Power Electronics Systems and Applications, 2009. PESA 2009. 3rd International Conference on*, pages 1–7. IEEE, 2009.

[81] S. Phatak and S. S. Rao. Logistic Map: A Possible Random-Number Generator. *Physical review E*, 51(4):3670, 1995.

[82] T. Yoshida, H. Mori, and H. Shigematsu. Analytic Study of Chaos of the Tent Map: Band Structures, Power Spectra, and Critical Behaviors. *Journal of Statistical Physics*, 31(2):279–308, 1983.

Curriculum Vitae

Affliation and Offcial Address: Faculty of Mathematics and Computer Science FernUniversität in Hagen, 58084 Hagen, Germany

Date and Place of Birth: 27 December 1980, Shanxi, P.R.China

Gender: Female

Languages: Chinese (native language), English

Education:

Ph.D. in Electrical Engineering, Faculty of Mathematics and Computer Science, FernUniversität in Hagen, Germany, 2012-2016

M.Sc. in Signal and Information Processing, School of Electronic Engineering, Xidian University, 2002-2005

B.Sc. in Management Engineering, School of Economic Management, Xidian University, 1998-2002

Specialisation:

(1)Main Fields: Intelligent control technology

(2)Present: Suppression of electromagnetic interference in power supplies

Die Reihen der Fortschritt-Berichte VDI:

1 Konstruktionstechnik/Maschinenelemente
2 Fertigungstechnik
3 Verfahrenstechnik
4 Bauingenieurwesen
5 Grund- und Werkstoffe/Kunststoffe
6 Energietechnik
7 Strömungstechnik
8 Mess-, Steuerungs- und Regelungstechnik
9 Elektronik/Mikro- und Nanotechnik
10 Informatik/Kommunikation
11 Schwingungstechnik
12 Verkehrstechnik/Fahrzeugtechnik
13 Fördertechnik/Logistik
14 Landtechnik/Lebensmitteltechnik
15 Umwelttechnik
16 Technik und Wirtschaft
17 Biotechnik/Medizintechnik
18 Mechanik/Bruchmechanik
19 Wärmetechnik/Kältetechnik
20 Rechnerunterstützte Verfahren (CAD, CAM, CAE CAQ, CIM ...)
21 Elektrotechnik
22 Mensch-Maschine-Systeme
23 Technische Gebäudeausrüstung

ISBN 978-3-18-3**85110**-2